To the Graduate Council:

I am submitting herewith a thesis written by Mahesh Sanganeria entitled "Studies on Embrittlement on ordered $Ni_4Mo$." I have examined the final copy of this thesis for form and content and recommend that it be accepted in partial fulfillment of the requirements for the degree of Master of Science, with a major in Metallurgical Engineering.

Charlie R. Brooks

C. R. Brooks, Major Professor

We have read this thesis
and recommend its acceptance:

Accepted for the council:

Vice Provost
and Dean of The Graduate School

# STUDIES ON EMBRITTLEMENT ON ORDERED $Ni_4Mo$

A Thesis

Presented for the

Master of Science

Degree

The University of Tennessee, Knoxville

MAHESH SANGANERIA

May 1989

# DEDICATION

This thesis is dedicated to my parents:

Mr. Govindram Sanganeria and Mrs. Gitadevi Sanganeria

# ACKNOWLEDGMENTS

The author would like to express deep gratitude to his major professor Dr. C. R. Brooks, for his unceasing guidance and help, in matters both technical and personal, through the entire course of this research.

The financial support provided by the Tennessee Eastman Corporation and through teaching assistantship by the Department of Materials Science and Engineering is greatfully acknowledged.

The author would like to thank Mr. Gary Whitaker Of Tennessee Eastman Corporation for providing useful technical informations on Hastalloy B-2 and Dr. Joe Klein of Haynes International for providing with chemical analysis of the material.

Thanks are extended to Dr. B. F. Oliver and Bimal Kad for their help in the preparation of the alloys.

Special thanks are expressed to Mr Doug Fielden, Head of the departmental machine shop and his amiable group especially Mr. Jack French for their patience in cutting Hastalloy B-2.

Help received from the electronic shop especially Michael R. Neal and Greg Jones is deeply appreciated.

Thanks are extended to Mr. Bob L. McGill for his help with scanning electron microscope and Mr. Albert W. Carter and Mrs. Aileen Cagle for supplying laboratory materials.

The author is greatful to Mrs. Sandra Maples and Mrs. Phyllis Davis for their goodwill and help with official matters.

A special thanks is expressed to Vikas Joshi and Rajen Patel for their help in the preparation of the thesis.

Last but not the least, the author would like to thank his fellow graduate students who provided a congenial work atmosphere.

# ABSTRACT

The alloy $Ni_4Mo$ in the ordered condition is strong and has potential for use at moderately high temperature (approx. $600^0C$), but it is extremely brittle in the ordered condition. $Ni_4Mo$ based commercial alloy Hastelloy B-2 is used in the disordered condition for its good strength and corrosion resistance. However, the possibility of ordering, and thereby embrittlement, during fabrication by welding is of concern. The present work involves an attempt to understand the phenomenon of embrittlement in ordered $Ni_4Mo$ with the aim of exploiting its potential use.

The alloy $Ni_4Mo$ undergoes an ordering transformation below $868^0C$ from a short-range order (SRO), FCC structure ($\alpha$) to a tetragonal structure ($\beta$), accompanied by a significant increase in hardness, yield strength and a drastic reduction in ductility. The $\alpha$ phase can be retained by rapid cooling from $868^0C$, and then the rate of ordering controlled by choice of aging temperature and time. On aging in the temperature range $700-800^0C$, an independent reaction commences, which involves the movement of high angle, former $\alpha$-boundaries.

Fracture in the embrittled ordered alloy occurs, clearly, along the high angle, former $\alpha$-boundaries. However at increased aging times, the fracture morphology

becomes finer (without any significant change in ductility) which does not correlate with the former α-grain size. It has been established in this work that this finer fracture surface morphology is associated with the fracture along the migrated, high angle boundaries.

Attempts were made to improve the ductility of ordered $Ni_4Mo$ by microalloying. Arc melted, microalloyed buttons were processed to obtain a fine grain, homogeneous α structure and then ordered by aging at 725°C for four hours. Thin slices of the ordered samples were bent to test for ductility. Elements Hf, Zr, Ce, Nb, Mg, La, and Mn were selected to act as a scavenger of impurities from the grain boundary but these elements did not seem to improve the ductility. Among the elements which are likely to segregate to the grain boundary and improve the strength of intrinsically weak boundaries, boron and beryllium were tested. Boron produced no observable change in ductility, however, beryllium appeared promising as the sample showed a little bending before fracturing.

The aging (up to 20 hours) behavior of cold worked, disordered structure α has been determined for 700°C, 775°C and 850°C ($T_c$ = 868°C) in terms of microstructural observation and microhardness measurement. Three degrees of cold work, 43%, 68% and 80% reduction in area, were

investigated. Aging at 850°C resulted in recrystallization of cold worked α into strain-free equiaxed α (with a marked hardness decrease), followed by short-range ordering and then long-range ordering (with a marked hardness increase). Then the long-range ordered structure on continued aging showed softening which appeared to be associated with domain growth. Aging at 700°C and 775°C did not result in recrystallization of cold worked α into strain-free α. Instead, it appears that long range ordering of cold worked disordered α (accompanied by a marked increase in hardness) followed by recrystallization into low dislocation density ordered β structure occurred. There is also a contribution of short-range ordering (which has been reported to exist at initial stages of aging cold worked α structure at 700°C) in increasing hardness in the initial stage of aging. Recrystallization of β was optically resolved on aging 43% cold worked sample for 150 minutes at 775°C or 300 minutes at 700°C.

The possibility of ordering and embrittlement, during fabrication by welding, in some Hastelloy B-2 components, in use at Tennessee Eastman Co., Kingsport, Tennessee was examined. Two samples were investigated to study the effect of welding. In the as-received condition these samples showed cracks on the surface which was exposed to chemicals in application. Metallographic observation

showed that these cracks were intergranular. However, bending samples with the cracks did not propagate them intergranularly. These samples showed an extensive bend ductility. The cause of the cracks is intergranular corrosion.

# TABLE OF CONTENTS

# LIST OF FIGURES

FIGURE PAGE

FIGURE PAGE

# CHAPTER 1

## INTRODUCTION

There is considerable interest in ordered alloys, as many are strong and show potential for use as high temperature structural materials(1). One such alloy is Ni-20at.%Mo, hereafter denoted as $Ni_4Mo$, for which the ordering reaction and strengthening have been extensiverly studied. The physical metallurgy and mechanical properties of this alloy (and other Ni-Mo alloys) have been recently reviewed (2). Although this alloy strengthens considerably upon ordering, a serious limitation of the use of it in the ordered condition is its extreme brittleness. No significant improvement in ductility of this alloy has yet been reported. An intensive study of the embrittlement in this alloy has been carried out in this work.

The alloy $Ni_4Mo$ undergoes an ordering reaction below $868^0C$ from a short-range ordered (SRO), FCC structure ($\alpha$) to a tetragonal structure ($\beta$), accompanied by a drastic reduction of ductility of polycrystalline samples in tension. Fracture in the embrittled ordered alloy occurs along high angle, former $\alpha$-boundaries. The $\alpha$ phase can be retained by rapid cooling from above $868^0C$, and then the rate of ordering controlled by choice of the aging

temperature and time. Also, single crystals of $\beta$ tested in tension show significant ductility.

Embrittlement in ordered alloys has drawn a significant interest and efforts are being put to understand this phenomenon. There is a striking similarity between embrittlement in ordered alloys and temper embrittlement in low alloy steels which has been extensively studied. Earlier workers, mostly working on temper embrittlement in low alloy steels, assigned the cause of embrittlement to grain boundary segregation of impurities; however this suggestion is not indisputable. A considerable effort is being made to arrive at a generalized model to explain the phenomenon of intergranular brittle failure. Many researchers are working towards a theory based on atomistic mechanisms. A brief review of these developments is presented in section 2.2.

The phenomenon of embrittlement in ordered alloys remains poorly understood. However, some remedial measures, involving microalloying (3,4), work very effectively in improving ductility in some specific systems. In the absence of a strong theoretical basis, our approach in this work has been to search for remedial measures for $Ni_4Mo$ based on the results available for other alloy systems. This essentially involves microalloying and thermo-mechanical treatments. A possible

rational, largely empirical, for these approaches is discussed in section 2.3.

The $Ni_4Mo$ based commercial alloys Hastelloy B and Hastelloy B-2, containing Fe and C, are used for their excellent corrosion resistance and good strength. The Fe present in Hastelloy B supresses formation of $\beta$ which is responsible for embrittlement. Hastelloy B-2 has a much lower Fe content (max 1%) and is very likely to undergo ordering during fabrication involving welding. The ductility drop associated with ordering is very sharp and a very small degree of ordering during fabrication may lead to catastrophic service failure. This work also investigates some Hastelloy B-2 components failed in service, for contribution of ordering in causing failure (samples supplied by Tennessee Eastman Corporation, Kingsport) and to evaluate the fabrication (welding) techniques in inducing ordering.

# CHAPTER 2

# LITERATURE REVIEW

## 2.1 INTRODUCTION TO $Ni_4Mo$ ALLOY

### Phase Diagram

Figure 2.1 shows the phase relations in the Ni-Mo system (5). There have been numerous investigations of the formation of $\beta$ from $\alpha$, but few give sufficient details about the exact composition of the alloys used to assist in defining $\alpha$-$\beta$ boundaries. However, considering the wealth of studies on $\beta$-alloys given as 20at%Mo, Brooks et al. (2) believe that $\beta$ encompasses the stoichiometric $Ni_4Mo$. Various investigators (6,7,8) have reported the decomposition temperature of $868\pm5^{o}C$.

### Crystal Structure of $Ni_4Mo$

The high temperature phase $\alpha$ is disordered and has a f.c.c. structure. The ordering reaction results in a slight tetragonal distortion of the cubic lattice resulting in body centered tetragonal phase $\beta$. Harker (9) determined the crystal structure and lattice parameters of $\beta$, and his results are reproduced in Fig.2.2. Similar results were obtained by several other workers (6,7).

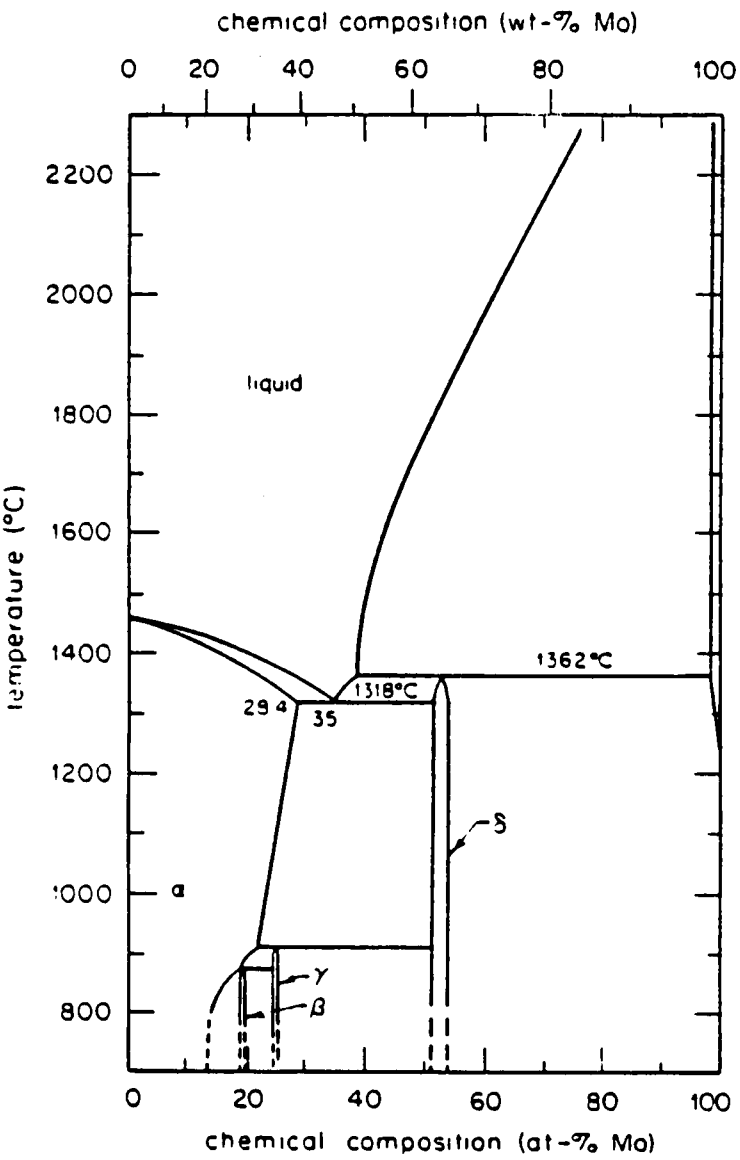


**Figure 2.1 The Ni-Mo phase diagram. (Ref. 5)**

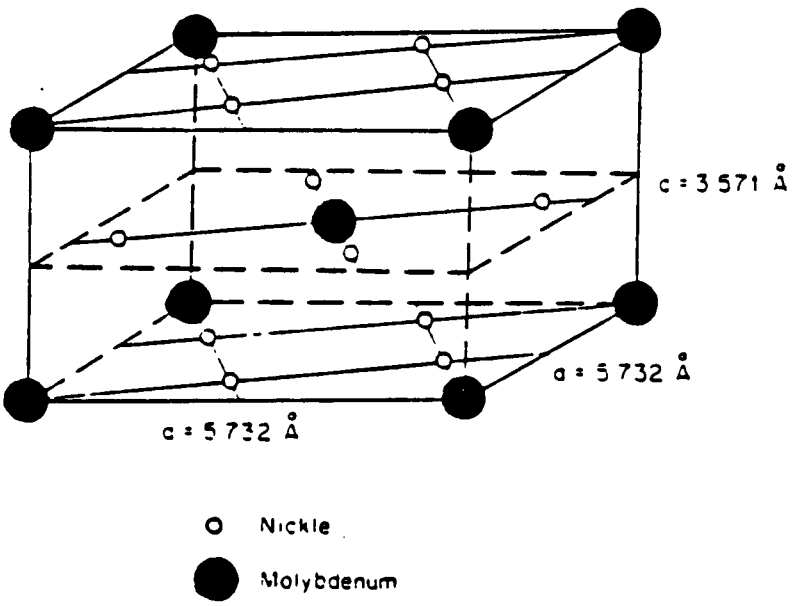


Figure 2.2 The crystal structure of $\beta(Ni_4Mo)$. (Ref. 9)

Orientation relationship between the $\beta$-phase and the parent fcc $\alpha$ solid solution may be understood by reference to Fig.2.3. During ordering the c-axis of the bct superlattice can be parallel to any of the three cube axes of the $\alpha$-phase. The bct a-axis can be inclined at either a positive or a negative angle to the cube axis. This gives 3 x 2 = 6 different orientation variants for the $\beta$-phase. For any given orientation the bct cell can have its origin at 5 different positions, so altogether there are 30 ways in which the bct cell can form from the fcc $\alpha$-matrix.

Domain Interfaces

Ruedl et al.(10) showed that the different domain boundaries could be classified as anti-phase domain boundaries (APBs), anti-parallel twins (APTs), or perpendicular twins (PTs). For APBs, the unit-cell axes of the superlattice in the adjacent domains are parallel across the boundary, as illustrated Fig. 2.4a and 2.4b for two possible displacement vectors. APTs correspond to the interfaces between two orientation variants in which the c-axes of the superlattice are anti-parallel (Fig. 2.4c). Two domain lattices may be displaced relative to each other, generating a combination APB and APT. When the c-axes of adjacent superlattice domains are approximately perpendicular to each other, i.e., when they are along

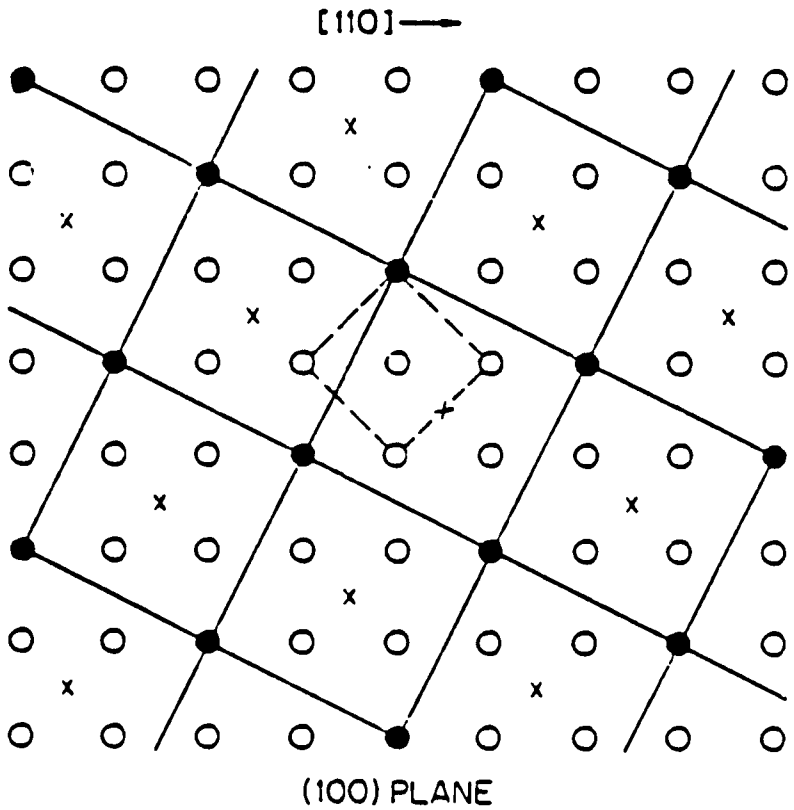


**Figure 2.3** Schematic diagram of $\beta$-lattice showing relation between fcc $\alpha$-lattice and bct ordered lattice; positions of Mo atoms in adjacent planes indicated by x. (Ref. 2)

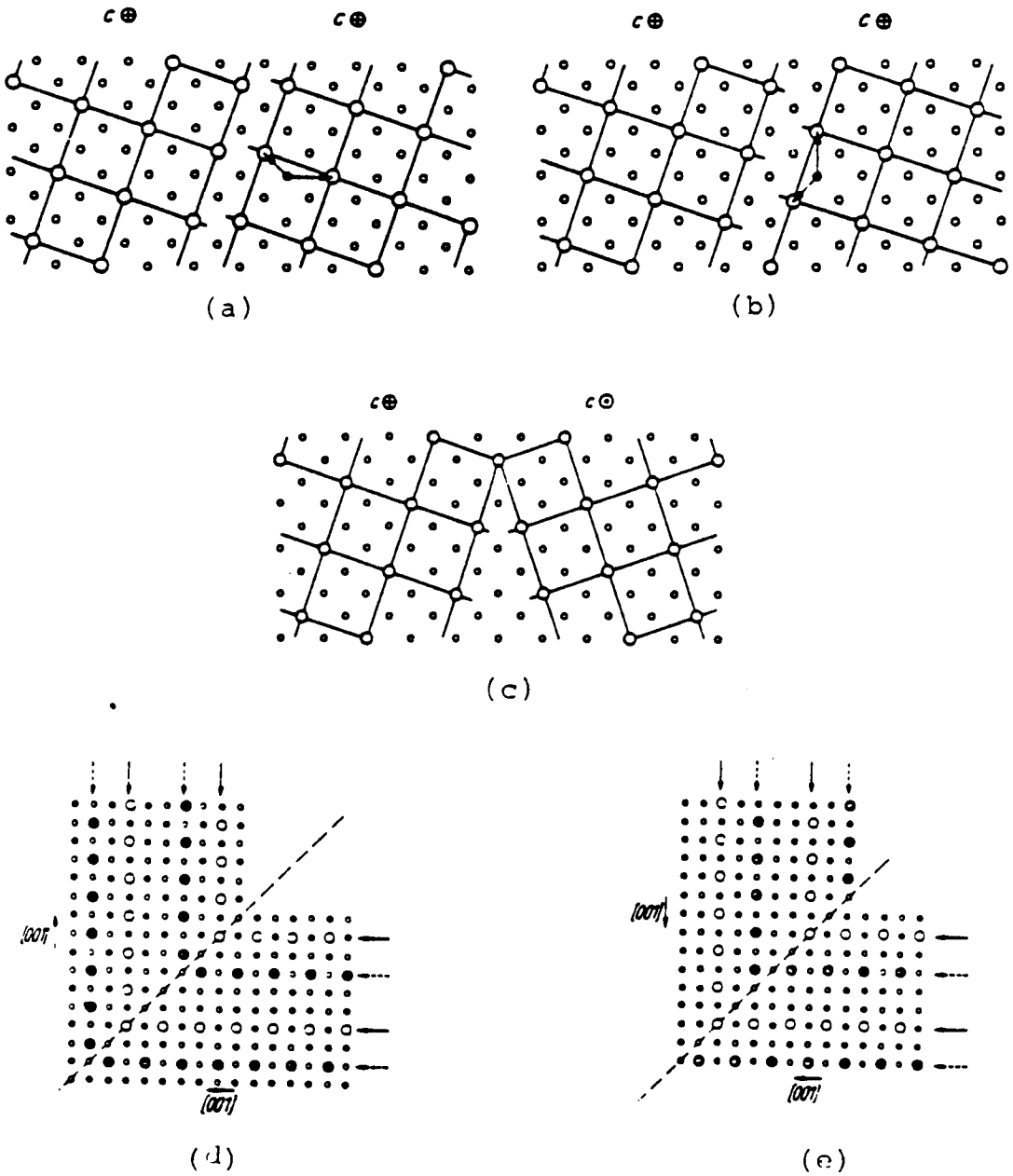


Figure 2.4 Models for $\beta$ domain boundaries (Ref. 10)
a), b) anti-phase boundary
c) anti-parallel boundary
d), e) perpendicular twins

different cube directions in the disordered lattice, the interface is a PT interface (Fig. 2.4d and 2.4e).

Phase Transformations

At solution-treatment temperatures in the range 900-1250°C, $Ni_4Mo$ is a SRO, single-phase, fcc solid solution (6,7,11). At temperatures below 868°C this alloy can transform to the LRO $\beta$-phase. The results obtained by Lei (12) show that during the transformation the electrical resistivity decreases while the hardness increases. The ordering transformation can also be detected by optical microscopy as $\beta$ shows an etching effect. However, this effect cannot be used quantitatively, e.g., in determining the extent of ordering or initiation of ordering.

The most direct methods of detecting the LRO $\beta$-phase is by means of X-ray and electron diffraction. However, the six orientation variants of the $\beta$-phase formed in a single $\alpha$-phase crystal produce a rather complex distribution of intensity in reciprocal space.

The first structural studies of SRO in $\alpha$-phase alloys, including quenched $Ni_4Mo$, were the X-ray diffuse scattering measurements made by Spruiell and Stansbury (11). They found that the diffuse scattering produced by SRO contained maxima located at the (1,1/2,0) positions in reciprocal space, as shown in Fig. 2.5 for quenched $Ni_4Mo$.

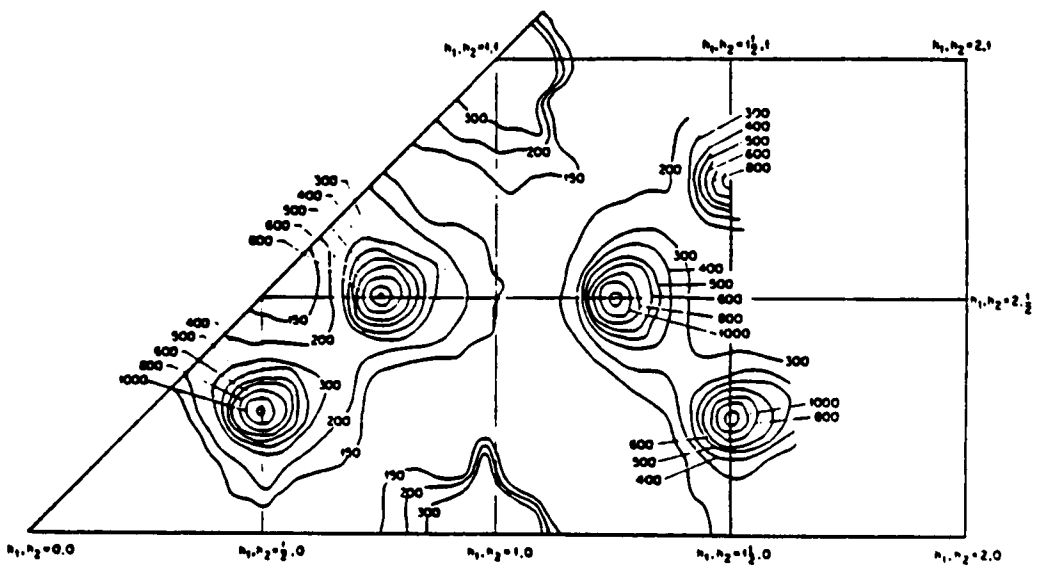

Figure 2.5 X-ray intensity distribution of diffuse intensity (at -167°C) in the $h_1$, $h_2$, 0 plane of reciprocal space for $Ni_4Mo$, quenched from 1000°C into ice water. (Ref. 11)

More support for a statistically non-random solid-solution model for the SRO state was provided by Clapp and Moss (13,14).

A detailed X-ray diffraction diffuse scattering study of SRO in quenched $Ni_4Mo$ alloy and the transition to the LRO state was carried out by Chakravarti et al.(15).There have been several other extensive studies of SRO in the $Ni_4Mo$ alloy and its transformation to LRO state using electron microscopy techniques (16-25). Although there is controversy over the nature of the SRO state in $Ni_4Mo$ and its role in the transition to the LRO state, there is reasonable agreement on the general features of the transformation. The (1,1/2,0) SRO maxima first become more intense (11,21), after which there is an increase in diffuse streaking in the diffraction patterns, followed by the formation of three-dimensionally isolated scattering at the $D1_a$ superlattice positions (11,22). At first the $D1_a$ superlattice reflections seem to coexist with the SRO maxima, but the latter soon disappear. Once the diffraction pattern shows the $D1_a$ superlattice reflections, the $\beta$-domains become clearly visible in dark-field images obtained when there are superlattice reflections (21).

Most investigators have interpreted the sequence of events described above to indicate a first-order phase transformation proceeding via nucleation and growth

(22,26-29), at least at temperatures above about 700°C. However, they do not exclude the possibility that the transformation can occur in a continuous fashion, as suggested by Cook (30), at lower aging temperatures.

The overall kinetics have been examined using microhardness (12,31) and electrical resistivity measurements (12). Ling and Starke (32) also have followed the development of the LRO parameter and domain size by wide-angle X-ray diffraction techniques. The ordering reaction shows a classical C-shaped time-temperature-transformation diagram, as shown in Fig. 2.6. This curve was dertermined from resistivity measurements made after cooling rapidly from about 1000°C to the transformation temperature (2).

The microstructural development during formation of $\beta$ involves first the formation of very fine $\beta$ domains in the $\alpha$ grains. These domains then grow, but in the range 700-800°C an independent grain boundary reaction commences, which involves the movement of high angle boundaries, with a coarser domain structure forming behind the moving interface (33), The microstructural changes are depicted schematically in Fig. 2.7.

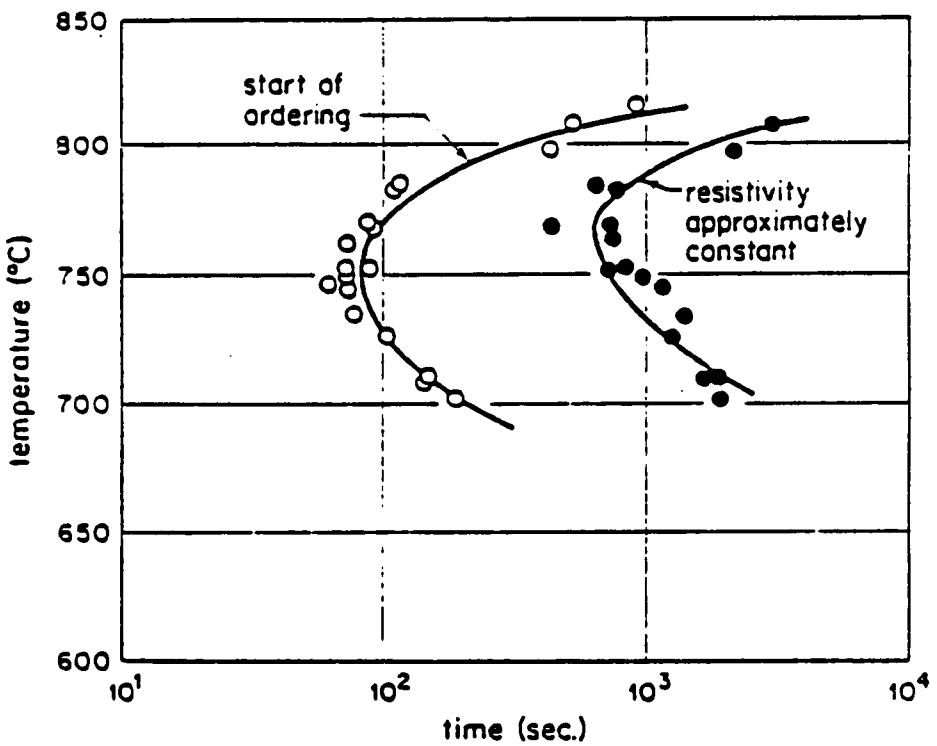


Figure 2.6 Isothermal time-temperature-transformation curve for ordering reaction in $Ni_4Mo$. (Ref. 2)

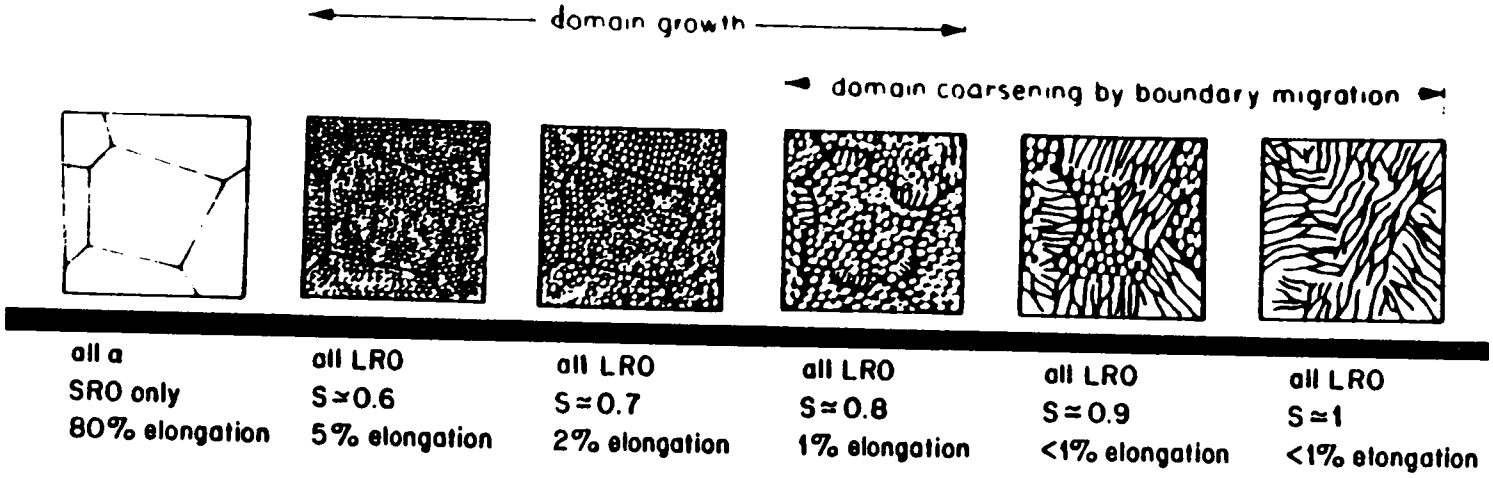


Figure 2.7 Schematic illustration of the sequence of microstructural development during aging of ordered $Ni_4Mo$ in the range 700-800°C. S is the long-Range order parameter. (Ref. 107)

## 2.2 GRAIN BOUNDARY SEGREGATION AND EMBRITTLEMENT IN METALS

In the course of processing, polycrystalline materials usually pass through a temperature range which promotes certain impurity elements to concentrate locally at interfaces.Interfacial and grain boundary adsorption or segregation in certain metals and alloys is known to be severely detrimental to many of their more important mechanical properties, causing problems such as some forms of embrittlement,temper brittleness (34-40), creep embrittlement(41), intergranular corrosion (42,43) and brittleness of some materials formed by powder metallurgy (44). One of the first detailed citations of the effect of impurities in iron is that of Arnold (45), who showed that As, P and S could all promote brittle failures exhibiting unusually bright crystalline fractures. However, it was not until near the end of the first world war that it was appreciated that temper brittle fractures were all intergranular and along prior austenite grain boundaries (46). Since then extensive work has been done to understand the causes of temper embrittlement and a myriad of literature is available reviewing the state of understanding of the subject (34-40). Some intermetallic compounds are known to exhibit similar intergranular fracture associated with segregation.

Choudhury et al. (47) have reported sulphur segregation to grain boundaries in fractured, ordered $Ni_4Mo$ alloy and they suspect that this contributes to the embrittlement. In light of this development it is appropriate to review the current state of knowledge in the field of grain boundary segregation.

Study of this field essentially involves developing a theory relating segregation to readily available parameters and precise measurement of segregation to confirm these theories. Also, a plausible theory relating embrittlement to segregation will provide the prospect of controlling the problem of embrittlement more predictably.

## Segregation Measurement

Attempts have been made to develop ever sophisticated techniques to measure the grain boundary segregation. Westbrook (48) has made an excellent review of indirect methods to detect grain boundary segregation. Seah, Hondros and Joshi (49-51) have reviewed in detail all available techniques assessing their merits and limitations. In the last decade two of the newer techniques, field ion microscopy and ion backscattering spectroscopy, have made specific contributions to the study of segregation. Far more productive than any other technique has been the application of Auger Electron Spectroscopy (AES) and, of the many alternative current

surface analytical techniques, there are no others which have produced significant new information about segregation. Stein et al. (52) have carefully discussed various aspects of AES with special emphasis on the application to metallurgically important problems.

## Theory of Grain Boundary Segregation

The first expression for grain boundary adsorption was derived by Mclean (53), using a statistical mechanical approach and assuming a partition of solute between lattice and grain boundary sites. The derived segregation equation for a solute of bulk concentration, $X_c$, at a grain boundary is:

$$X_b/(1-X_b)=[X_c/(1-X_c)]\exp(E_1/RT) \quad \text{---------(1)}$$

where $X_b$ is the adsorption level as a molar fraction of a monolayer and $E_1$ is the molar heat of adsorption of the segregant at the grain boundary.

The derivation of the above equation assumes a grain boundary structure consisting of a fixed number of well defined sites, with identical binding energies. A saturation segregation level is achieved when all the sites are filled. The recent measurements by AES (49) show that segregation levels can occur well beyond this. These experimental results could not be reconciled with the

above model in which segregation is limited to fixed number of sites. A generalized treatment, described below, of equilibrium segregation was presented by Seah and Hondros (49) which allows for multilayer formation and includes the McLean segregation as a particular case.

One of the most used gas phase isotherms that allows for multilayer adsorption is that of Brunaur, Emmett and Teller (54), the so called BET isotherm. The solid/solid interface analogue of the above relation is represented as:

$$(1/X_b)/(X_c/(X_{co}-X_c))=1/K+[(k-1)/K][X_c/X_{co}] \quad \text{------(2)}$$

where symbols are as in equation (1) except $X_{co}$ which is the solublity limit and K is $\exp[(E_1-E_L)/RT]$ where $E_1$ and $E_L$ are heat of adsorptions of the first and subsequent layers, respectively, at the grain boundary.

Grain Boundary Segregation and Brittle Fracture

Many authors link segregation induced low temperature fracture with the Griffith approach (55-59) where

$$\sigma_F = (2E\Gamma'\pi c)^{0.5} \quad \text{----------(3)}$$

$\sigma_F$ being the stress at which a crack of length c begins to propagate in a material with elastic modulus E. In a brittle material, $\Gamma'$ is the total energy required in

creating unit area of surface by the crack and is composed of the surface energy and a plastic work term. It is argued that segregation of impurities at the fractured surface decreases the surface energy and thereby decreases the fracture strength. Seah (60) has reviewed these models and concludes that this reduction in surface energy can not account for the low temperature intergranular failure. However, the role of this factor in some high temperature intergranular failures, i.e., creep embrittlement, was not ruled out.

Seah (60) has proposed a model for segregation-induced lowering of grain boundary fracture strength and reports that this model predicts, with reasonable accuracy, the effect of segregation on the transition temperature and also the relative embrittlement of the four main embrittling species in steel. The argument proposed is that the decrease in grain boundary fracture strength is due to an increase in the average interatomic distance at the grain boundary associated with the segregation of atoms of larger size. This model explains the remedial effect of some smaller atoms like B and Be on the low temperature embrittlement of some steels.

The macroscopic models discussed above provide a qualitative understanding of the subject under discussion. However, it is realized that the process of fracture involves the breaking of bonds at the atomistic level and

a more precise explanation may be generated working microscopically. A considerable effort is being made to find a generalised theory based on atomistic mechanisms.

White and coworkers (4) report two possible effects of solute segregation on grain boundary decohesion. In case(a), the solute segregates much more strongly to the free surface than to the grain boundary and causes embrittlement whereas in case(b) the solute segregates more strongly to grain boundary, giving rise to the increased grain boundary cohesion. They found that (61) S (case a) and B (case b) segregation in $Ni_3Al$ conforms to this prediction.

Explaining the effect of substitutional third elements and alloy stoichiometry on the brittleness of $Ni_3Al$, Takasugi et al. (62-64) conclude that the degree of intergranular brittleness is related to the valency difference between constituent atoms in the alloy. The discrepancies that were observed in the ranking of brittleness as a function of these valency differences were attributed to the additional effect of atomic size differences. The structural features of the grain boundaries were incorporated into the argument.

Attempts have been made to rationalize the effect of segregant on the basis of characterstic of chemical bond. Eberhart et al. (65) have addressed the issue of

embrittlement of Ni by S considering the directionality of the bonds (Ni-Ni, Ni-S, S-S) at the grain boundary of Ni. They conclude that the presence of S-S bonds facilitates electron transfer that drives the fracture process.

In a series of publications, Farkas et al. (66-69) have analyzed the structural features of ordered grain boundaries and arrived at a conclusion that these boundaries are inherently weak and segregation of impurities is not responsible for the embrittlement. However they do not provide any argument for the beneficial effect of some impurities.

A number of investigations are underway and in the present state of understanding their applicablity is limited to particular systems. Application of results of atomistic calculations to real grain boundaries are complicated and cumbersome. Also their predictive capablities have not been evaluated systematically.

## 2.3 DUCTILIZING INTERMETALLICS

Many strongly ordered intermetalic compounds have excellent physical and mechanical properties which make them potentially useful for structural applications. For example, some intermetalic compounds show an increase of yield strength with increasing temperature, accompanied

with good structural and chemical stablities. Kao et al. (70) have reported high temperature strength of ordered $Ni_4Mo$ and their results are summarised in Fig. 2.8.

However, it is well known that the intermetallic compounds are usually very brittle, particularly at low temperatures. Therefore, they are difficult to fabricate into useful shapes and have not seen practical uses. The fracture in most intermetallic compounds occurs along high angle grain boundaries.

Factors, inherent to crystal lattice, which may lead to the brittle failure of intermetallics include a limited number of easy slip systems, a large slip vector and restricted cross slip. However, the fact that a number of intermetallic single crystals show considerably high ductility rules out these factors as the only reasons for their brittleness.

Segregation of impurities to grain boundary, which has been traditionally applicable to metals and alloys, is another possible mechanism and was discussed in section 2.2. However, brittleness was observed in $Ni_3Al$ and $Ni_3Si$ where the grain boundary was found to be clean by Auger Electron Spectroscopy measurements (71,72). A recent study concerning intergranular fracture mechanisms suggests that grain boundary fracture directly relates to the structure and bond environment of the grain boundary itself (73). Another argument proposed is that the difficulty of slip

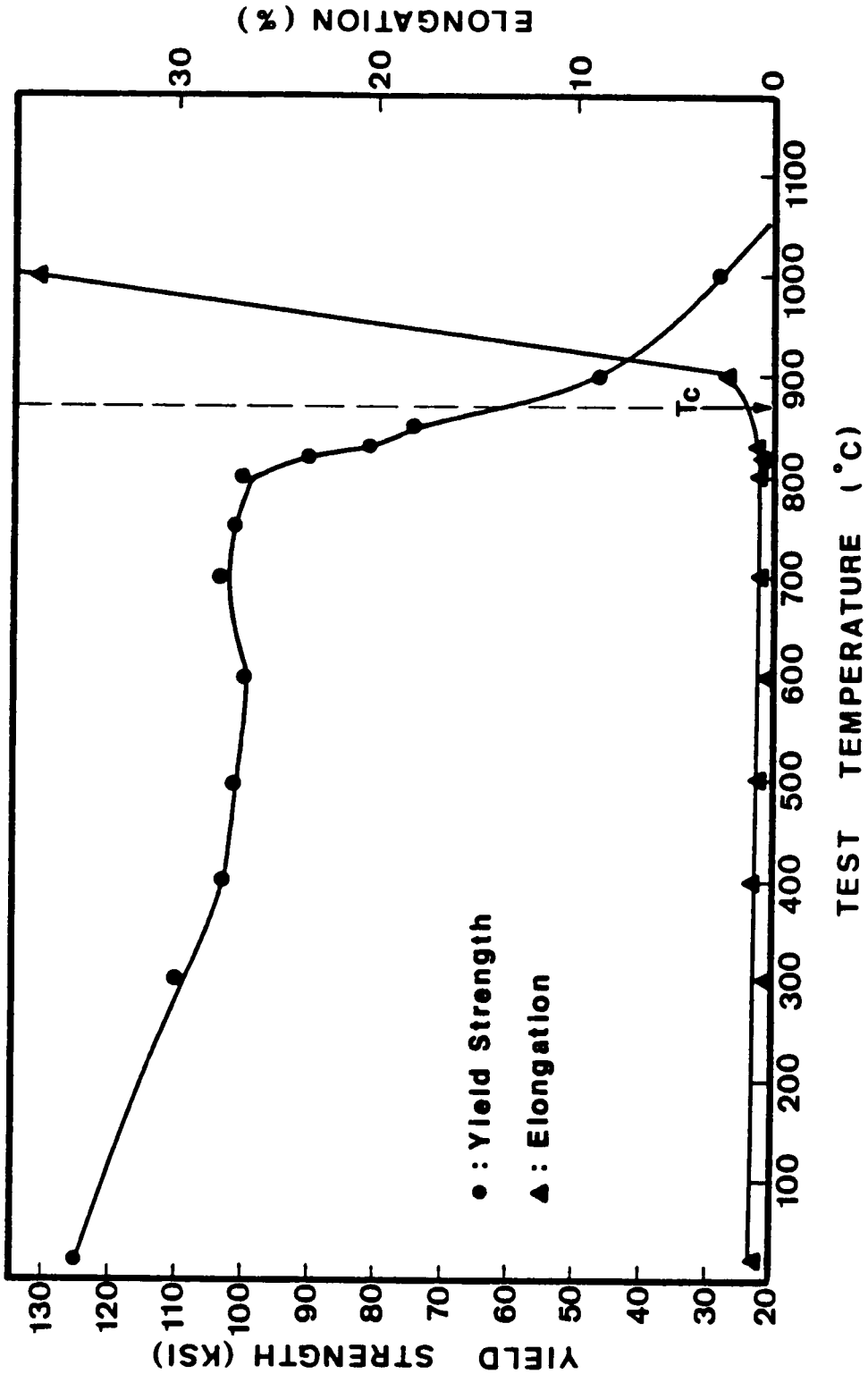


Figure 2.8 Yield strength and elongation as a function of test temperature for ordered $Ni_4Mo$. $T_c$ denotes the critical temperature of 868°C. (Ref. 70)

propagation across grain boundaries leads to stress concentrations which results in intergranular brittle fracture (74-76).

In the present state of understanding, the exact mechanism of intergranular fracture is not known. However, various attempts to improve ductility of intermetallics have produced interesting results and provide a clue to an experimental approach in solving the problem. A review of these experimental techniques is presented here which will be utilised in designing our experimentation of attempts to ductilize ordered $Ni_4Mo$.

Microalloying

Mircoalloying involves control of composition by the addition of minor concentrations (in ppm range) of elements. Two types of microalloying additions (dopants), depicted schematically in Fig. 2.9, have been used to improve the ductility of intermetallics. Type I dopants are scavengers of harmful impurities from grain boundaries. Type II dopants enhance grain boundary cohesion by altering the atomic bonding characterstics at the grain boundaries.

Small additions of boron to $Ni_3Al$ increase the room temperature elongation from 0 to over 50% (3,4) and changes the fracture mode from wholly intergranular to a mixture of intergranular and transgranular. Boron is known

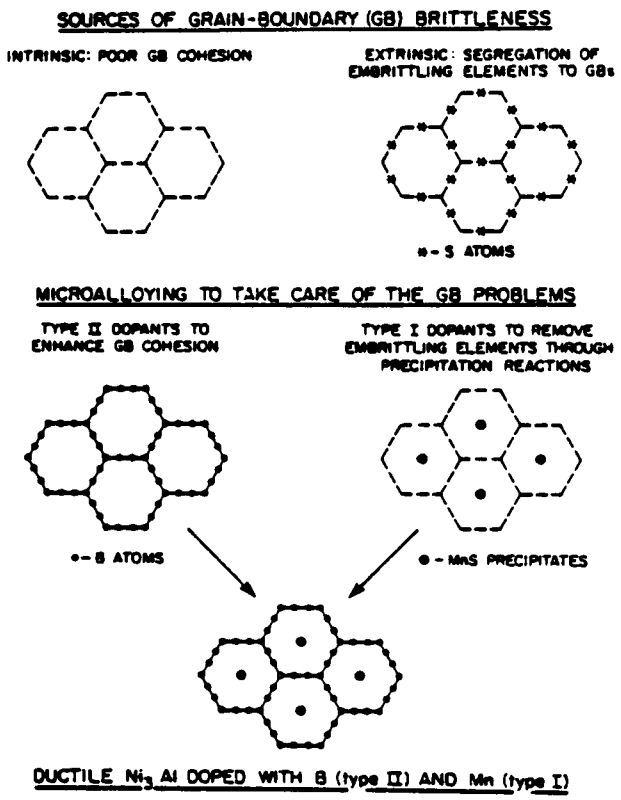


Figure 2.9 Design of ductile $Ni_3Al$. (Ref. 4)

to segregate to grain boundaries in $Ni_3Al$ (4,77,78) and promotes nickel enrichment (aluminum depletion), effectively disordering the grain boundary (79). This eliminates intergranular fracture by either easing slip transmittal (75), improving the cohesive strength of the grain boundary (4), or a combination of both. Choudhury et al. (80) have made an excellent presentation of the role of boron in $Ni_3Al$.

Boron has also been used to improve the room temperature ductility of isostructural intermetallics $Ni_3Ga$ (64,81,82), $Ni_3Si$ (64,81) and $Ni_3(Si,Ti)$ (83). Again this boron-induced ductility improvement works better with increasing nickel-rich deviation from stoichiometry (e.g. for $Ni_3Ga$ (64), tensile elongation is 11, 19 and 28% for 75, 76 and 77at% Ni, respectively). Boron addition to FeAl (84) did not appear to improve ductility but did change the fracture mode from intergranular fracture to transgranular cleavage.

It appears that for microalloying to improve ductility, the intermetallic must first have sufficient slip systems for plastic flow and that the microalloying element must also segregate to the grain boundary.

Macroalloying

Macroalloying (i.e., alloying additions greater than about 1 at% ) may be used in several ways: to change the crystal structure to one of higher symmetry and/or small unit cell size, to promote the operation of different additional slip systems, to change electron-to-atom ratio, to produce a second phase, or to make the alloy susceptible to a (stress-induced) phase transformation.

Excellent ductility has been realized in $(Co,Fe)_3V$, $(Ni,Co,Fe)_3V$ and $(Ni,Fe)_3V$ (85,86) using macroalloying. In these systems macroalloying brings about a change in the crystal structure of the alloy from hexagonal to ordered cubic, which permits operation of a larger number of slip systems, and a change in electron-to-atom ratio. While other intermetallics may respond to this solution, it is unlikely to be successful if applied to cubic crystals structures which are brittle.

Macroalloying can be used to produce a finely dispersed second phase with the aim of promoting slip homogenization (87) and, hence, reducing local stress concentrations. Seybolt (88) used mechanical alloying to add fine dispersions of $Al_2O_3$, $Y_2O_3$ and $ThO_2$ to NiAl and $Al_2O_3$ to FeAl and found that the low temperature ductility problem was exacerbated. While this approach is unpromising for an intermetallic such as NiAl in which the fine dispersion is unlikely to affect the lack of

sufficient slip systems, it can not be ruled out as a viable technique for intermetallics with suficient slip systems, as long as processing techniques are carefully controlled.

It may be possible to use macroalloying to favor a stress-induced transformation to a martensite structure. The B2 alloy NiTi is ductile at room temperature and this ductility has been ascribed to such a transformation (89). It is argued that the martensitic transformation relieves stress concentrations at grain boundaries before the intergranular fracture stress is reached.

Thermomechanical Treatment

Thermomechanical treatment involves subjecting material to a combination of plastic deformation and heat treatment. Many intermetallics are disordered at higher temperatures (above $T_c$) and this disordered structure can be retained at room temperature by water quenching. The disordered structure can be cold worked considerably (the structure resulting from cold working of quenched disordered structure will be referred to as 'prior cold worked' structure in subsequent discussions) before subsequently ordering by annealing at higher temperature (below $T_c$). It has been recently reported that prior cold work can increase ductility of ordered alloys with superstructures such as $L1_2$ (90), $L1_o$ (91), B2 (92).

However, information provided in these papers is not sufficient to conclude that this will be an effective way of ductilizing ordered intermetallics. Akoi and Izumi (90) cold deformed and recrystallized a single crystal of high purity $Ni_3Al$. The polycrystalline $Ni_3Al$ so obtained was found to give a tensile elongation of 15% compared to almost nil elongataion of conventionally processed polycrystalline $Ni_3Al$. According to Kawahara (92), an increase in tensile elongation up to 15% was observed in a prior cold worked, ordered FeCo-2V alloy. However, ductility was found to decrease with increasing time at the ordering temperature for the duration investigated (up to 16 hours). While there is considerable gain in ductility over the undeformed condition the possiblity of the ductility dropping to a practically insignificant value for a longer time at the ordering temperature can not be ruled out.

The problem of ductilizing intermetallics must be viewed with high temperature application in mind. An effect achieved must not deteriorate with time at high temperatures. Again this approach of thermomechanical treatment, even if successful, may not be very promising for applications requiring fabrication by welding but it will certainly contribute a great deal to the understanding of this poorly known subject.

An interesting question arises in this regard- "whether a cold deformed, disordered structure recrystallizes during annealing below $T_c$?". The available information concerning this effect is in many cases inconsistent. Greenberg et al. (93,94) have documented the inconsistencies and have discussed recrystallization features of ordered alloys with respect to dislocation structure in various superlattices, e.g., $L1_0$, $L1_2$, B2.

A detailed study of the ordering and recrystallization for FeCo-0.4%Cr alloy revealed the existence of three temperature intervals below $T_c$ where prior cold worked alloy exhibited different behavior (95,96); this is schematically represented in Figure 2.10. At a temperature immediately below $T_c$ the alloy recrystallizes, then orders. As the temperature is decreased, recrystallization does not occur (with annealing time of about 100 hours),but ordering does; finally recrystallization is observed again over a lower temperature interval, followed by ordering. According to Vidoz et al. (97), a prior cold worked $Ni_3Fe$ alloy does not recrystallize at $T<T_c$; at the same time an alloy of non stoichiometric composition, which is incapable of being ordered, recrystallizes at these temperatures. CuAu is reported to recrystallize (98) during ordering without

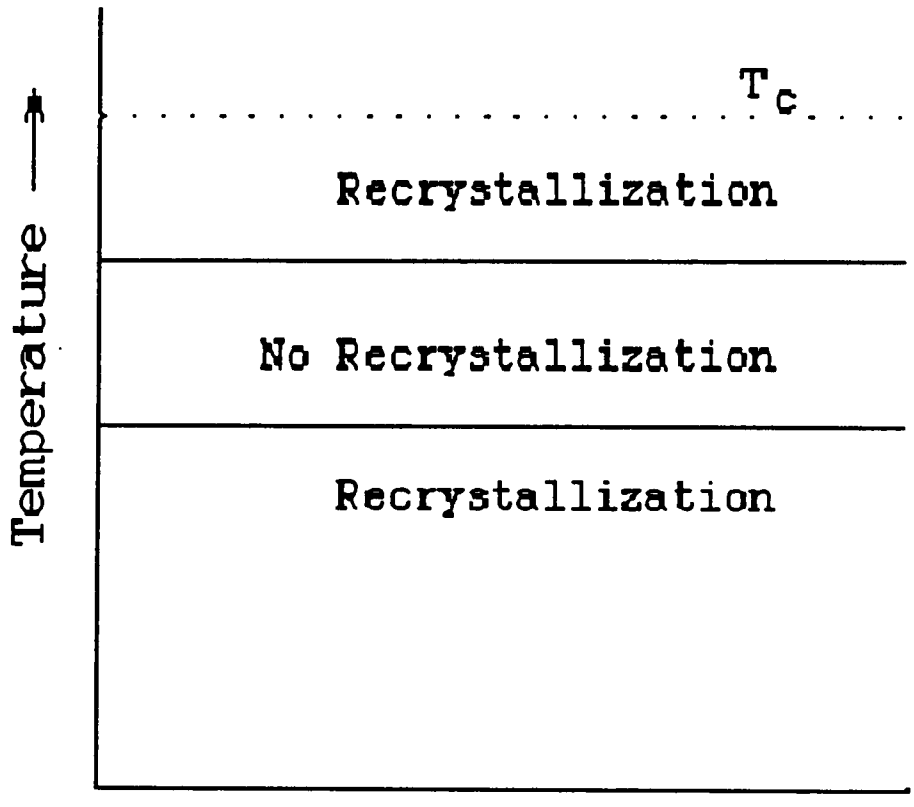


Figure 2.10 Schematic representation of recrystallization behavior of prior cold worked Fe-50Co-0.4%Cr.

any prior cold work; however, Zemtsova et al. (99) recently observed no recrystallization in CuAu without prior cold work.

From the results of work described above, it appears that when a prior cold worked structure aged below $T_c$ orders, recrystallization and grain growth almost stops. This fact can be utilized to develop a very fine grain structure. The grain refinement should improve the ductility of ordered intermetallics. The theoretical basis and experimental evidence for this is discussed in the next section on rapid-solidification.

Besides this, a careful control of ordering and recrystallization, e.g.,

1) recrystallization followed by ordering,
2) recrystallization preceeded by ordering, or
3) recrystallization and ordering simultaneously,

may favorably alter the state of stress at high angle grain boundaries which might result in ductility improvement.

Rapid Solidification

Rapid solidification can be used to produced very fine grain sizes in ordered intermetallics, and this should increase the ductility. Schulson (100) suggested that for NiAl a critical grain size exists below which cracks nucleated are stable. It was proposed (101) that

below a critical crack size the stress required to nucleate cracks is less than the stress to propagate them. NiAl with grain size below 20$\mu$m was found to show a ductility up to 40% at 400$^{o}$C (102). The variation of ductility in NiAl with grain size (103) is shown in Fig. 2.11. It was argued (103) that stable microcracks allowed the initial elongation (say 5%), and the subsequent extensive ductility could have been the result of activation of additional slip systems at higher stress. Also in structures with sufficient slip systems, individual grains can deform as single crystals without being constrained by a grain boundary, since the grain boundaries are cracked. Fine grain size also leads to slip homogenization and thereby greater ductility.

Rapid solidification also leads to better alloy homogeneity and cleaner grain boundaries. However the principal drawback of this process is that the material must be consolidated in some useful form.

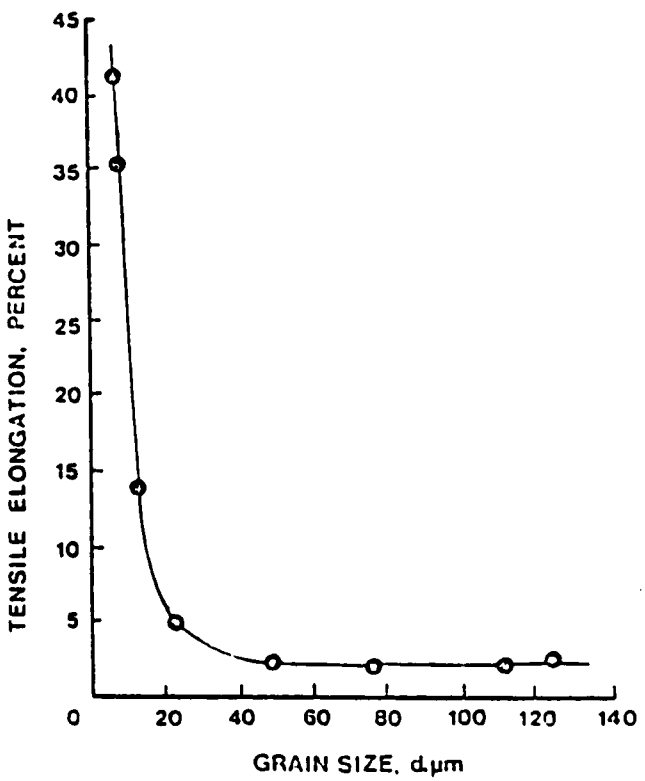


Figure 2.11 Tensile elongation as a function of grain size for NiAl at 400°C. (Ref. 103)

# CHAPTER 3

## EXPERIMENTAL METHODS

The experimentation was aimed at studying the following aspects of embrittlement in ordered $Ni_4Mo$:

I. The fracture process and its relation to microstructural features, degree of ordering, etc.

II. Attempts to ductilize it by various processing techniques:

A. Microalloying

B. Thermomechanical Treatment

III. Investigating the role of welding in inducing ordering and consequently embrittlement in some $Ni_4Mo$-based commercial alloy components (to be used in disordered condition).

Different sets of experiments were conducted for the studies described above and these experiments will be referred to as Fracture in Ordered $Ni_4Mo$, Ductilizing Ordered $Ni_4Mo$, and Ordering in Hastelloy B-2 in subsequent discussions.

## 3.1 FRACTURE IN ORDERED $Ni_4Mo$

A high purity Ni-Mo alloy containing nominally 19.97 at.% Mo was fabricated in the form of a plate about 3 mm x 5 mm x 20 mm long. To develop an appropriate $\alpha$ grain size for revealing the migrated boundaries upon aging, the alloy was heated for 1800 s at 1250°C, then cooled in about 1200 s to 1000°C, then water quenched. The sample was cooled to 1000°C before quenching because quenching directly from 1250°C resulted in quench cracks in samples, even in the $\alpha$ condition. It was then aged at 727°C for 720 h, which developed a structure of fine domains within the former $\alpha$ grains and with the high-angle boundaries just beginning to migrate. One side of the plate was metallographically polished then etched to reveal the migrated boundaries. The sample was then loaded in a three point bending device till cracks were visible in an optical microscope. The three point bending device used is illustrated in Fig. 3.1. The sample was examined with a scanning electron microscope (SEM) to determine the crack propagation direction relative to the microstructural features. Regions were photographed, the sample loaded additionally to advance the cracks, and the sample again observed in the SEM. Finally the sample was broken into two pieces and it was observed in SEM at approximately 45° so that metallographic and fracture surface could be examined simultaneously.

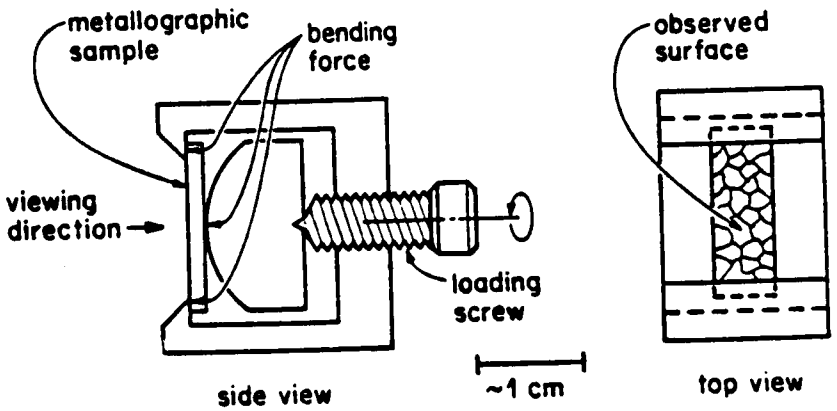


Figure 3.1 Schematic diagram of the three-point bending device used to initiate cracking in the alloy.

## 3.2 DUCTILIZING ORDERED $Ni_4Mo$

### A. Microalloying

Nine alloys, containing different alloying elements, were prepared. The alloy designations, corresponding compositions are tabulated in Appendix A. The alloys were prepared from $Ni_4Mo$ of the composition listed in Table 3.1. 10-15 grams of each alloy were melted in water cooled, copper hearth, electric arc furnace under a constant flow of argon. To limit contamination from air the furnace chamber was first evacuated and then purged with argon four to five times before a constant flow of argon was established. The alloy buttons were inverted and remelted twice to ensure homogeneity. In case of high melting point alloying additions, a master alloy was made with approximately 15% alloying element and this master alloy was used as alloying element addition.

The alloy buttons were cold rolled to break the cast structure, with intermediate anneal in argon at 1000°C for 30 minutes. The alloys were then encapsulated in argon-filled silica tubes and homogenized at 1100°C for 120 h, then quenched by breaking the capsules in water to retain the disordered structure. To obtain a fine grain size, the buttons were again cold worked and annealed at 1000°C for 30 minutes, then quenched.

Table 3.1 Chemical composition (weight%) of alloy used for microalloying and thermomechanical treatment.

| Element | Wt % |
|---|---|
| Al | < 0.02 |
| C | < 0.002 |
| Ca | < 0.1 |
| Cr | < 0.1 |
| Cu | 0.01 |
| Fe | 0.11 |
| Mn | 0.02 |
| Mo | 28.5 |
| Ni | 70.65 |
| Si | < 0.02 |
| V | < 0.01 |
| W | < 0.1 |
| Zr | 0.01 |

A thin slice was cut from each alloy and subjected to an ordering treatment at 725°C for 4 hours. Each slice was then put in a vice and broken with pliers. The fracture surface was examined in a stereo optical microscope. This was the only test performed on these alloys.

B. Thermomechanical Treatment

A preliminary investigation of this experiment was conducted on alloys NMCRO and NMCR6 for which the compositions are tabulated in Appendix B. The method of preparing and processing of these alloys has been described by Vasudevan (104). The samples were received in (i) the cold worked condition, and (ii) the cold worked and aged at 700°C for 480 minutes condition. The preliminary work involved optical metallography, microhardness measurement and fracture surface examination for samples aged at 700°C and 850°C for different times. Following the results of this investigation a more structured experiment was conducted on an alloy of different composition and this experiment is described below.

The alloy of composition listed in Table I was machined to a 1.9 cm diameter rod and then swagged with intermediate anneal at 1000°C so as to obtain rods of final diameter 0.3 cm and cold worked to 80% reduction in area (RA), 68% RA and 43% RA. These cold worked rods were

cut into approximately 0.5 cm long pieces and subjected to various aging treatments. Aging temperatures of 700°C, 775°C, 850°C, and 885°C were used. The aging time for 700, 775, and 850°C was 1, 3, 5, 7, 10, 30, 60, 150, 300, 600, and 1200 minutes. Aging for 1, 3, 5, 10 and 30 minutes was done at 885°C. The aging treatments for time up to 30 minutes were conducted in a salt bath furnace.

Optical Metallography and Hardness Measurement

The aged specimens were mounted in bakelite in such a way so as to observe the transverse surface metallographically. The transverse surface was obtained by grinding off one half of the sample after mounting. The mounted samples were polished with rough grinding wheels (1200 and 600 micron) and subsequently polished with polishing cloth using 9.0, 1.0 and .06 micron alumina powder.

Hardness measurements were made on polished surfaces using a Tukon Hardness Tester with a 5 Kg load. Three impressions were read and averaged to yield a Diamond Pyramid Number, DPH. (Hardness calibration blocks were not tested, so the reported hardness values are only approximately absolute. They are correct relatively.)

For metallographic examination the etchant used was a mixture of one part solution of $CrO_3$ and three parts 20% HCl. The $CrO_3$ stock solution was prepared by mixing 30 gms of $CrO_3$ with 300 ml of water.

## 3.3 ORDERING IN HASTELLOY B-2

Eight samples, cut from varous components which had been in service at Tennessee Eastman Co., Kingsport, were supplied for the examination. The following experiments were conducted.

### Surface Examination

The surface of samples were examined for presence of cracks under a stereo optical microscope. Pieces were cut from sample F and G shown in Fig 3.2. These pieces were put in SEM to examine the surface at higher magnifications. Some samples, including sample H, were inadvertently cleaned using 20% HCl. However on comparison with uncleaned specimens, it was observed that chemical cleaning did not affect the appearance of the surface.

Figure 3.2 Optical macrographs showing samples in as-received condition a) Sample F b) Sample H.

Bend Test

Pieces from the same samples containing surface cracks were cut from relevant portions on the basis of results of the surface examination and machined from one side (non-crack side) to reduce the thickness to 0.4 cm. These were then bent by 60, 120 and 180 degrees and examined in SEM after each bend to follow up the opening of cracks.

Metallography and Hardness Measurement

Pieces were cut from samples F and G, mounted with epoxy resin and polished using the method described earlier for hardness measurement and metallographic observation. The through-thickness surface was examined.

# CHAPTER 4

## RESULTS AND DISCUSSIONS

The results of this work are discussed in three different sections: Fracture in and Ordered $Ni_4Mo$, Ductilizing Ordered $Ni_4Mo$, Ordering in Hastalloy B-2.

### 4.1 FRACTURE IN ORDERED $Ni_4Mo$ (also published in references (106) and (107))

The fracture in ordered $Ni_4Mo$ occurs along the former $\alpha$, high angle grain boundaries. Therefore, it is obvious that the grain boundary structure and chemistry plays an important role in the fracture process and should be carefully studied in order to develop an understanding of brittle fracture. The effect of aging (below $T_c$) on the fracture surface appearance has been reported by Kao (105). Fractographs (after Kao) of tensile specimens for different aging times at $725^0C$ are presented in Fig. 4.1.

In the as-quenched, SRO, $\alpha$-structure condition, fracture occurs by void coalesence, as shown by the dimpled structure in Fig. 4.1a. Aging for one minute produces no change in fracture mechanism (Fig. 4.1b). However, aging for 3 minutes produced a marked change in fracture surface topology (Fig. 4.1c); some intergranular fracture has occurred. Aging for 10 minutes produces a

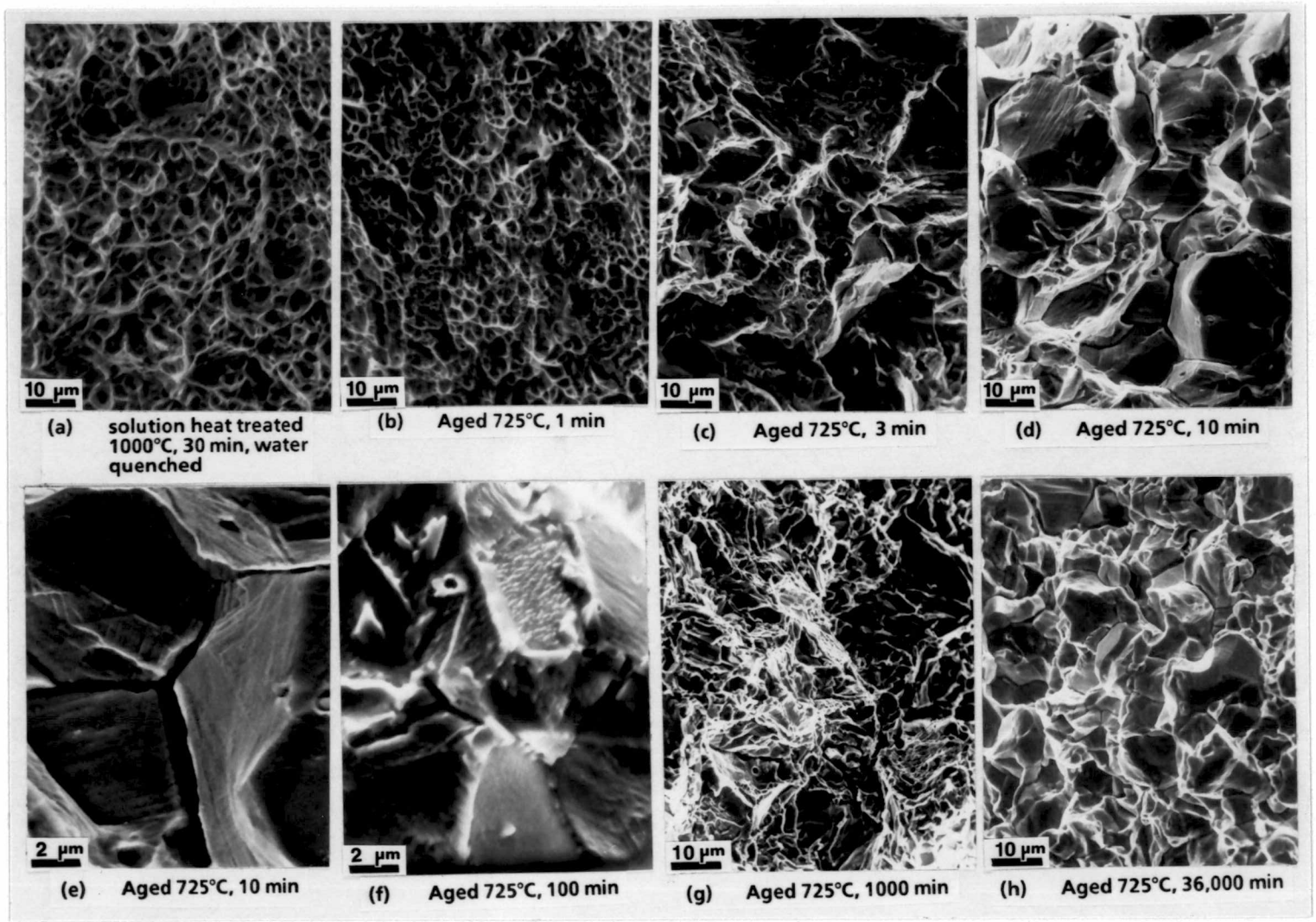


Figure 4.1 Fractography of tensile samples aged at 725°C.(Ref. 105)

fracture surface topology which is essentially completely intergranular and fracture is along the high angle, former α-boundaries (Fig. 4.1d). In the sample aged 100 minutes, the fracture surface undergoes a change. There is still the appearance of intergranular fracture (Fig. 4.1f), but the surface is not as smooth as for the shorter aging times (Fig. 4.1e). Aging for 1000 minutes produced a fracture topology even finer (Fig. 4.1g). There is no evidence of dimples, but the fracture surface is quite uneven. Aging for 36,000 minutes produced a fracture surface which is more intergranular in appearance (Fig 4.1h), but these features are finer than that for short aging times (Fig. 4.1d) The transition in fracture surface topology was suspected to have a relation to microstructural changes occurring during aging (See Fig. 2.7). The following discussion will confirm that the finer fracture topology at long aging periods is associated with fracture along migrated grain boundaries.

Fig. 4.2 shows regions illustrating the migrated boundaries. Note that the position of the original, straight boundary, prior to migration, can be clearly seen. Also note that the regions inside the grains show little contrast with the etchant used, even though the structure consists of very fine domains. Fig. 4.3 shows at low magnification the structure after deformation sufficient to show cracking.

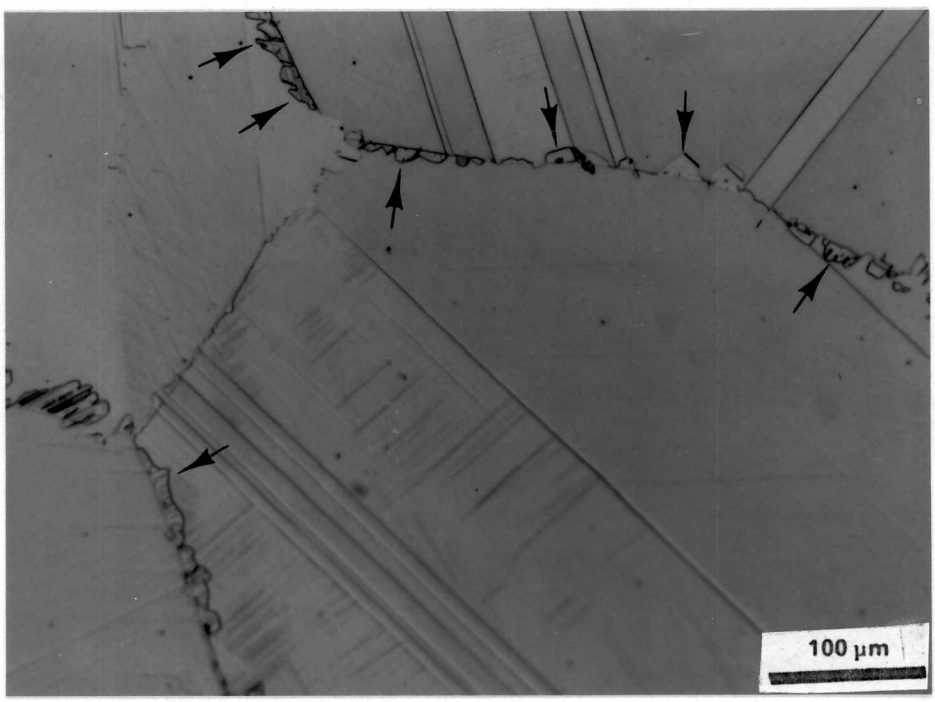


Figure 4.2 Examples of migrated boundaries (arrows) in ordered $Ni_4Mo$ (optical micrograph).

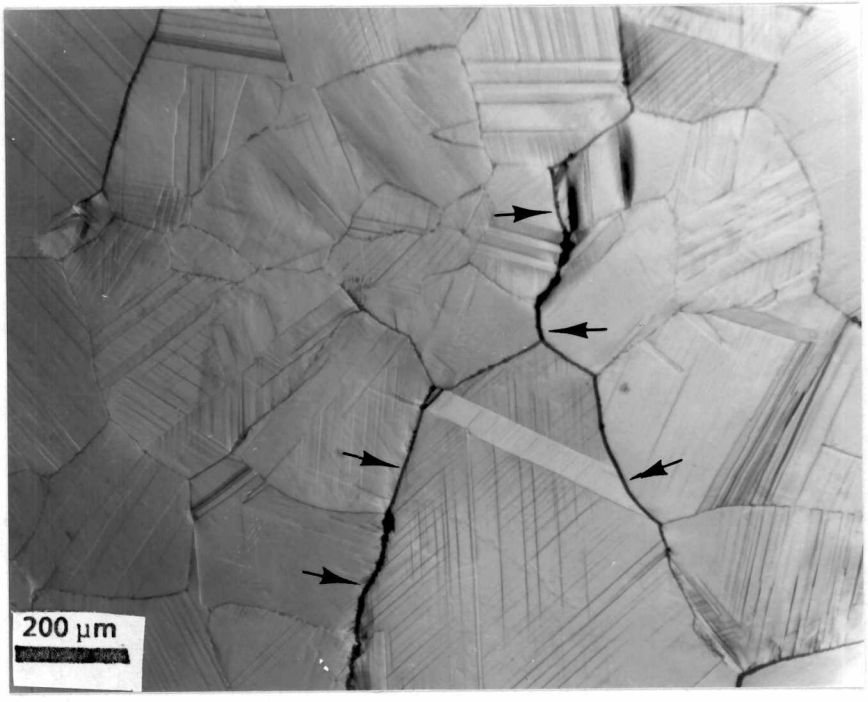


Figure 4.3 The metallographically etched surface after sufficient bending to initiate cracks (arrows). Note the slip traces in all the grains.

Since the etchant not only revealed the position of the migrated boundary but also the location of the boundary before migration (see Fig. 4.2), the relation of the crack path relative to these two locations could be observed. Examples which clearly show that cracking occurred along the migrated boundaries are shown in Fig. 4.4 and Fig 4.5.

Although the ductility is low, clear evidence of slip is seen on both the fracture surface and on the metallographically polished surface (Fig. 4.3). Slip traces on the fracture surface of a sample aged for short times having no migrated boundaries are shown in Fig. 4.6. They also can be seen on the fracture surface of migrated boundaries (Fig. 4.5b). The continuity between the slip traces on the fracture surfaces of the migrated boundaries and the metallographically prepared surface is illustrated in Fig. 4.7. Also note in Fig. 4.5b, 4.5c and 4.7 that on the metallographically prepared surface the same slip traces extend from the former $\alpha$ grains, which contains a fine domain structure, into the coarser domain structue which develops behind the migrated boundaries. This shows the crystallographic continuity of the domain structure as the boundary migrates.

Auger spectroscopy of the fracture surface of an ordered $Ni_4Mo$ sample has revealed sulphur concentrated along the former $\alpha$, high angle boundaries (47). Sulphur

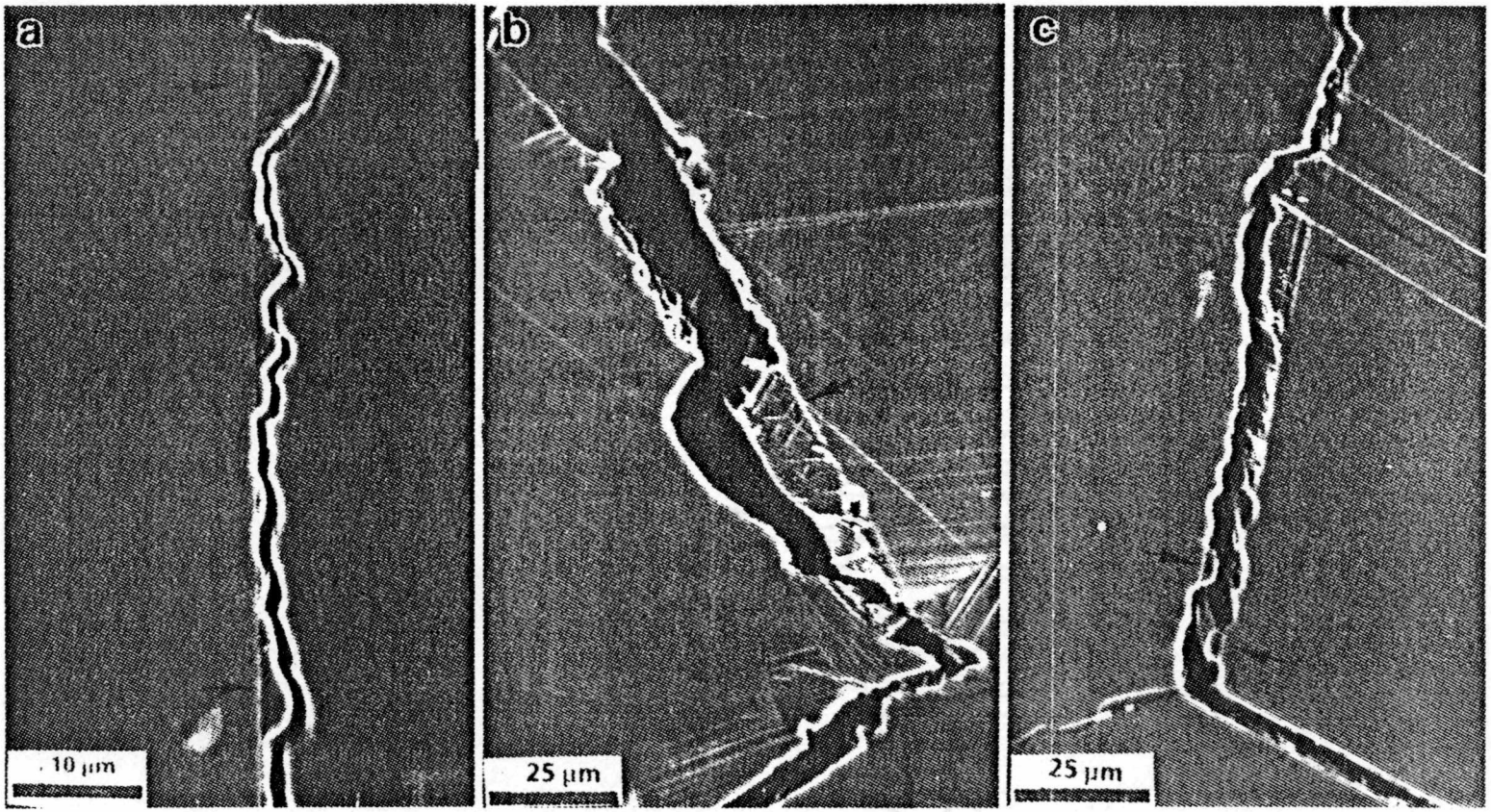


Figure 4.4 Examples of fracture along migrated boundaries in ordered $Ni_4Mo$. The arrows point out the location of the original boundaries prior to migration.

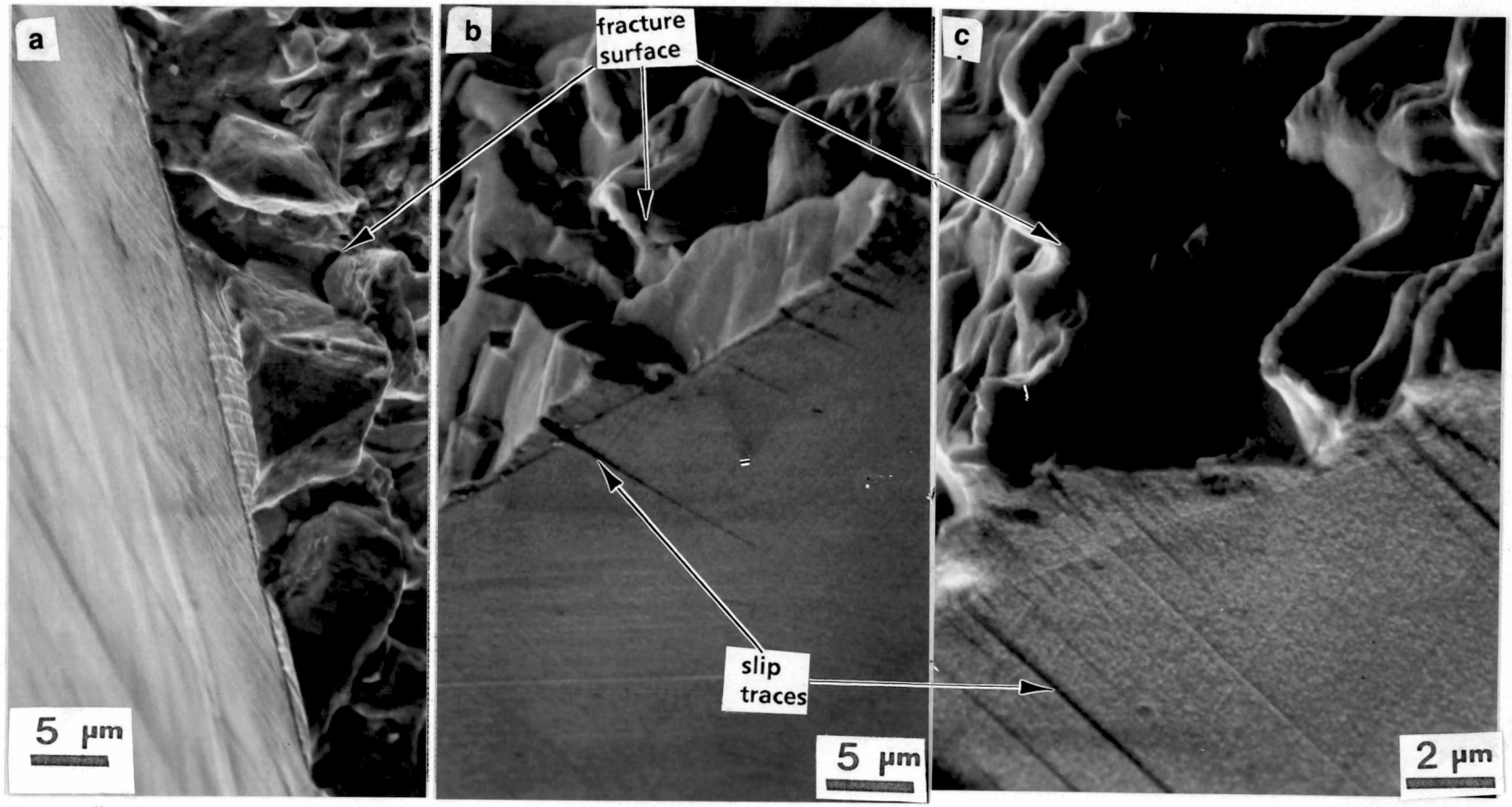


Figure 4.5 Fractographs of the intersection of the fracture surface and metallographic surface illustrating fracture along migrated boundaries.

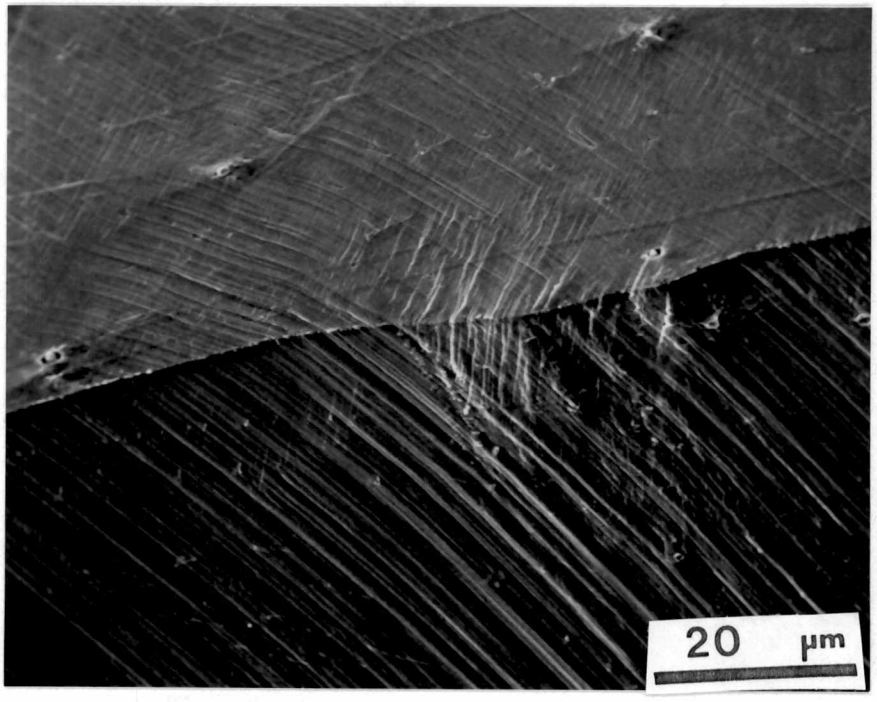


Figure 4.6 Fractograph of sample aged 210 min. at 725°C showing slip traces on the fracture surface.

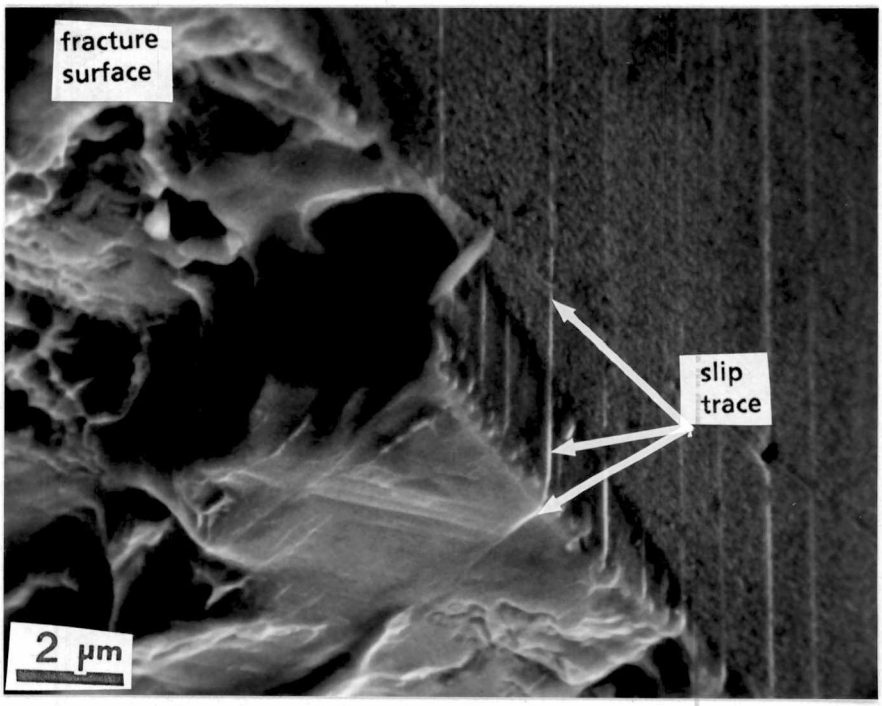


Figure 4.7 Fractograph of intersection of fracture surface and metallographic surface, showing continuity of slip traces in the original grain and region behind the migrated boundary.

was also detected on the fracture surface of a sample of the same alloy after heat treating to develop migrated boundaries. Thus it appears that the sulphur is diffusing rapidly enough during aging to maintain a high concentration at the migrating boundary. If sulphur is responsible for the grain boundary weakness, this would explain why fracture occurs along the migrated boundaries.

## 4.2 DUCTILIZING ORDERED $Ni_4Mo$

### A. Microalloying

Microalloying is known to improve ductility in certain ordered intermetallics. In this research, $Ni_4Mo$ was microalloyed with eight elements with the aim of improving ductility in the ordered condition. It should be recalled here that the melts were made in an electric arc furnace, cold worked to break the cast structure and subsequently homogenized. Following homogenizing, the alloy buttons were cold worked and solution heat treated for grain refinement. Thin slices from each button were cut and ordered at $725^0C$ for 4 hours and subjected to bending to test for ductility.

The amount of alloying additions in this work was approximately 0.1 wt.%. The samples appeared quite clean after melting. Weight losses in the process of melting were less than 0.1% except for the Zr alloyed melt. This

leads to the conclusion that there will be significant amount of retained alloying elements; however, the actual amount was not ascertained.

It is believed (4) that microalloying elements act in improving ductility by i) segregating to grain boundary and improving intrinsic strength of the boundary, or ii) by scavenging impurity elements, which cause weakening of the grain boundary, from the grain boundary.

The first kind of effect is likely to be provided by atoms of smaller size. Boron and beryllium were used as microalloying elements in this work to test this effect. Boron addition does not have any effect on the ductility of ordered $Ni_4Mo$. However, there appears to be some effect of beryllium addition. Bend tests on the alloy with beryllium addition gave a bending of approximately $15^0$ compared to almost no bending in cases of similarly treated alloys without beryllium. In this experiment the alloy contained approximately 1250 ppm of beryllium which may not be the optimum amount and it is possible that ductility can be improved by controlling the amount of beryllium addition.

Elements which were investigated to produce the second kind of effect include Hf, Zr, Ce, Nb, Mg and La. None of these elements produced any noticable change in ductility. Mn addition of the order of 1.0% was also investigated for this category of effect but was found to

have no effect. Although this amount of addition does not fall in the catagory of microalloying, it was examined here because it was added to act as scavenger for sulphur which is reported to segregate at the grain boundary in ordered $Ni_4Mo$ (47). This order of addition is commonly added in steels for scavenging sulphur.

On the basis of the above observations, further work in this area should be concentrated on investigating the effect of beryllium. This should involve exploring ductility improvement with varying amount of beryllium additions, e.g., 50, 100, 250, 500, 750, 1000, 1250, 1500 ppm. It will be interesting to determine the grain boundary concentration of beryllium using Auger Electron Spectroscopy to ensure that this element segregates to the grain boundary which is necessary in order that it improve the ductility by the first mechanism. Also, if this investigation shows an improvement in ductility, the effect of the second catagory of elements in conjuction with beryllium should be examined.

B. Thermomechanical Treatment

Thermomechanical treatment means subjecting material to a combination of plastic deformation and heat treatment. In this experiment the term will be restricted to mean cold working $Ni_4Mo$ in the disordered ($\alpha$) condition

(referred to as prior cold work) and subsequent aging below $T_c$.

This work was initiated with an aim of studying the fracture behavior of ordered $Ni_4Mo$ obtained by aging prior cold worked structure below $T_c$. In the process of fracturing an 80% prior cold worked and ordered (at $700^0C$ for 8 hours) $Ni_4Mo$ alloy (NMCRO), it was found that the alloy bent by about $15^0$ before fracturing. This is in contrast to almost no bending in the as-quenched and then ordered condition. Also, the literature survey, discussed in Section 2.3, revealed a significant ductility improvement in ordered Fe-50Co-2V alloys processed in a similar way (92). These observations led to the conclusion that prior cold work might give rise to a ductility improvement in ordered $Ni_4Mo$.

No attempt, at this stage, was made to measure ductility quantitatively. This was because of two reasons. i) The ductility achieved was not significant enough to account for time and cost involved in performing standard mechanical properties tests. ii) It was not known whether the sample tested had the same or higher long-range order parameter compared to similarly aged as-quenched samples (used for comparing bend test results), which should be established before any claim regarding ductility improvement in the ordered condition could be made. It was

thus concluded that further investigations should be made in the following stages:

1) characterizing the aging behavior of prior cold worked $Ni_4Mo$ in terms of microstructural developments and hardness changes,

2) studying the variation of long-range parameter with aging using electron diffraction or x-ray diffraction,

3) conducting non-standard bend tests and developing a qualitative relationship between the results of bend tests and microstructure,

4) designing a thermomechanical treatment to give the best ductility on the basis of results from stage (3) and testing this treatment using the non-standard bend test, and

5) performing standard mechanical properties tests if the results of stage (4) appear encouraging.

It is step 1) which was conducted in this research. Because of the time constraints, the work was limited to optical metallographic observations and microhardness measurements.

On the basis of the literature review (section 2.3), possible aging behavior (at temperatures below $T_c$) of a prior cold worked alloy in terms of microstructural development and hardness variations will be presented and used in the discussion of the results obtained for $Ni_4Mo$.

(Ordering occurs in a similar way as $Ni_4Mo$, i.e., follows a C-shaped time-temperature transformation curve for isothermal ordering.)

Cold working results in an increase in hardness and a change in other physical and mechanical properties. In an alloy with no ordering reaction, aging at sufficiently high temperature results in the formation of new equiaxed recrystallized grains and this is associated with the recovery of physical and mechanical properties to those of the undeformed condition. However, the presence of an ordering reaction at the aging temperature complicates the recrystallization process and the following possiblities exist. (In the following discussions the disordered structure will be denoted by $\alpha$ and ordered by $\beta$.):

Case 1) The cold worked disordered structure ($\alpha$) upon aging recrystallizes into strain free equiaxed $\alpha$-grains resulting in softening and this is followed by ordering and hardening. Schematic hardness variation with aging time in this case is presented in Fig. 4.8. It is assumed that commencing of ordering will inhibit grain growth thereby stopping further softening. Also since the starting structure for ordering is strain-free $\alpha$-grains, the ordering is expected to follow similar kinetics as that of the solution heat treated condition. The only difference here will be finer grain size obtained in the former case.

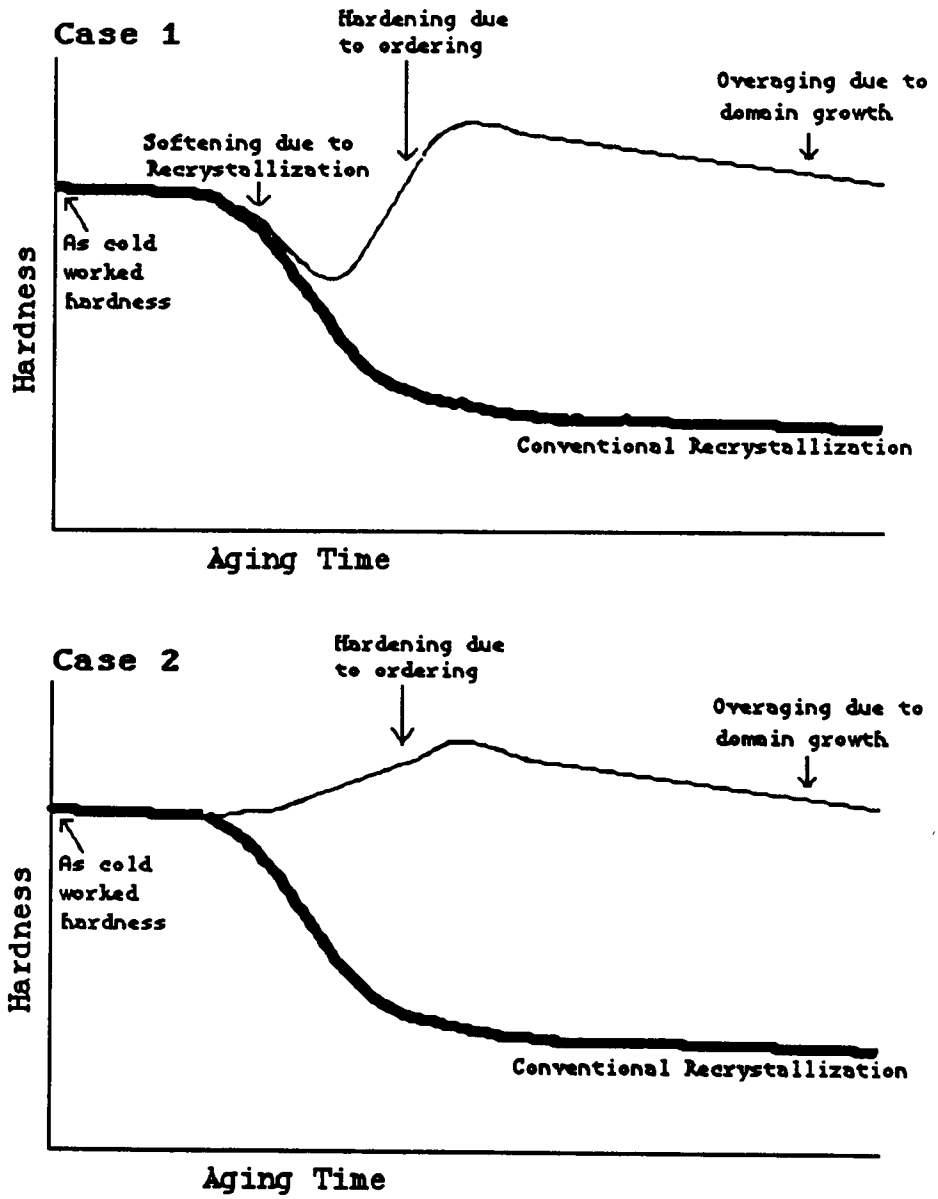


Figure 4.8 Schematic representation of various possibilities of hardness variation with aging a prior cold worked generic alloy, undergoing disorder-order transformation below melting point,at a temperature below $T_c$. All the curves are compared with a curve which will be obtained in the absence of ordering at temperature.

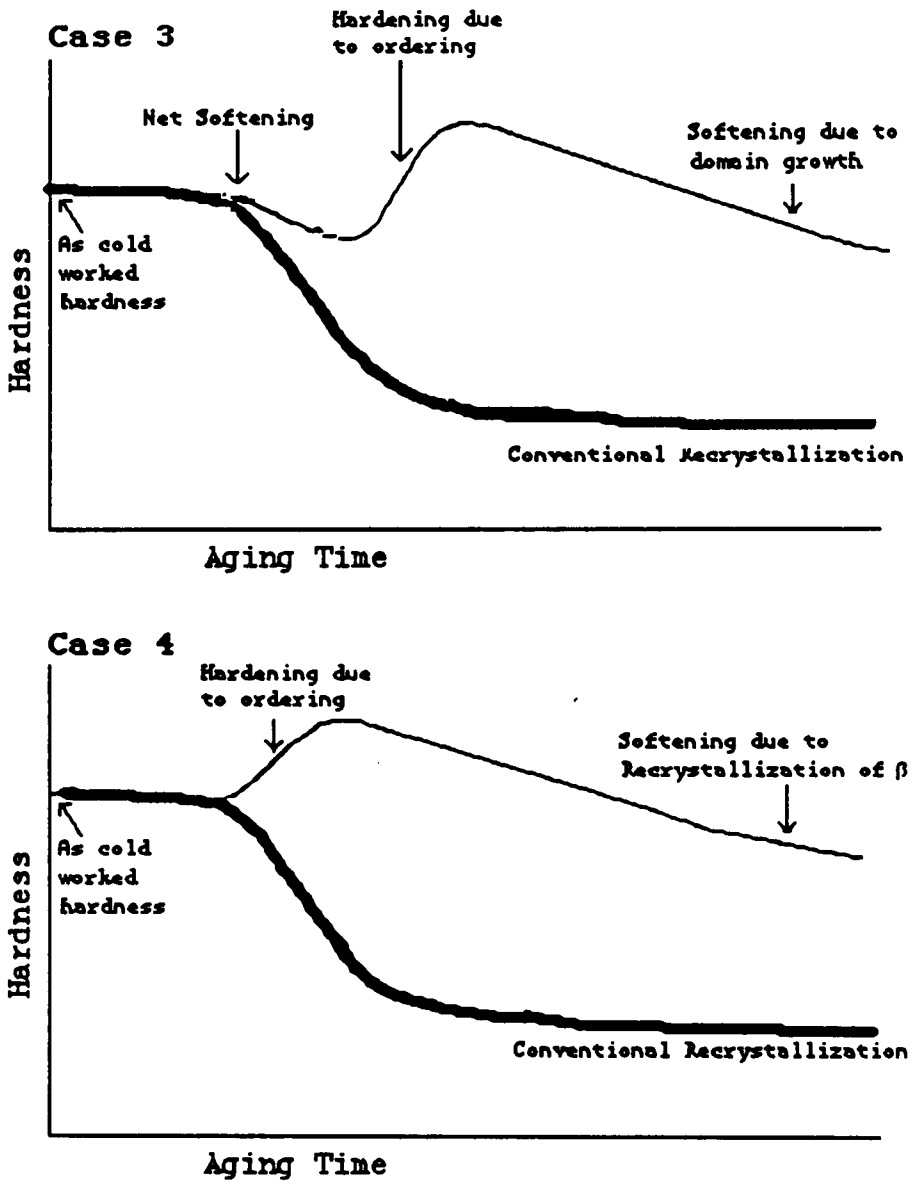


Figure 4.8 continued

Case 2) The cold worked disordered structure ($\alpha$) upon aging orders and there is no recrystallization, i.e., the only high angle boundaries are former $\alpha$ grain boundaries as in the cold worked condition. This is similar to ordering in conventional aging, except that $\beta$ has inherited a high dislocation density from the cold worked $\alpha$. Fig. 4.8 shows a schematic representation of hardness variation with aging time. No recrystallization occurs in this case and the softening is due to domain growth.

Case 3) Ordered $\beta$ recrystallizes from the cold worked structure ($\alpha$). This case is different from case (2) in the sense that now there exist high angle boundaries between strained (high dislocation density) $\alpha$-grains and recrystallized (low dislocation density) $\beta$-grains. Since this recrystallization is associated with a phase transformation, it will be termed "pseudo-recrystallization", in subsequent discussions. There are two factors to be considered here to predict the hardness variation: i) the formation of long range-order giving rise to an increase in hardness and ii) the formation of new $\beta$ grains which should relieve stresses in the cold worked $\alpha$ matrix by elimination of dislocations, leading to a decrease in hardness. It is difficult to predict the hardness variation with aging time in this case. However, from the experimental results to be discussed, it appears that the net effect at short time will be softening

followed by a hardening associated with an increase in long-range order parameter. Finally $\beta$-grain growth will result in softening.

Case 4) The cold worked structure upon aging orders which results in formation of strained $\beta$. This is followed by recrystallization and the formation of strain-free - grains from a strained $\beta$-matrix. The hardness will initially increase because of ordering and will be followed by a decrease associated with softening due to recrystallization of $\beta$. Note here that the softening rate associated with recrystallization is shown to be much slower than that in the recrystallization of $\alpha$ (case 1) based on the experimental results.

The effect of aging below $T_c$ in prior cold worked $Ni_4Mo$ has been studied in this work for three degrees of cold work: 43% Reduction in Area (RA), 68% RA and 80% RA. Ordering kinetics in as-quenched specimens follow a C-shaped curve (see Fig. 2.6), with the maximum ordering rate at about $775^0$C. Thus three aging temperatures, $775^0$C, $700^0$C and $850^0$C, were choosen for aging cold worked $\alpha$. Short time aging treatments at $885^0$C (just above $T_c$) were performed for a comparision with the response of alloy without any ordering reaction.

Fig. 4.9 shows the variation of hardness as a function of degree of cold work. Note a remarkably high work hardening rate. The microstrutural changes associated

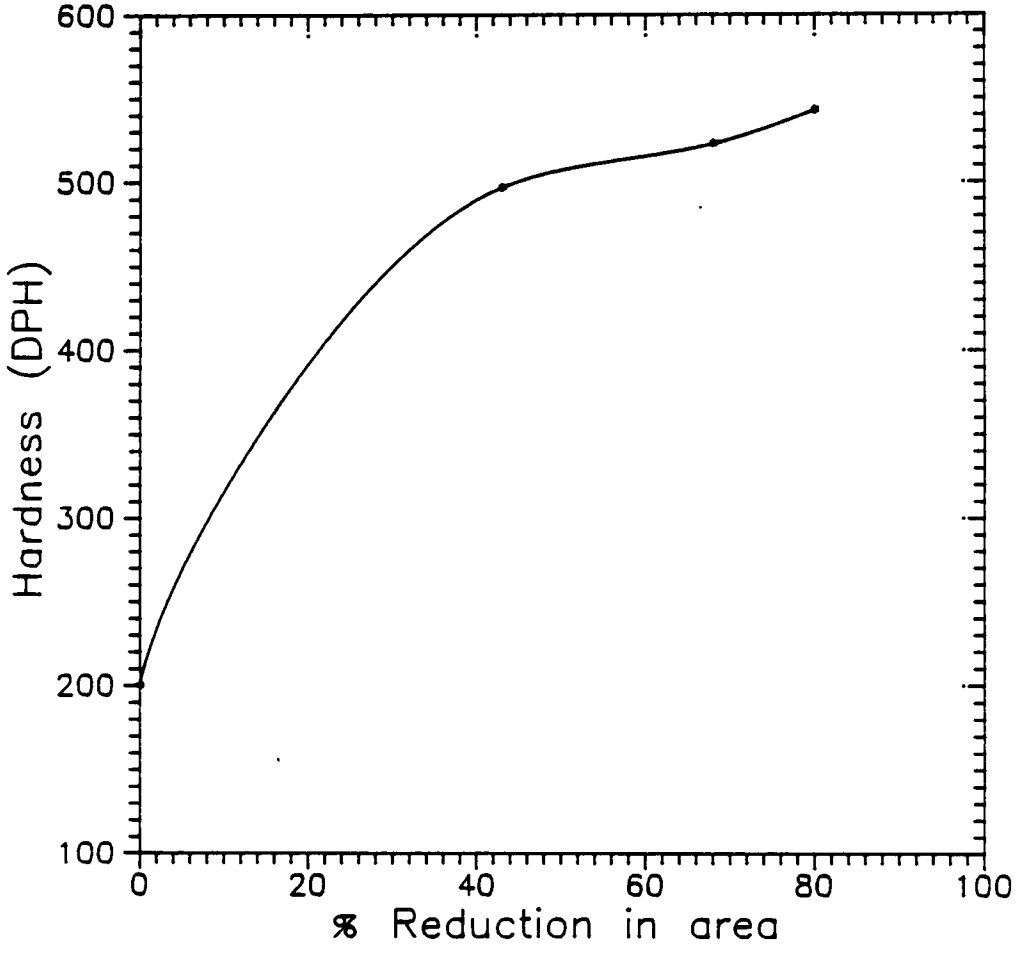


Figure 4.9 Hardness of disordered (α) $Ni_4Mo$ as a function of the degree of cold work.

with cold working are shown in Fig. 4.10. Fig. 4.10a, which is for 43% RA condition, clearly shows α-grain boundaries which becomes less clear for 68% RA (Fig. 4.10b) and almost unresolved for 80% RA (Fig. 4.10c).

The effect of aging in cold worked α at $850^0$C, $775^0$C and $700^0$C will be discussed here in two sections - i) at $850^0$C and ii) at $775^0$C and $700^0$C. This is because at $700^0$C and $775^0$C the response appears to be the same. The hardness values reported here must be taken with some reservations. The cold working was performed by swaging rods of $Ni_4Mo$. Swaging introduces a variation in degree of cold work from center to the surface. An attempt was made to restrict indentations to the center of the samples for a fair comparison. However, the possibility of certain off-center indentations exist. This, coupled with experimental error, resulted in the scattering in hardness values by about ±15 DPH. (Also some micrographs show some elongated black features. These are particles believed to be introduced during preparation of the alloy which have been elongated during the process of swagging. They were found in the as-received material.)

Effect of aging at $850^0$C

Fig. 4.11 shows the change in hardness on aging cold worked α at $850^0$C. The hardness decreases considerably till about 5 min., and then there is a slight increase,

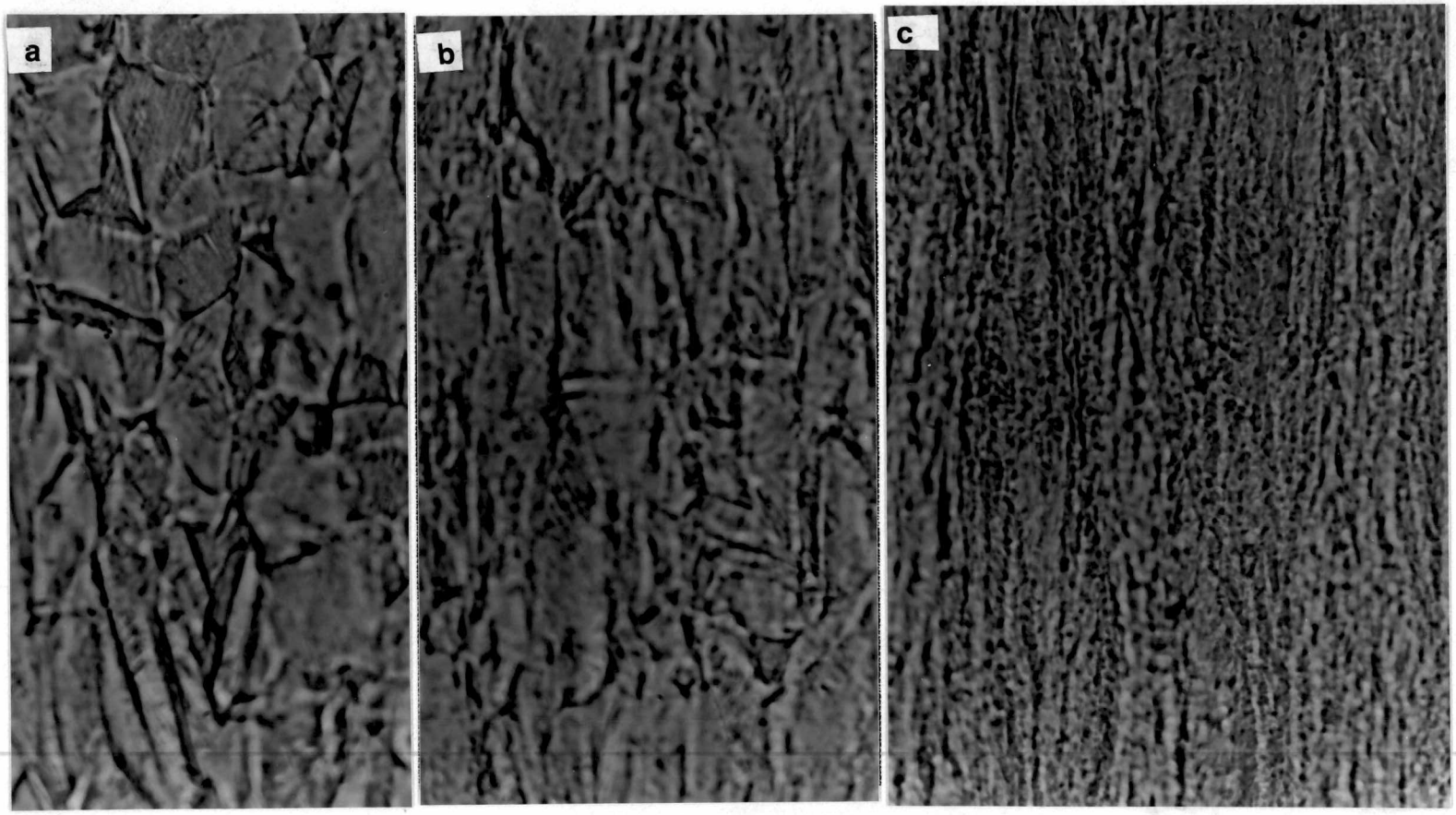


Figure 4.10 Optical micrograph showing microstructure of cold worked disordered (α) $Ni_4Mo$. a) 43% RA, b) 68% RA, c) 80% RA. 1000X

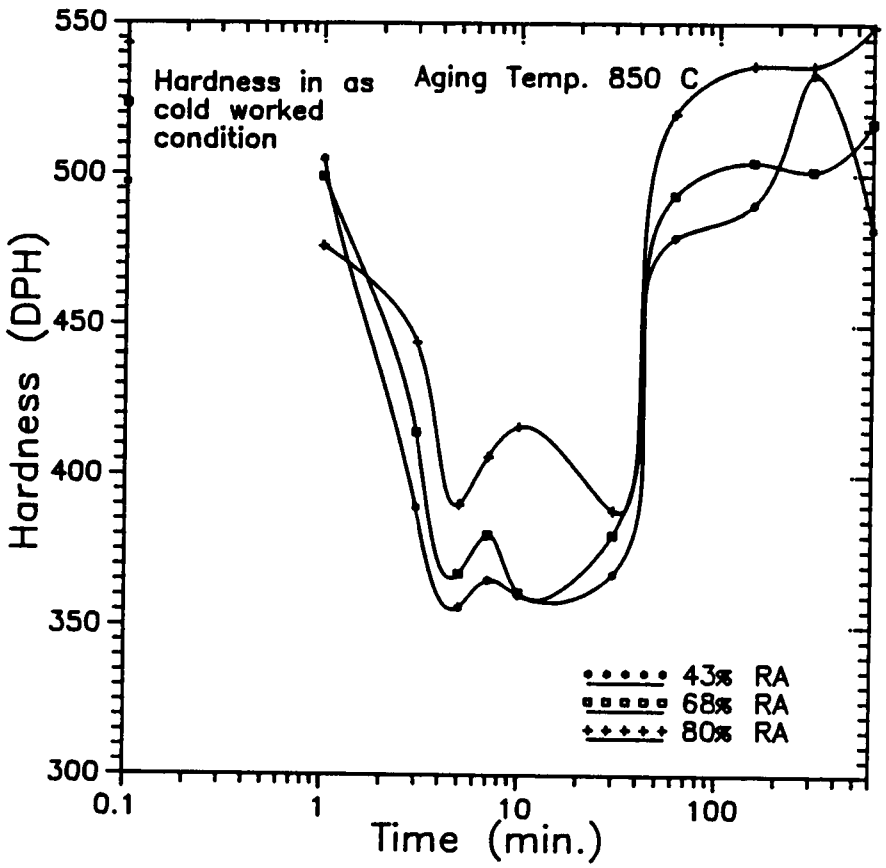


Figure 4.11 Hardness as a function of aging time at $850^0$C for prior cold worked $Ni_4Mo$.

followed by a slight decrease again and then a considerable increase in hardness from 30 to 60 minutes. The slight increase in hardness at aging times around 10 minutes does not appear to be a statistical scatter, because this effect is consistently observed in all three cold work conditions.

This variation can be accounted for in the following way. The aging for 5 minutes results in complete recrystallization of the cold worked $\alpha$ structure and thereby a decrease in hardness. This is further corroborated by metallographic examination (see Fig. 4.12). Note that the hardness level achieved (350-400 DPH) is still much above the typical solution heat treated hardness of approximately 200 DPH. The high hardness of strain-free $\alpha$ grains is probably due to very fine grain size and not because of an ordering effect. This explanation can be confirmed by a comparison with hardness values achieved (Fig. 4.13) by aging at $885^{0}$C (above $T_{c}$), a temperature where no long-range ordering will occur. At this temperature recrystallization is complete in 3 minutes (confirmed by metallographic observation (Fig. 4.14)) and the hardness level and grain size are the same as those achieved at $850^{0}$C in 5 miuntes. The faster recrystallization at $885^{0}$C is due to a higher temperature increment of $35^{0}$C. The fact that no ordering occurs in minutes at $850^{0}$C is also consistent with the fact that

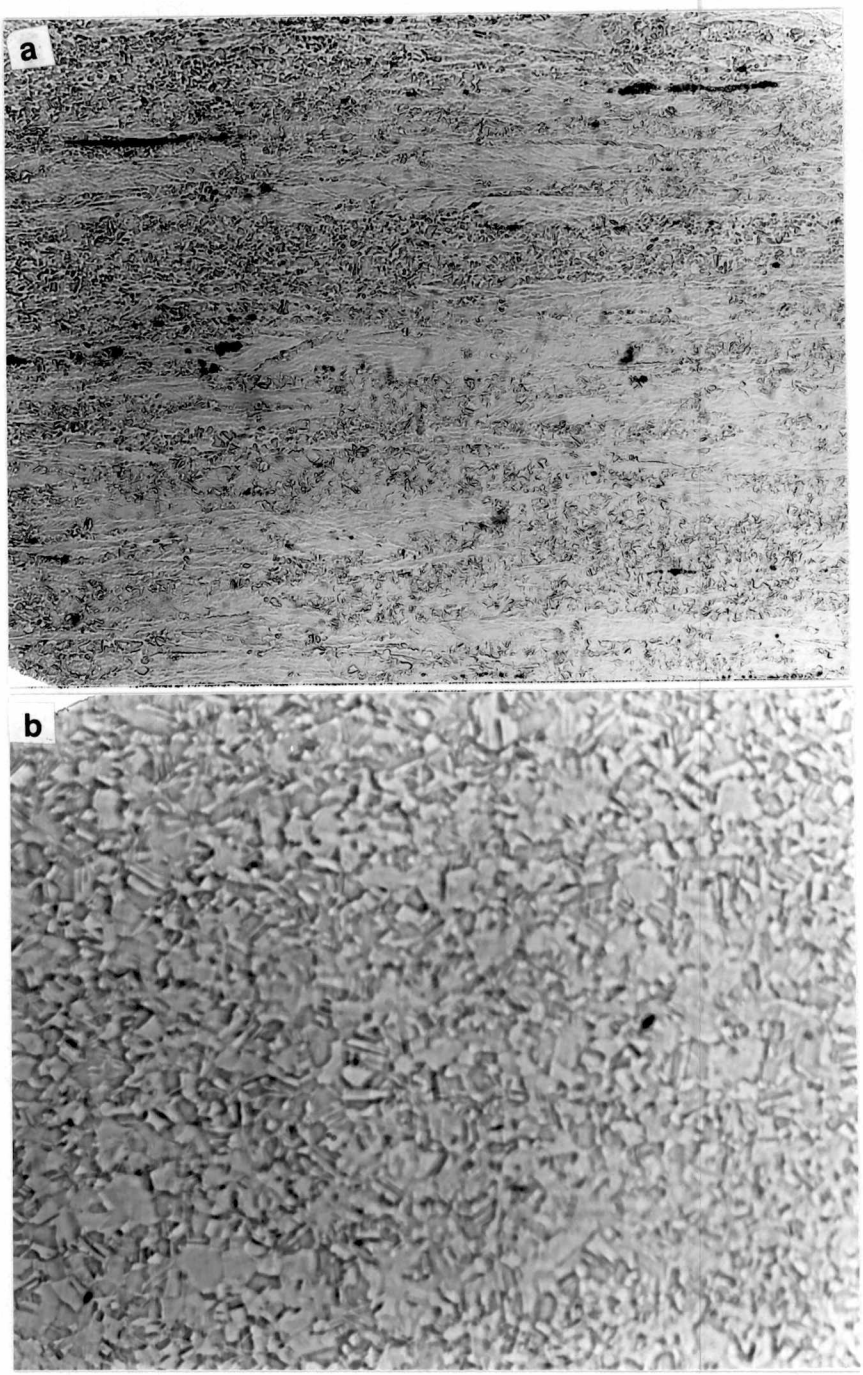


Figure 4.12 Optical micrographs showing microstructural development on aging 80% prior cold worked $Ni_4Mo$ at 850°C. a) 1 minute and b) 5 minutes. 1000X

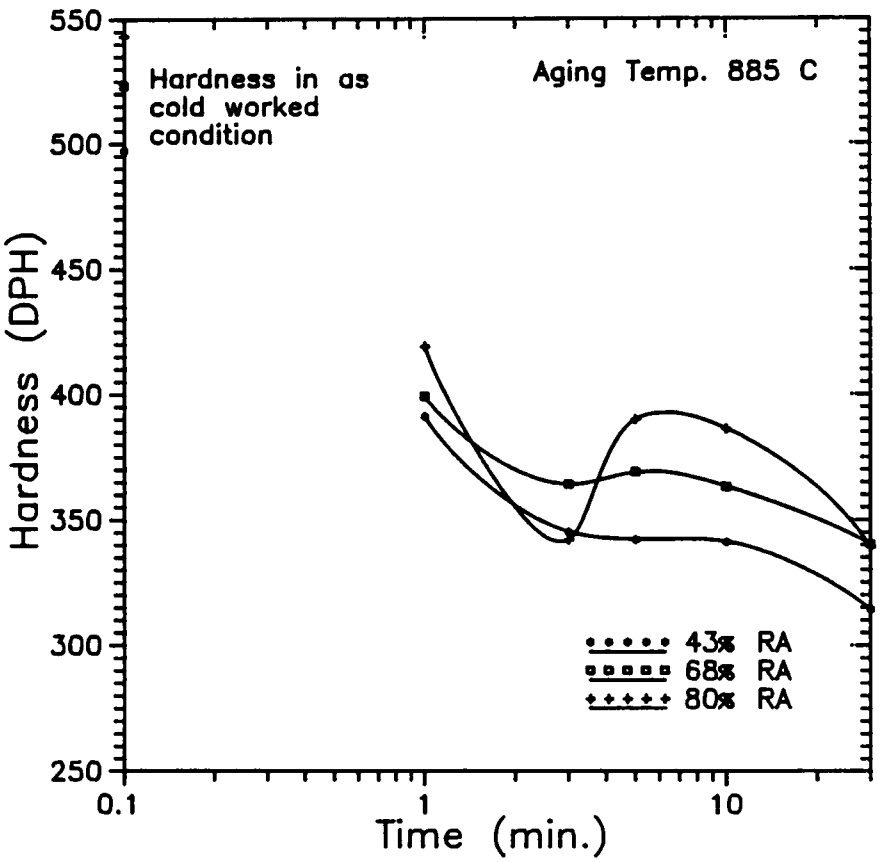


Figure 4.13 Hardness as a function of aging time at $885^0$C (above $T_c$) for prior cold worked $Ni_4Mo$.

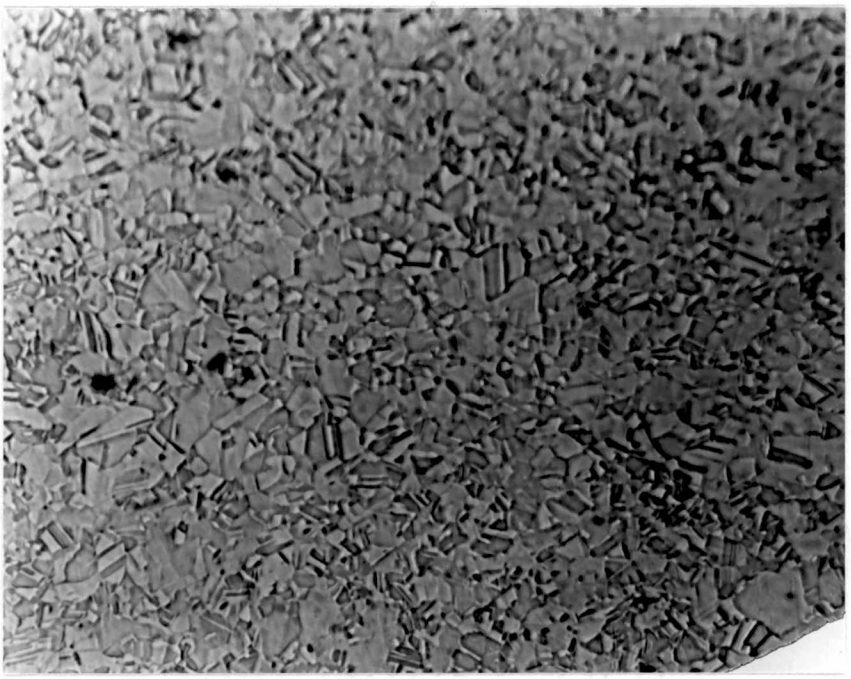

Figure 4.14 Optical micrograph showing equiaxed recrystallized grains obtained by aging prior cold worked $Ni_4Mo$ at $885^0C$ (above $T_c$) for 3 minutes. 1000X

ordering in as-quenched samples at 850$^0$C does not start until 10 minutes.

The slight increase in hardness beyond 5 minutes aging is probably due to establishment of SRO in the recrystallized $\alpha$ grains and the subsequent decrease is associated with continued grain growth of SRO $\alpha$ grains. This is consistent with the aging behavior at 885$^0$C where SRO will exist (Fig. 4.13). There is a slight increase in hardness immediately following completion of recrystallization which is probably due to the short-range ordering. At 885$^0$C, aging for longer time results in grain growth and therefore softening. However, on continued aging at 850$^0$C, ordering commences and hardness increases greatly on aging for 60 minutes. The subsequent aging is likely to follow ordering kinetics similar to that of as-quenched specimens because of the reason discussed in case (1) of the generic recrystallization behavior. It was found that upon aging a similar alloy (NMCR6) at 850$^0$C the former $\alpha$ grain growth from aging time of 60 minutes to 50 hours is very slow which is illustrated in Fig. 4.15. This is consistent with the fact that ordering inhibits grain growth.

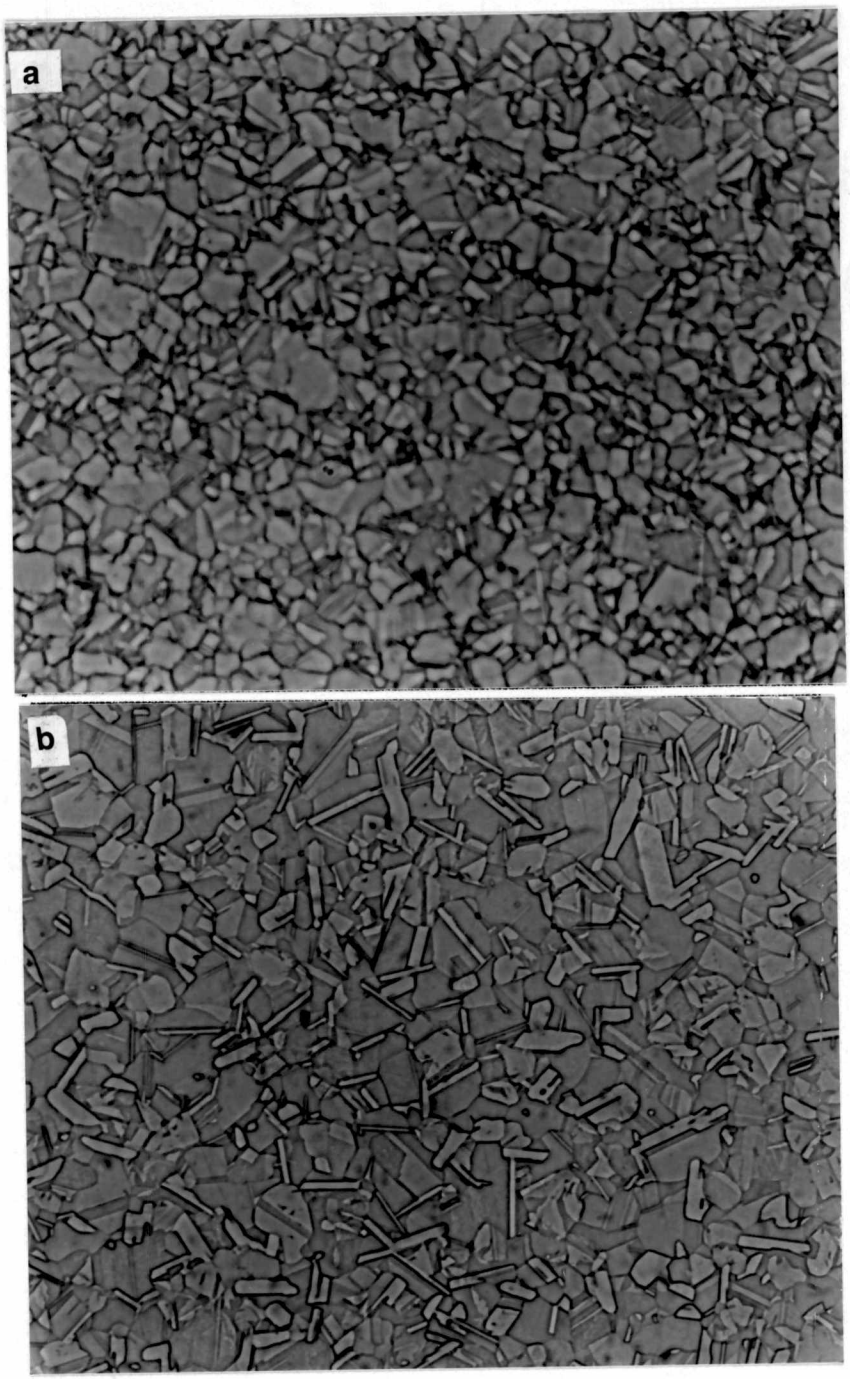


Figure 4.15 Optical micrographs illustrating a very slow grain growth on aging 80% cold worked $Ni_4Mo$ (NMCR6) at $850^0C$ for a) 60 minutes and b) 50 hours. 1000X

Effect of aging at $700^0$C and $775^0$C

The variation of hardness on aging cold worked $\alpha$ at $775^0$C and $700^0$C is shown in Figs. 4.16 and 4.17, respectively. The general trend of variation is an increase in hardness for an aging time of 3 to 5 minutes, followed by a slight decrease in hardness. Continued aging results in again an increase in hardness and then a decrease. The initial slight decrease in hardness is observed in all three cold work samples and for both the aging temperatures. Ling et al. (108) have also reported a slight decrease in hardness on aging a 60% cold work $\alpha$ structure at $700^0$C and $650^0$C. However, this slight decrease was observed at much longer times, of the order of 100-200 minutes. With only information available from hardness and metallographic observation, the exact reason for the slight decrease in hardness can not be determined.

An increase in hardness for aging at very short times of 1 minute at both the temperatures indicates that there is no recrystallization. Microstructural observation showed no change over the cold worked condition. The increase in hardness is provided either by formation of tiny domains of $\beta$ in strained $\alpha$ matrix (as explained in case (2)) or by the establishment of SRO in $\alpha$ which was destroyed by cold working. For the aging temperature of $700^0$C the later hypothesis is supported by the results of resistivity measurements by vasudevan (104) at $700^0$C on

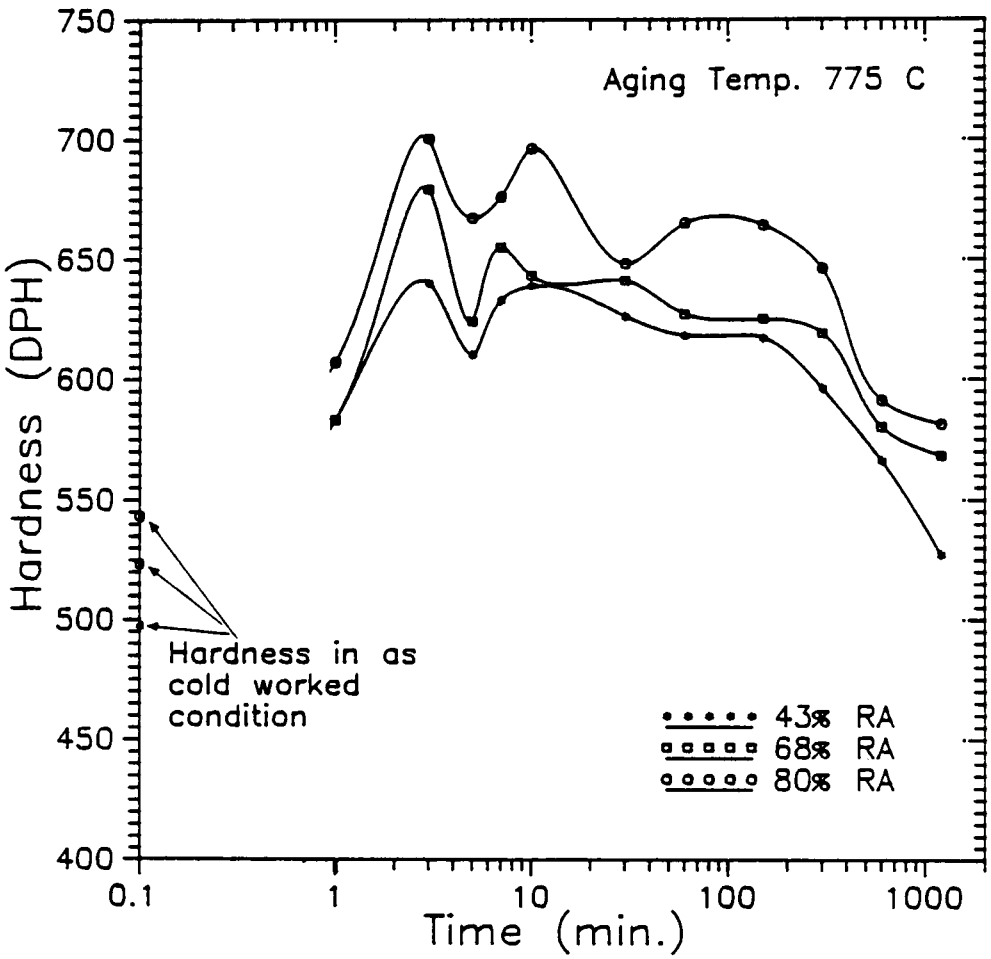


Figure 4.16 Hardness as a function of aging time at $775^0C$ for prior cold worked $Ni_4Mo$.

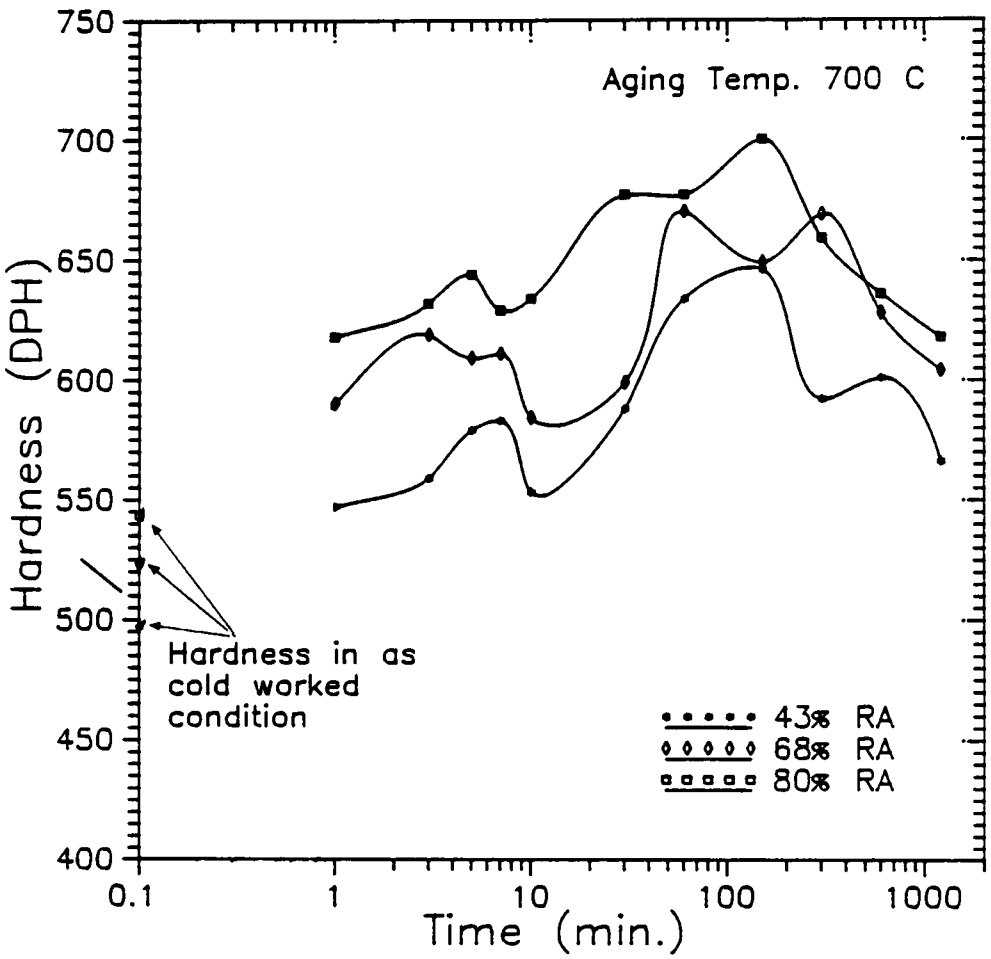


Figure 4.17 Hardness as a function of aging time at $700^0$C for prior cold worked $Ni_4Mo$.

0%. 28%, 44% and 68% cold worked structure. It was observed that, irrespective of the degree of cold work, resistivity increases for aging times up to 4 minutes and then there is a decrease in resistivity. The increase in resistivity is typical of transition to SRO whereas recrystallization and long-range ordering results in a decrease in resistivity. The first hardness maximum in our experiment appears approximately 5 minutes for aging at $700^0$C. The hardness change associated with this 5 minute aging period at $700^0$C is of the order of 75 DPH and this might not be only due to SRO. It is likely that initially recovery of short-range ordering provides a hardness increase and following this there is an additional contribution to the hardness increase by the formation of very small $\beta$ domain inside the short-range ordered (high dislocation density) $\alpha$-grains.

The subsequent slight drop in hardness might be due to pseudo-recrystallization at the grain boundary, as described in case (3), which is not resolved optically at 1000x. Continued aging at $700^0$C results in an increase in the hardness which is perhaps associated with increase in long-range order. Aging beyond about 150 minutes results in softening associated with the recrystallization of $\beta$. Note that below 30 minutes aging times, the hardness curves for all three degrees of cold work seem to follow a similar pattern, but beyond this there is a difference in

the shape of these three curves. This may be due to the fact that aging up to times of 30 minutes was done in a salt bath which gives a high rate of heating and a closer control of temperature and therefore is less likely to give experiemental scatter. Because of the consistencies in the curves the small changes in hardness have been considered real for aging times up to 30 minutes whereas beyond this period the fluctuations in hardness variations are considered to be experimental scatter.

Aging at $775^0$C resulted in increase in hardness by about 150 DPH in 3 minutes which is possibly due to formation of $\beta$ domains inside cold worked $\alpha$-grains. Although there is no experimental evidence, it is likely that long-range ordering is preceeded by short-range ordering and it also contributes a hardness increase in the initial stages of aging. The high hardness, compared to aging at $700^0$C, achieved in a shorter aging time of 3 minutes might be due to faster ordering rate at this temperature compared to $700^0$C. The hardness drop on aging beyond 3 minutes appears to be of the similar nature as discussed for $700^0$C and the subsequent increase is perhaps due to increase in long-range order parameter. The final softening associated with the recrystallization of $\beta$ strarts in about 10 minutes aging.

The existence of recrystallization of $\beta$ can be concluded from microstructural examination. Fig. 4.18 shows microstructures obtained in 43% prior cold worked structure on aging at $775^0$C for 60 and 150 minutes. The micrograph for 60 minutes shows some activity at grain boundaries, however, recrystallization of $\beta$ is clearly resolved in the microstructure for 150 minutes aging. From the microstructural examination the time of nucleation of $\beta$ could not determined. It is possible that $\beta$ nucleates in the early stages of ordering by pseudo-recrystallization as described in case 3 and subsequently grows or it could have nucleated in ordered $\beta$ as described in case 4. The similar observation is made for 68% and 80% prior cold worked structure. The micrograph for 80% prior cold worked structure is presented in Fig. 4.19. Similar recrystallization behaviour is obtained for aging at $700^0$C except for the fact that the recrystallized $\beta$ grain could be resolved only in the sample aged for 300 min. The microstructure obtained on aging 43% cold worked structure at $700^0$C illustrating recrystallization of $\beta$ is shown in Fig. 4.20.

Whatever be the mechanism of nucleation of strain-free $\beta$, the growth characterstics are the same as those observed in recrystallization without ordering. These characterstics are listed below:

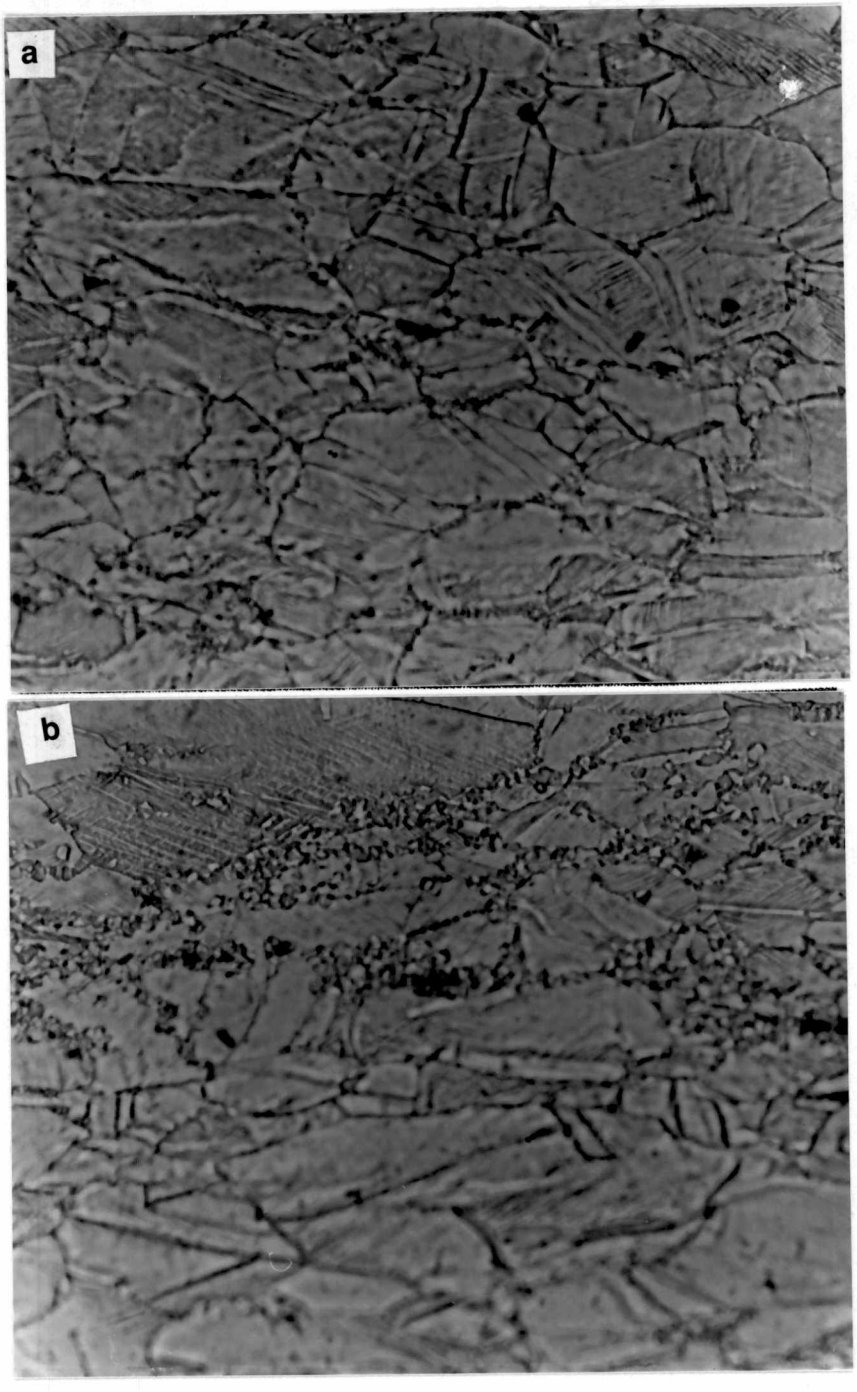


Figure 4.18 Optical micrographs showing recrystallization of $\beta$ upon aging 43% prior cold worked $Ni_4Mo$ at $775^0C$. a) 60 minutes and b) 150 minutes. 1000X

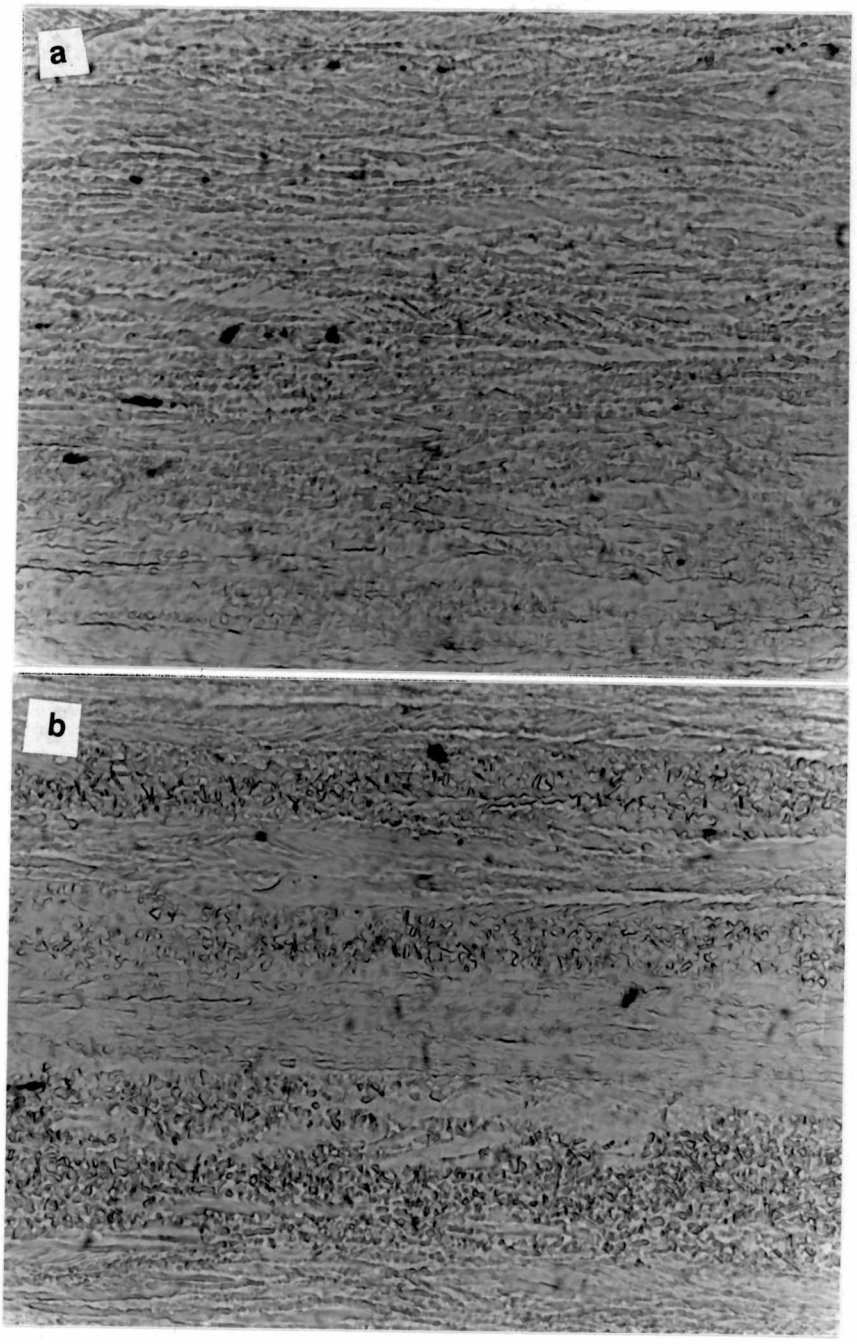


Figure 4.19 Optical micrographs showing recrystallization of $\beta$ upon aging 80% prior cold worked $Ni_4Mo$ at $775^0C$. a) 60 minutes and b) 150 minutes. 1000X

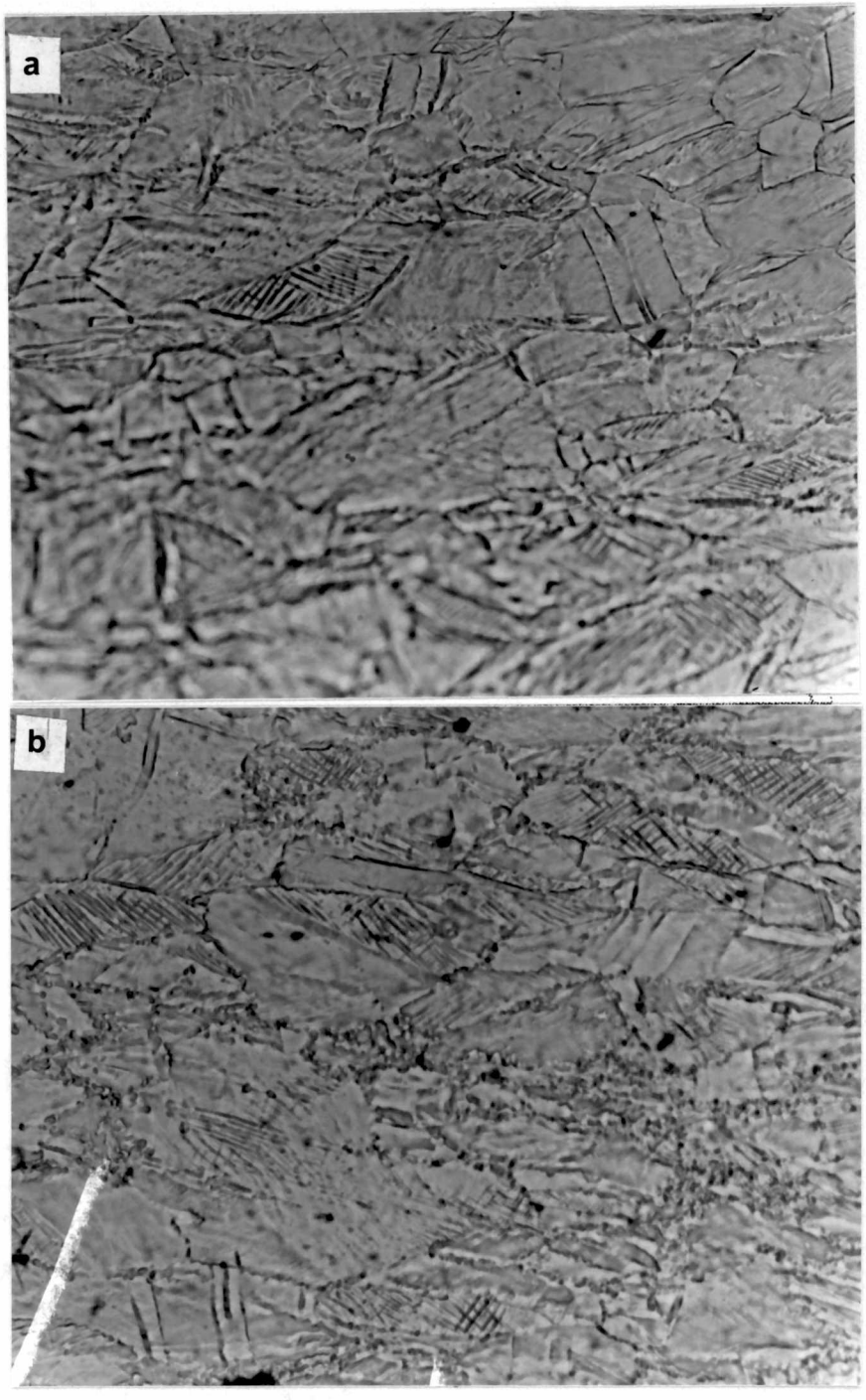


Figure 4.20 Optical micrographs showing recrystallization of $\beta$ upon aging 43% prior cold worked $Ni_4Mo$ at $700^0$C. a) 150 minutes and b) 300 minutes. 1000X

i) For the same degree of cold work, the extent of recrystallization (fraction recrystallized) is greater in the sample aged at higher temperature, aging time remaining the same. This is obvious on comparing Figs 4.18b and 4.20a. In Fig 4.20a, which was obtained on aging at $700^0$C for 150 min., recrystallization is not resolved whereas the sample aged at $775^0$C for the same time (Fig 4.18b) clearly shows recrystallized $\beta$.

ii) For the same aging temperature and time, recrystallization is more complete in samples with higher degree of cold work. This is illustrated in Figs 4.21 and 4.22 which shows microstructures on aging at $775^0$C and $700^0$C for 20 hours for three degrees of cold work, respectively. The fraction recrystallized is the most in the sample with 80% cold work and the least in 43% cold worked sample.

iii) For the same aging time and temperature, the higher degree of cold work will develop a finer initial, recrystallized grain size. This is again illustrated in Figs 4.21 and 4.22. It is observed that the recrystallized $\beta$ grain size is the finest in 80% cold worked structure and coarsest in 43% cold worked structure.

All micrographs show that the recrystallization occurs in bands parallel to the axis of the rod shaped samples. It should be recalled here that samples were prepared by cold working (swagging) a 1.9 cm diameter rod

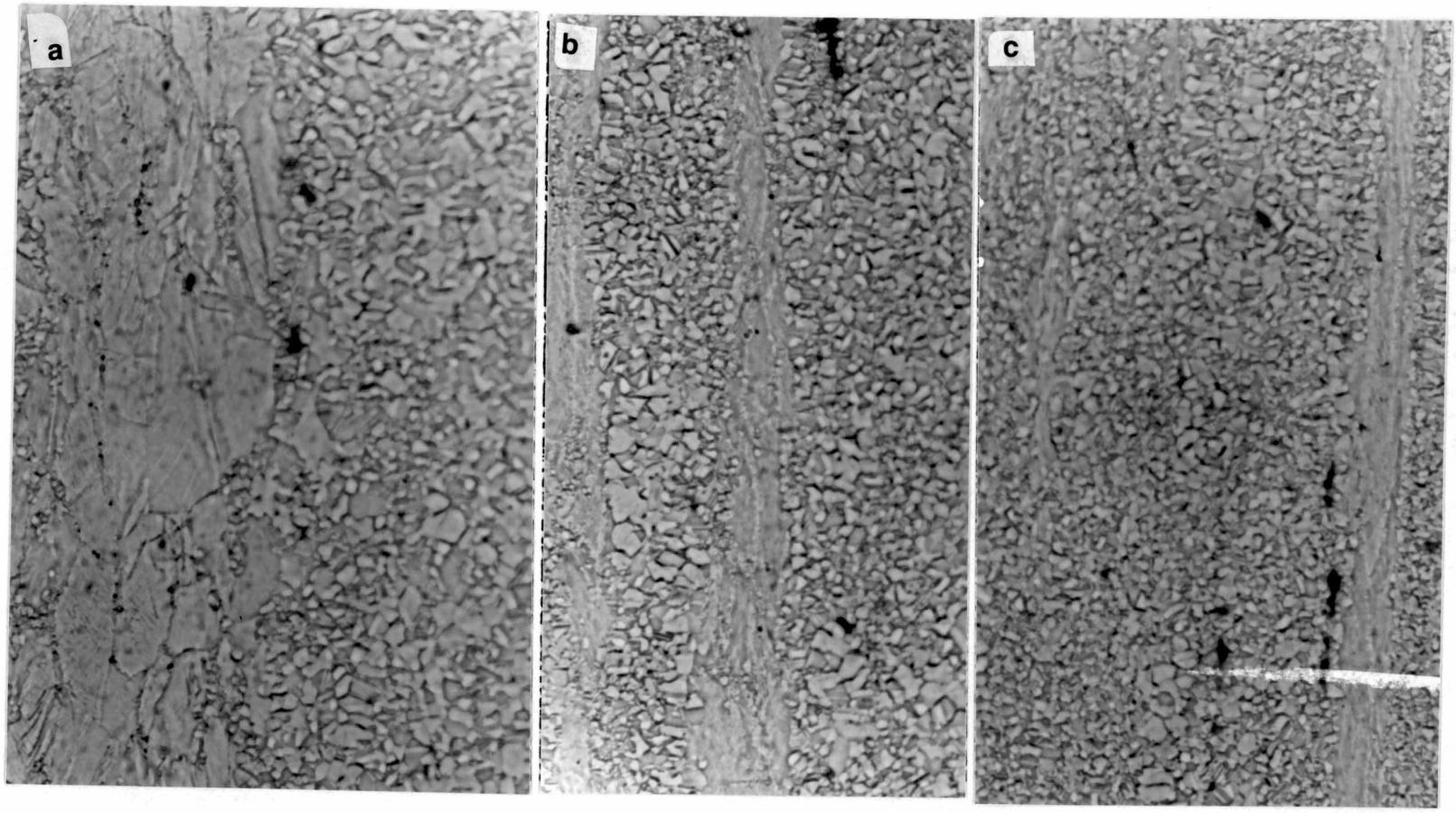


Figure 4.21 Optical micrographs illustrating recrystallized $\beta$ grain size and extent of recrystallization upon aging prior cold worked $Ni_4Mo$ at $775^0C$ for 1200 minutes. a) 43% RA, b) 68% RA and c) 80% RA. 1000X

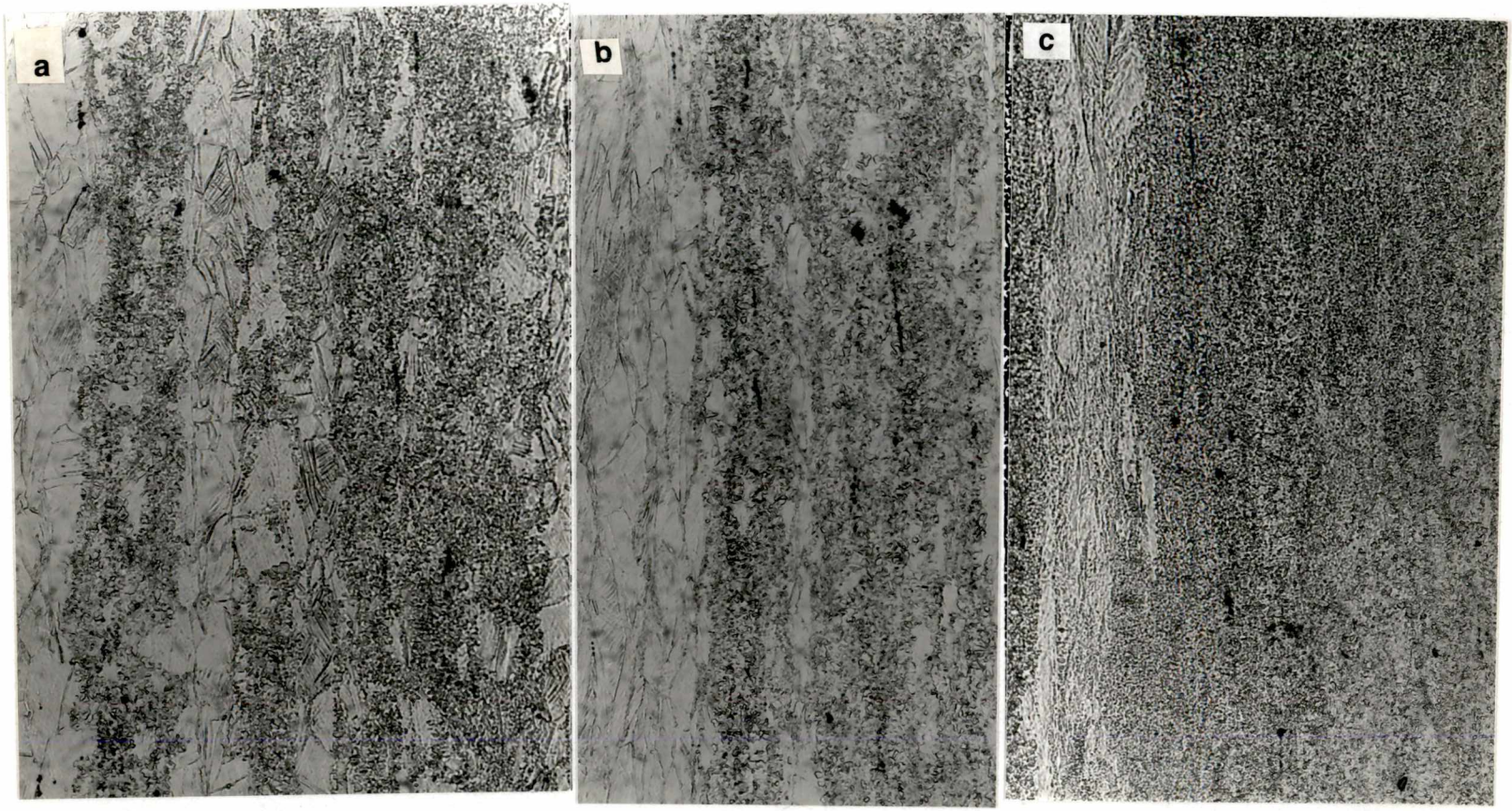


Figure 4.22 Optical micrographs illustrating rescrystallized $\beta$ grain size and extent of recrystallization upon aging prior cold worked $Ni_4Mo$ at $700^0C$ for 1200 minutes. a) 43% RA, b) 68% RA and c) 80% RA. 400X

with intermediate anneals to a final size of 0.125 cm. It is possible that this processing introduces a texture which results in non-homogeneous strain resulting in non homogeneous recrystallization. Note that this behavior is not something typical of recrystallization of $\beta$. The recrystallization of $\alpha$ also occurs in bands which is illustrated in Fig. 4.12a.

It must also be mentioned here that $\beta$ recrystallization is not complete at $775^0$C in 20h.

An attempt was made to improve the ductility by grain refinement. This utilized the fact that a fine grain size develops on aging at $850^0$C which does not coarsen on sunsequent ordering. The thermomechanical treatment given was - cold work by 80% and then recrystallize at $860^0$C in 6 miuntes followed by again a cold work of 60% and recrystallized at $860^0$C. This treatment however did not give a grain size any finer then cold work and recrystallize only once. The sample was given an ordering treatment at $725^0$C and then tested for bend ductility. The second set of treatment did not seem to increase the ductility.

## 4.3 ORDERING IN HASTELLOY B-2

Hastelloy B and Hastelloy B-2 are used in the chemical industry for their excellent corrosion resistance and good strength. These alloys have a $Ni_4Mo$-based composition with some alloying elements, mainly Fe and C. Fe retards the ordering reaction. Hastelloy B-2 has a much lower Fe and C content, so it is very prone to ordering during fabrication. Hastelloy B-2 is being used at Tennessee Eastman Co., Kingsport, Tennessee, where some components made of this alloy failed in service.

It is believed that the failed components were subjected to improper heat treatment prior to service. However, it was realized that there is a possibility of ordering during fabrication, especially welding. This prompted a need to examine the possibilty of ordering in other components. The maximum service temperature is $200^0C$ and therefore the possibility of ordering during service is unlikely.

Nine pieces, numbered A through G, were cut from different components and supplied for this investigation. One of the pieces, numbered D, was from a failed part. It showed clear cracks joining the fracture surface. A piece was cut from this sample so that the cracked region could be separated for examination of the fracture surface. (The preexisting fracture surface was not suitable for

examination because of improper handling.) The fracture surface was examined in an SEM and showed clear intergranular fracture (Fig 4.23). This indicates the presence of ordering and it was further confirmed by a microhardness value of 370 DPH. Typically, solution heat treatment at 1000oC for 30 minutes then quenching gives a microhardness value of 200 DPH. It is suspected that this component was given an improper heat treatment.

Other samples on surface examination in a stereo optical microscope showed the presence of cracks in certain regions. The cracks were observed only on the surface exposed to the chemical; no cracks were seen on the outer surface. Also the cracks were concentrated in a region where the surface was ground to remove the weld cap.

Cracks were more obvious in sample F and H and therefore these two samples were chosen for further investigation. SEM pictures of the surface in the as-received condition are presented in Fig. 4.24. These pictures have been taken from general regions of the heat-affected zone where grinding was done. The grinding marks appear as bands in the pictures. Note that cracks do not appear sharp, as would be expected in intergranular crack propagation in a material with straight grain boundaries.

Extensive ductility was observed in bend tests (a non-standard test described in section 3.3). The samples

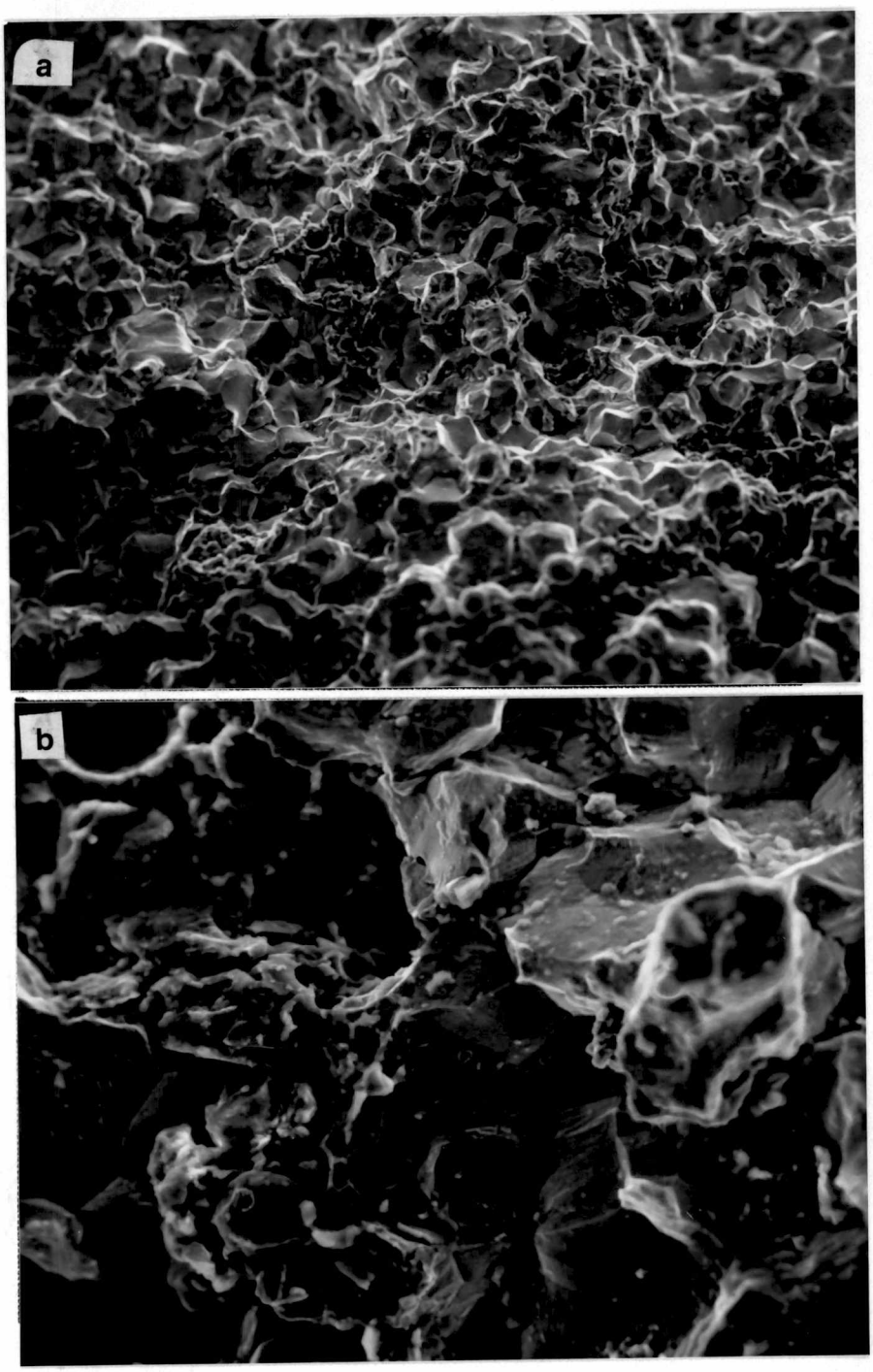


Figure 4.23 SEM pictures showing intergranular fracture in an improperly heat treated Hastelloy B-2 sample D. a) 100 x, b) 500 x

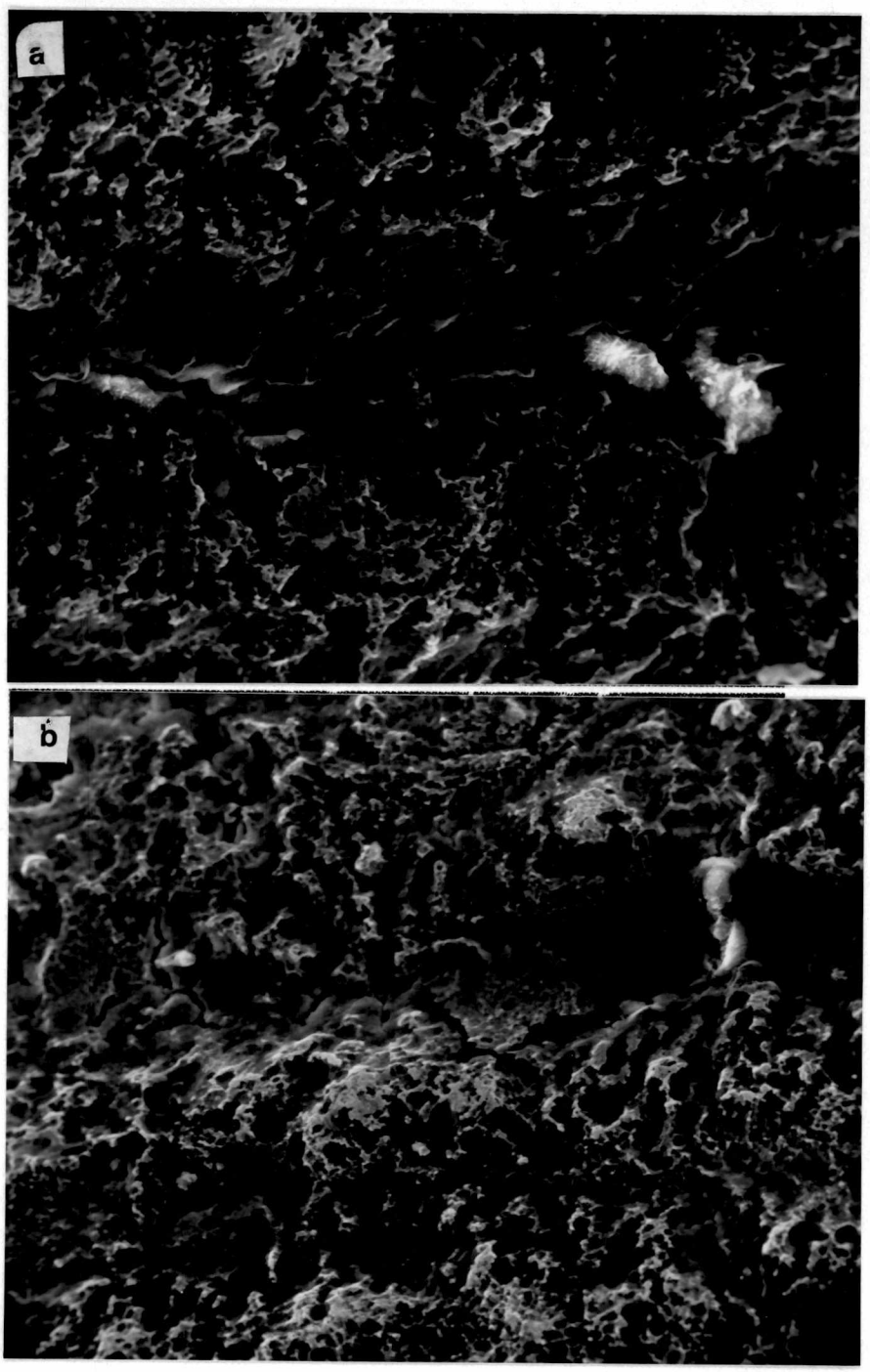


Figure 4.24 SEM pictures of surface in as-received condition. Grinding marks appear as band. a) and b) sample F, 400 x; c) and d) sample H, 140x.

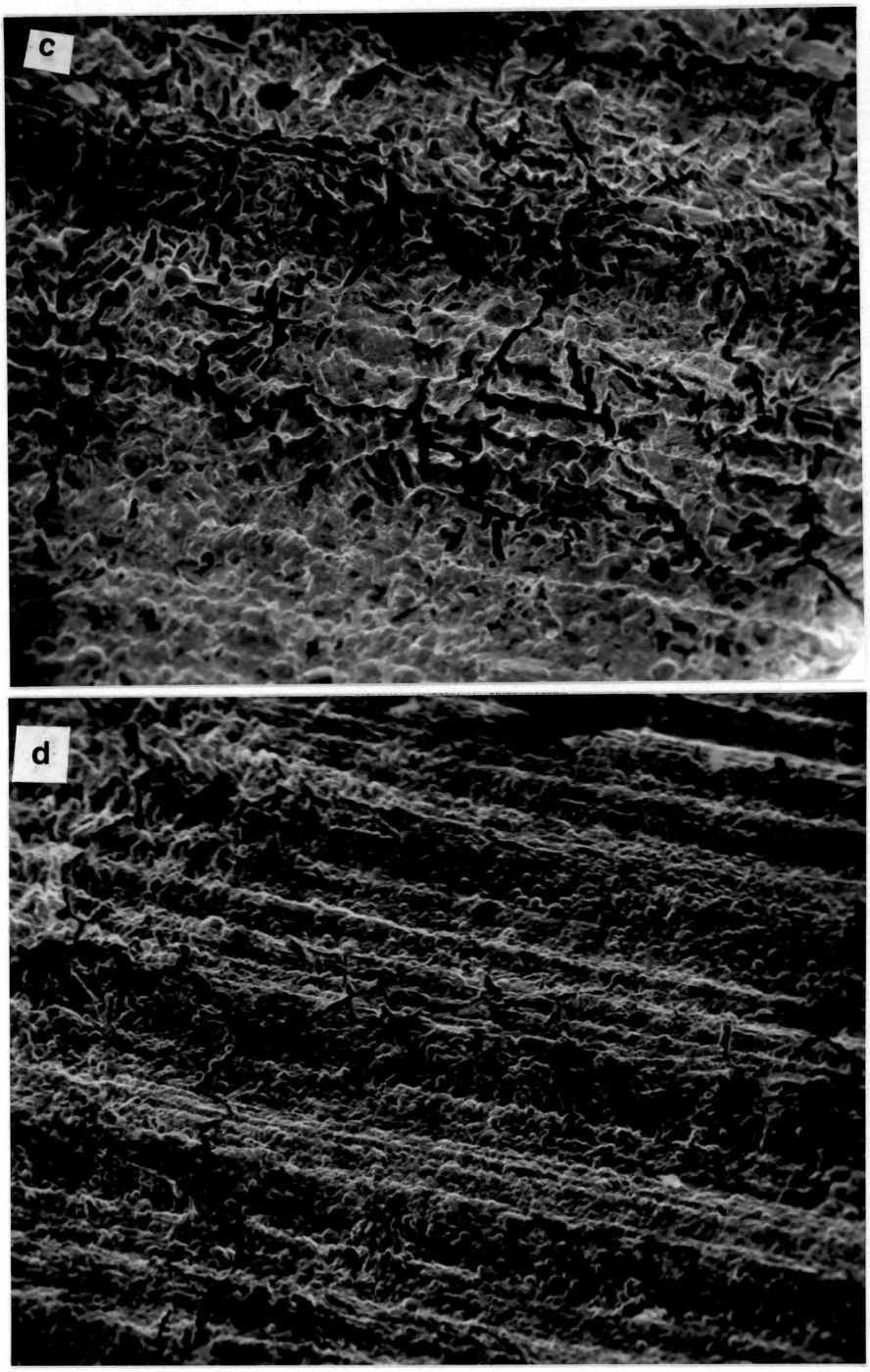


Figure 4.24 continued

did not break even after a bend of 180 degrees. Although the cracks opened up and became blunt, but they did not propagate intergranularly. Pictures of cracks taken for different degrees of bending are presented in Fig. 4.25. This crack blunting is more obvious in Fig. 4.26 which was obtained in SEM by focussing into the crack in Fig. 4.25c. The high bend ductility and the appearance of the cracked regions suggest no ordering.

Metallographic examination of cross-sectional views in the etched and unetched condition reveals the depth of cracks in the sample. SEM micrographs of this observation are shown in Fig. 4.27. Note that cracks do not necessarily extend to the surface, but the possiblity of these cracks meeting the surface at a different cross-section is very likely. The fact that cracks appear only on the chemically exposed surface was also confirmed by this observation. Higher magnification micrographs of cracks are presented in Fig. 4.28. It appears that a grain has fallen out, possibly during polishing. Note that these cracks are intergranular; however the fact that these intergranular cracks do not propagate intergranularly under a bending load leads to the conclusion the these crack are the result of a corrosion process such as intergranular stress corrosion. Fig. 4.29

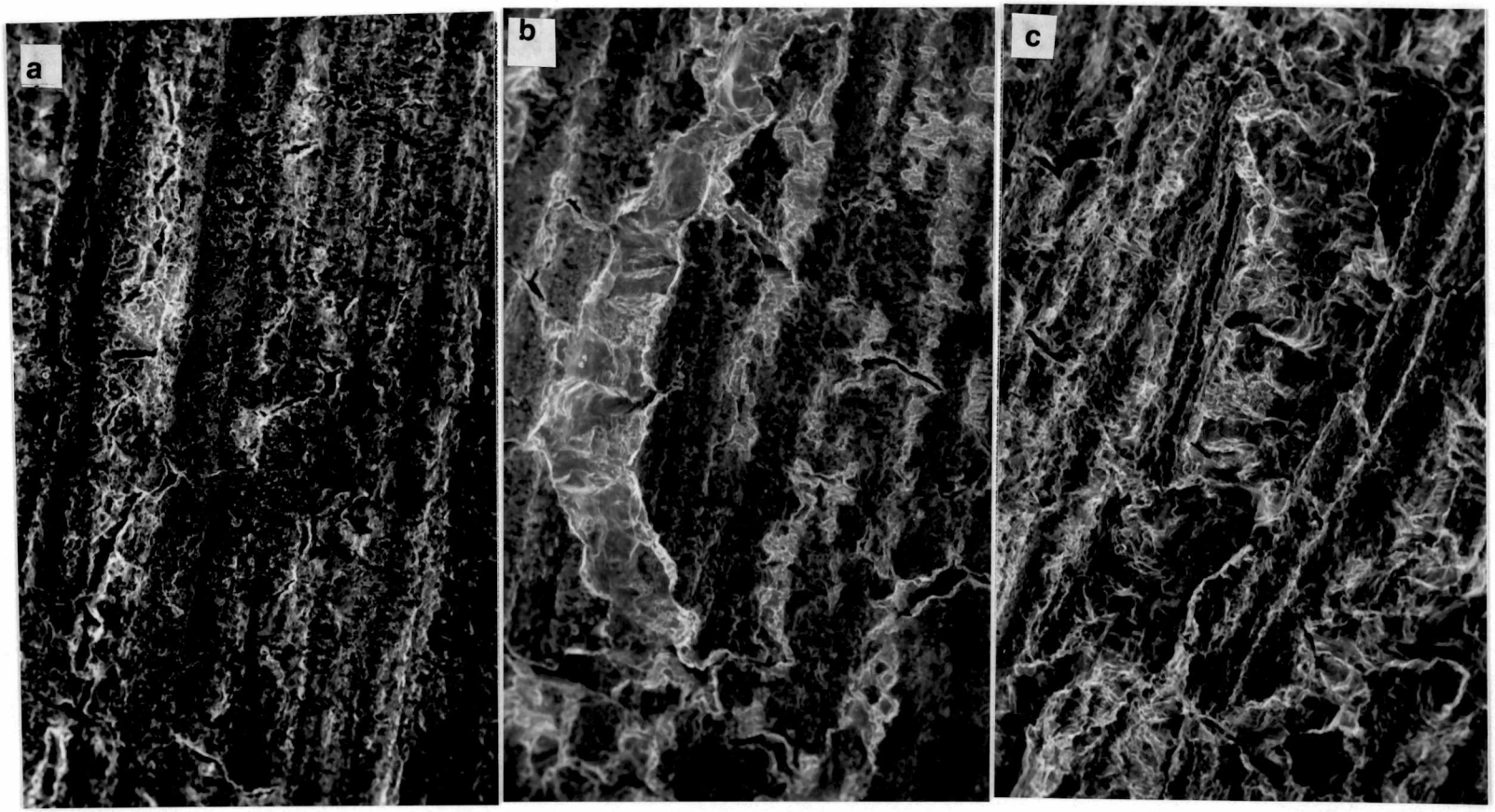


Figure 4.25 SEM pictures showing opening up of surface crack in sample F on bending a) $60^{o}$ bend, 80x b) $120^{o}$ bend, 100x c) $180^{o}$ bend, 100x.

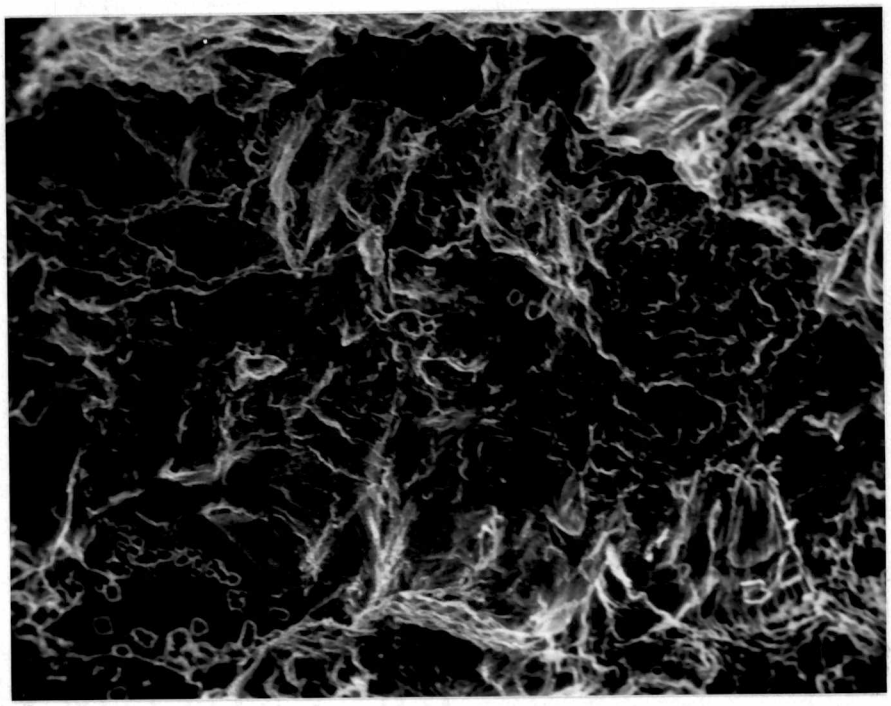

Figure 4.26 SEM pictures obtained by focussing inside a crack in Figure 4.25c. Sample F, 500x.

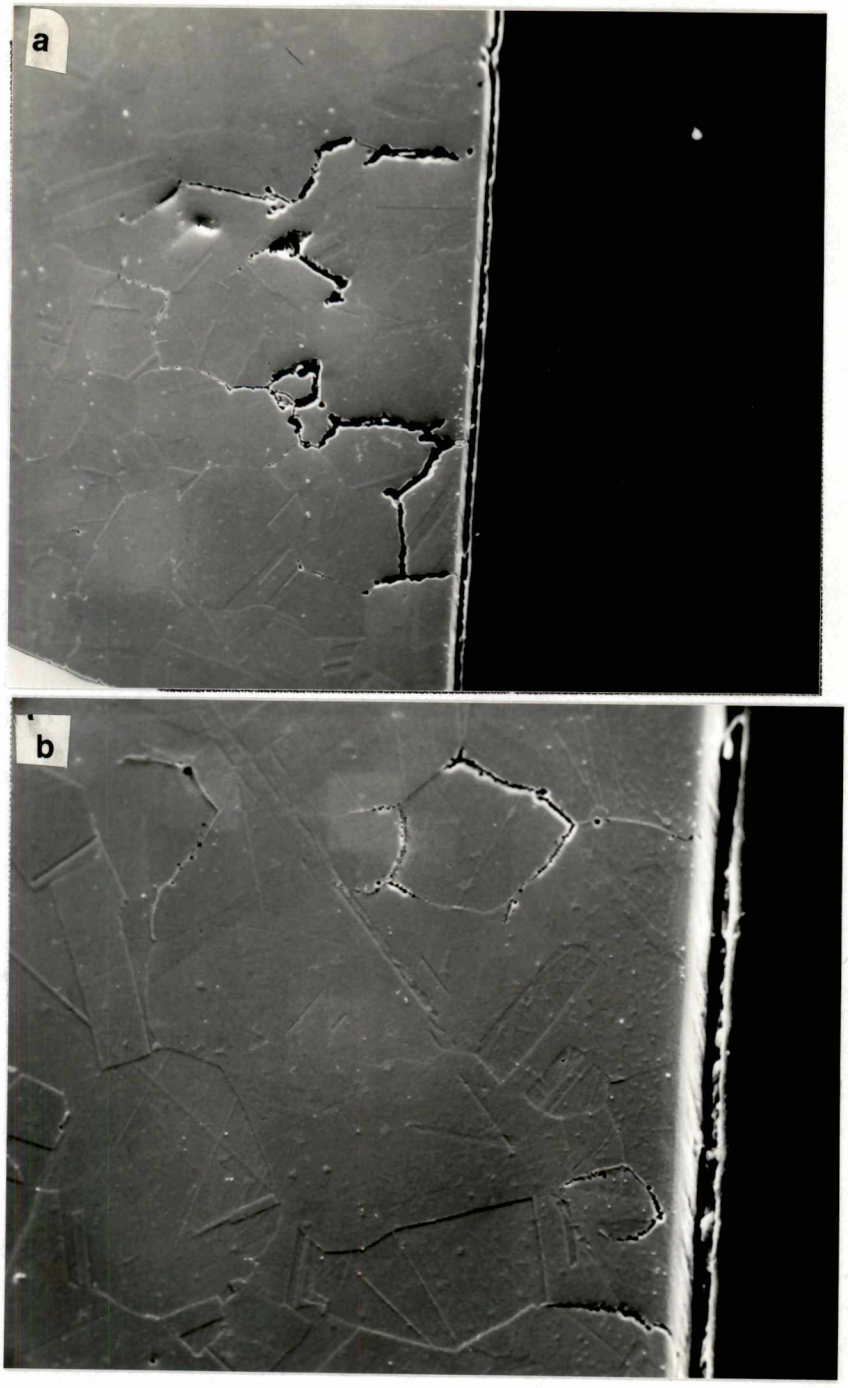


Figure 4.27 SEM pictures of metallographically polished cross-sectional surface showing cracks. a) and b) sample F, polished; c) and d) sample H, etched. a) 200x; b), c) and d) 500x.

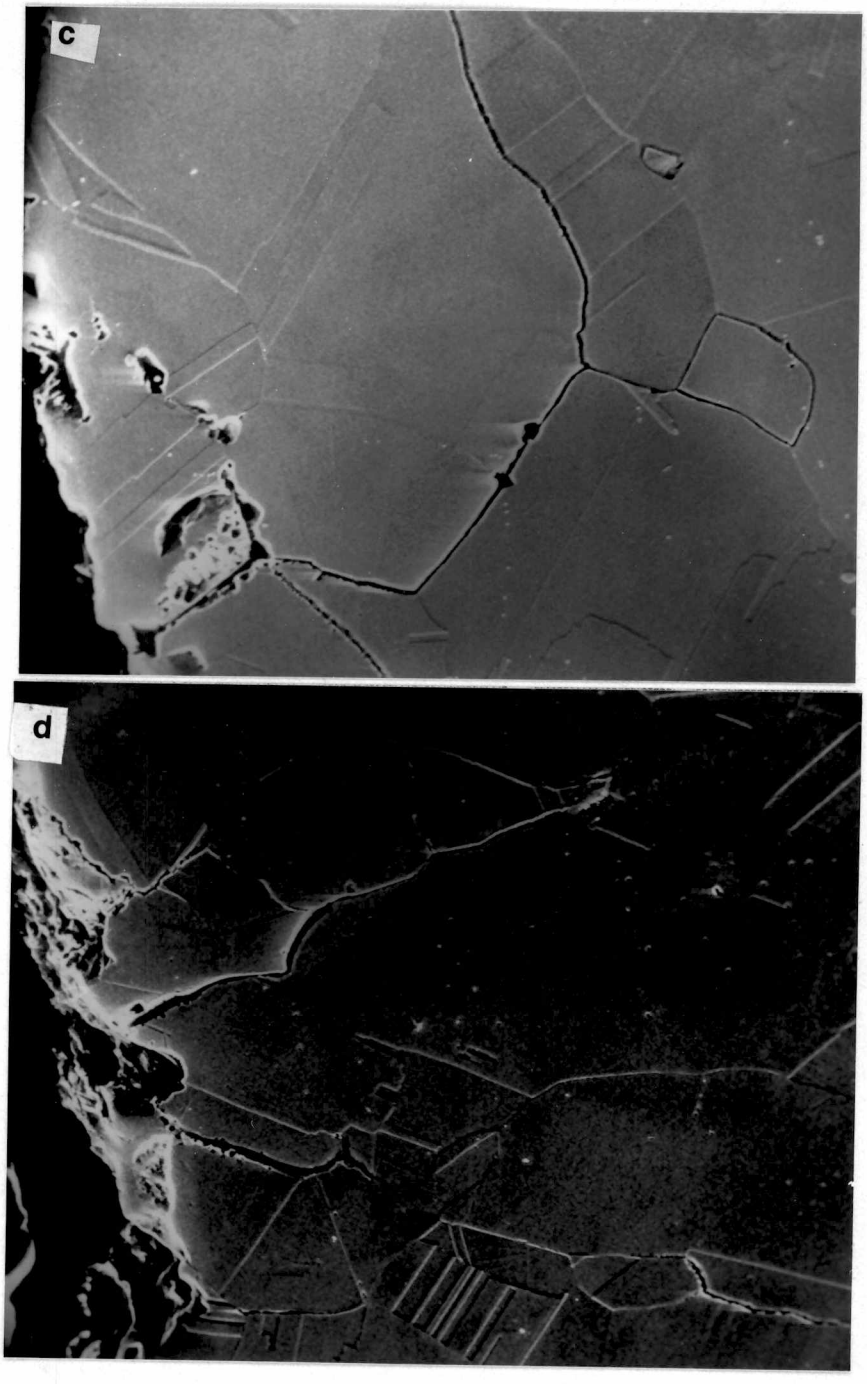


Figure 4.27 continued

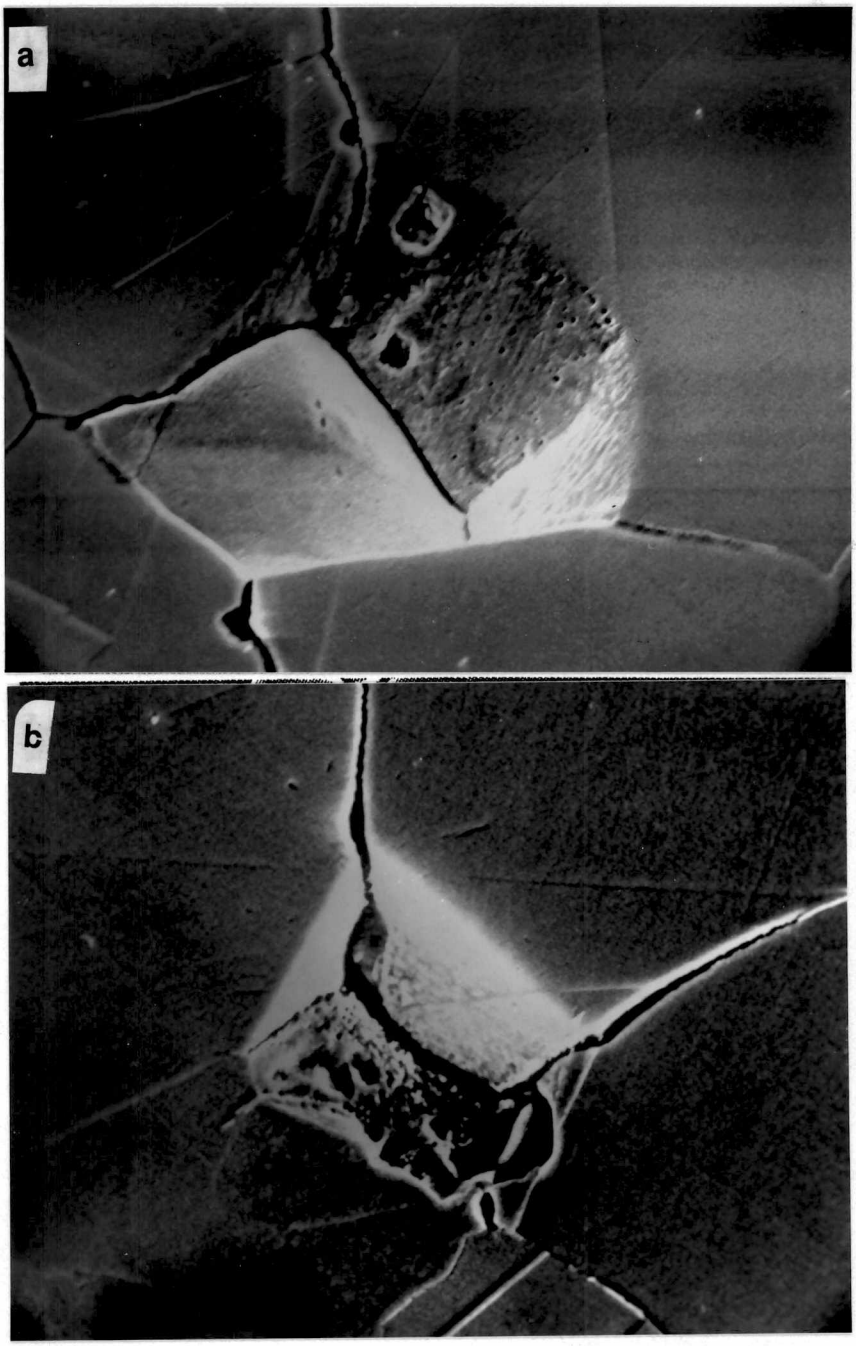


Figure 4.28 SEM pictures of metallographically polished and etched cross-sectional surface showing cracks and falling out of a grain illustrating intergranular cracks. Sample H, 2000x.

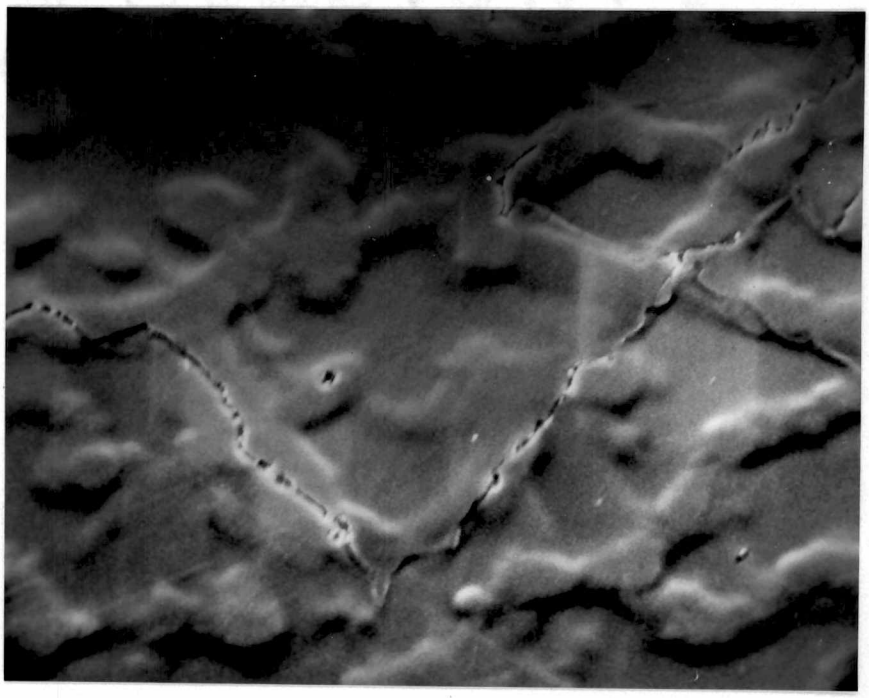

Figure 4.29 SEM pictures of polished and etched cross sectional surface in weldment region showing etching effect at grain boundary. Sample H, 2000x.

shows a microstructure of the weldment. Note the crack-like feature along the grain boundaries. However, this feature does not appear in the unetched condition, and thus this is an etching effect.

# CHAPTER 5

# CONCLUSIONS

The conclusions of this research are presented in three sections: Fracture in Ordered $Ni_4Mo$, Ductilizing Ordered $Ni_4Mo$ and Ordering in Hastelloy B-2.

## 5.1 FRACTURE IN ORDERED $Ni_4Mo$

1. Fracture in ordered $Ni_4Mo$, with migrated prior $\alpha$ high angle boundaries (obtained by aging for sufficiently long times at the temperature range 700-800$^0$C), occurs along the migrated boundaries.

2. The fine fracture morphology associated with long aging times is due to fracture along migrated boundaries.

3. Ordered $Ni_4Mo$ undergoes a very small plastic deformation by slip, evident in slip lines observed on metallographic and fracture surfaces, before fracturing intergranularly.

4. There is crystallographic continuity between prior $\alpha$-grains and the area formed by the migrated boundaries, evident in continuity of slip lines across the grains up to the migrated boundaries.

## 5.2 DUCTILIZING ORDERED $Ni_4Mo$

1. The following two conclusions were drawn from the experiment on ducilizing ordered $Ni_4Mo$ by microalloying:

i) Microalloying with elements producing a scavenging action does not seem to improve the ductility of ordered $Ni_4Mo$. This conclusion is based on the lack of ductility of ordered $Ni_4Mo$ microalloyed with Zr, Ce, Mg, Nb, Hf and La.

ii) Among the smaller sized atoms, which are likely to improve the ductility in the ordered condition, boron did not produce any beneficial effect. However, beryllium addition appears promising. The effect of lithium, which has a smaller atom size than beryllium and boron, should be investigated in future work.

2. Thermomechanical treatment appears promising for improving the ductility of the ordered $Ni_4Mo$. However, this was not established in this work. A preliminary investigation which involved studying aging behavior of the prior cold worked (disordered) $\alpha$ was performed and the conclusions are listed below:

i) Upon aging at $850^0C$ ($T_c = 868^0$), the prior cold worked (43% RA, 86% RA and 80% RA) $Ni_4Mo$ recrystallizes completely in about 5 minutes, to eqiaxed $\alpha$ grains. This is followed by short-range ordering and finally long-range ordering.

ii) There is almost no grain growth on aging at $850^0C$ from 1 hour to 50 hours. This implies that ordering inhibits growth rate.

iii) Aging at $700^0C$ and $775^0C$ results in, first recovery of short-range order, followed by long-range ordering and finally recrystallization of $\beta$ into fine grains. The mechanism of the nucleation of $\beta$ grains could not be ascertained.

iv) Recrystalliztion of $\beta$ has the same characterstics as that of conventional recrystallization of disordered alloys.

v) The recrystallization of $\beta$ is very slow as it is not complete for 80% prior cold worked structure in 20 hours for an aging temperature of $775^0C$.

vi) Grain refinement, to the extent of about 5 micro meter grain size obtained by thermomechanical treatment, did not make a significant contribution to the ductility of the ordered $Ni_4Mo$.

## 5.3 ORDERING IN HASTELLOY B-2

1. Sample D, which was suspected to have been given a improper heat treatment, was found to be ordered.

2. Samples F and H showed extensive bend ductility which implies that they were not ordered.

3. Cracks, observed on the as-received surface and the metallographically polished surface, are due to intergranular corrosion.

# LIST OF REFERENCES

# LIST OF REFERENCES


1 N.S.Stoloff, "Ordered Alloys - Physical Metallurgy and Structural Applications," Int. Metals Rev., Vol. 29, P. 123, 1984.

2 C.R.Brooks, J.E.Spruiell and E.E.Stansbury, "Physical Metallurgy of Nickel-Molybdenum Alloys," Int. Metals Rev., Vol. 29, P. 210, 1984.

3 K.Aoki and O.Izumi, "Improvement in Room Temperature Ductility of the $L1_2$ Type Intermetallic Compound $Ni_3Al$ by Boron Additions," Nippon Kinzoku Gakkaishi, Vol. 43, P. 1190, 1979.

4 C.T.Liu, C.L.White and J.A.Horton, "Effect of Boron on Grain Boundaries in $Ni_3Al$," Acta Metall., Vol. 33, P. 213, 1985.

5 R. P. Elliott, Constitution of Binary Alloys, First Suppliment, McGraw-Hill, New York, 1958.

6 P. V. Guthrie and E. E. Stansbury, "X-ray and Metallographic Study of the Nickel-rich Alloys of the Nickel-Molybdenum System II," Report ORNL 3078, Oak Ridge National Laboratory, Oak Ridge, Tenn., 1961.

7 R.E.W.Casselton and W.Hume-Rothery, "The Equilibrium Diagram of The System Molybdenum-Nickel, "J. Less-Common Met., Vol. 7, P. 212, 1964.

8 K.Vasudevan, "Transmission Electron Microscopy Study of Phase Transformations in Ternary $Ni_4Mo$ based Alloys Containing 0-4% Chromium," PhD Dissertation, University of Tennessee, Knoxville, 1986.

9 D.Harker, "The Crystal Structure of $Ni_4Mo$," J. Chem. Phys., Vol. 12, P. 315, 1944.

10 E.Ruedl, P.Delavignette, and S.Amelinckx, "Electron Diffraction and Electron Microscopic Study of Long- and Short-Range Order in $Ni_4Mo$ and of the Substructure Resulting from Ordering," Phys. Status Solidi, Vol. 28, P.305, 1968.

11 J.E.Spruiell and E. E. Stansbury, "X-Ray Study of Short-Range Order in Nickel Alloys Containing 10.7 and 20.0 at% Molybdenum," J. Phys. Chem. Solids, Vol. 26, P. 811, 1965.

12 T.S.Lei, "The Effect of 0-8% Iron on Transformations of Alpha Phase Ni-Mo-Fe Alloys with Ni:Mo Ratio Equal to 4:1," PhD dissertation, University of Tennessee, 1979.

13 P.C.Clapp and S.C.Moss, "Correlation Functions of Disordered Binary Alloys.III," Phys. Rev., Vol. 171, P. 764, 1968.

14 P.C.Clapp and S.C. Moss, "Correlation Functions of Disordered Binary Alloys.I," Phys. Rev. Vol. 142, P. 418, 1966.

15 B. Chakravarti, E.A.Starke,Jr, C.I.Sparks, and R.O.Williams, "Short-Range Order and the Development of Long-Range Order in $Ni_4Mo$," J. Phys. Chem. Solids, Vol. 35, P. 1317, 1974.

16 G.van Tendeloo, "Short-Range Order Considerations and Development of Long-Range Order in Different Ni-Mo Alloys," Mater. Sci. Eng., Vol. 26, P. 209, 1976.

17 T.Saburi, K.Komatsu, M.Yamamota, S.Nenno and Y.Mizutani "A New Metastable Phase $Ni_2Mo$," Trans. AIME, Vol. 245, P. 2348, 1969.

18 S.K.Das, P.R.Okamoto, P.M.J.Fisher, and G.Thomas, "SRO in Ni-Mo, Au-Cr, Au-V, and Au-Mn Alloys," Acta Metall., Vol. 21, P. 913, 1973.

19 P.R.Okamoto and G.Thomas, "On Short-Range Order and Micro-Domains in the $Ni_4Mo$ System," Acta Metall., Vol. 19, P. 825, 1971.

20 S.K.Das and G.Thomas, "On Structural Interpretation of Short-Range Order" in Order-Disorder Transformation in Alloys, eds. Hans Warlimont, Springer-Verlag, New York, 1974.

21 W.M.Stobbs and J.-P.Chevalier, "The Classification Of Short-Range Order By Electron Microscopy," Acta Metall., Vol. 26, P. 1197, 1979.

22 J.-P.Chevalier and W.M.Stobbs, "Short-range Order and The Disorder-Order Transformation in Stoichiometric $Ni_4Mo$," Acta Metall., Vol. 27, P. 1197, 1979.

23 M.Yamamoto, S.Nenno, T.Saburi, and Y.Mizutani, "Structural Changes during Isothermal Annealing of the Quenched $Ni_3Mo$ Alloy(I)," Trans. Jpn Inst. Met., Vol. 11, P. 120, 1979.

24 J.-P.Chevalier and W.M.Stobbs, "An Electron Diffraction Study of Short-Range Order in Quenched $Ni_4Mo$ Alloy," Acta Metall., Vol. 24, P. 535, 1976.

25 G.Thomas and R.Sinclair, "Discussion of 'An Electron Diffraction Study of Short-Range Order in Quenched $Ni_4Mo$'," Acta Metall., Vol. 25, P.231, 1977.

26 W.B.Snyder and C.R.Brooks, "Mechanical Properties and Domain Structure of Ordered $Ni_4Mo$," in Ordered Alloys, eds. B.H.Kear, C.T.Sims, N.S.Stoloff and J.H.Westbrook, Claitor's Publishing Division,Baton Rouge,La, 1974.

27 T.Saburi, E.Kanai, and S.Nenno, "Domain Structure in $Ni_4Mo$ Alloy," J. Less-Common Met., Vol. 37, P. 59, 1974.

28 T.Saburi, K.Komatsu. amd S.Nenno, "Transition from Short-range to Long-range Order in $Ni_4Mo$," Philos. Mag., Vol. 20, P. 1091, 1969.

29 F.-W.Ling and E.A.Stark,Jr, "The Development of Long-range Order and the Resulting Strengthening Effects in $Ni_4Mo$," Acta Metall., Vol. 19, P. 759, 1971.

30 H.E.Cook, "Continuous Transformations," Mater. Sci. Eng., Vol. 25, P. 127, 1976.

31 S.J.Block, "Hardness Changes during The Ordering Reaction of Three Nickel-Molybdenum Alloys," MS Thesis, University of Tennessee, 1961.

32 F.-W.Ling and E.A.Starke, "The Disorder-Order Transformation in $Ni_4Mo$," in Advances in X-ray analysis, ed. K.F.J.Heinrich, C.S.Barrett, J.B.Newkirk and C.O.Rudd, Plenum, New York, Vol. 15, P. 319, 1974.

33 K.Vasudevan, H.P.Kao, C.R.Brooks and E.E.Stansbury, "Domain Coarsening by Grain Boundary Migration in Ordered $Ni_4Mo$," in Proc. 44th Annual Meeting of the Electron Microscopy Society of America, G. W. Bailey, ed., San Francisco Press, San Fransisco, P.560, 1986.

34 J.H.Hollomon, "Temper Brittleness," Trans. ASM, Vol. 36, P. 473, 1946.

35 B.C.Woodfine, "Temper-Brittleness: A Critical Review of the Literature," J. Iron Steel Inst., Vol. 173, P. 229, 1953.

36 J.R.Low, Fracture of Engineering Materials (American Society of Metals, Metals Park, Ohio), P. 127, 1964.

37 C.J.McMahon, "Temper Brittleness - An Interpretive Review," in Temper Embrittlement in steel, American Society for Testing and Materials, Philadelphia, PA, P. 127, 1968.

38 L.G.Emmer,C.D.Clauser and J.R.Low, WRC Bull., Vol. 183, P. 1, 1973.

39 R.Narayan and M.C.Murphy, "A Review of Temper Embrittlement as it Affects Major Steam Turbine and Generator Roter Forgings," J. Iron Steel Inst., Vol. 211, P. 493, 1973.

40 R.Bruscato, "Temper embrittlement and Creep Embrittlement of 2.25 Cr-1 Mo Shielded Metal Arc Weld Deposites," Weld. J. Res. Suppl., Vol. 49, P. 1488, 1970.

41 H.R.Tipler and D.McMlean, "Influence of Interface Energy on Creep," Met. Sci J., Vol. 4, P. 103, 1970.

42 K.T.Aust, J.S.Armijo, E.F.Koch and J.H.Westbrook, "Intergranular Corrosion and Mechanical Properties of Austenitic Stainless Steels," Trans. ASM, Vol. 61, P. 270, 1968.

43 A.Joshi and D.F.Stein, "Intergranular Brittleness Studies in Tungsten Using Auger Spectroscopy," Corrosion, Vol. 28, P. 321, 1972.

44 A.Joshi and D.F.Stein, "Intergranular Brittleness Studies in Tungsten Using Auger Spectroscopy," Met. Trans., Vol. 1, P. 2543, 1970.

45 J.O.Arnold, "The Physical Influence of Elements on Iron," J. Iron Steel Inst., Vol. 45, P. 107, 1894.

46 H.P.Philpot, Proc. Inst. Auto Eng., Vol. 12, P. 235, 1917-18.

47 A.Choudhury, H.P.Kao, C.R.Brooks and C.L.White,"Auger Analysis of the Fracture Surfaces of Ordered $Ni_4Mo$," Scr. Metall., Vol. 22, P. 1057, 1988.

48 J.H.Westbrook, "Segregation at Grain Boundaries," Met. Rev., Vol. 9, P. 415, 1964.

49 M.P.Seah and E.D.Hondros, "Grain Boundary Segregation," Proc. Roy. Soc. Lond., Vol. 335, P. 191, 1973.

50 E.D.Hondros, "Grain Boundary Segregation: Assessment of Investigative Techniques," in Grain Boundary Structure and Properties, eds. D.A.Chadwick and D.A.Smith, Academic Press, London, P. 265, 1976.

51 A.Joshi, "Experimental Techniques to Study Segregation," in Interfacial Segregation, eds., W.C.Johnson and J.M.Blakely, American Society for Metals, Metals Park, Ohio, P. 39, 1977.

52 D.F.Stein, W.C.Johnson and C.L.White, "Study of Grain Boundary Segregation using Auger Electron Spectroscopy," in Grain Boundary Structure and Properties, eds. D.A.Chadwick and D.A.Smith, Academic Press, London, P. 301, 1976.

53 D.McLean, Grain Boundaries in Metals, Oxford Univ. Press, London, 1957.

54 S.Brunauer, P.H.Emmett and E.Teller, "Adsorption of Gases in Multimolecular Layers," J. Am. Chem Soc., Vol. 60, P. 309, 1938.

55 P.V.Ramasubramanian and D.F.Stein, "An Investigation of Grain-Boundary Embrittlement in Fe-P, Fe-P-S and Fe-Sb-S Alloys," Met. Trans., Vol. 4, P. 1735, 1973.

56 A.Joshi and D.F.Stein, "Temper Embrittlement of Low Alloy Steels," in Temper Embrittlement of Alloy steels, American Society for Testing and Materials, Philadelphia, PA, P. 59, 1972.

57 A.Joshi and D.F.Stein, "An Auger Spectroscopy Analysis of Bismuth Segregated to Grain Boundaries in Copper," J. Inst. Metals, Vol. 99, P. 178, 1971.

58 J.M.Capus, "The Mechanism of Temper Brittleness," in Temper Embrittlement in steel, American Society for Testing and Materials, Philadelphia, PA, P. 3, 1968.

59 J.R.Low, "Impurities, Interfaces and Brittle Fracture," Trans. TMS-AIME, Vol. 245, P. 2481, 1969.

60 M.P.Seah, "Interface Adsorption, Embrittlement and Fracture in Metallurgy," Surface Science, Vol. 53, P. 168, 1975.

61 C.T.Liu and J.O.Stiegler, "Ductile Ordered Intermetallic Alloys," Science, Vol. 226, P. 636, 1984.

62 T.Takasugi and O.Izumi, "Electronic and Structural Studies of Grain Boundary Strength and Fracture in $L1_2$ Ordered Alloys-I. On Binary $A_3B$ Alloys," Acta Metall., Vol. 33, P. 1247, 1985.

63 T.Takasugi, O.Izumi and N.Masahashi, "Electronic and Structural Studies of Grain Boundary Strength and Fracture in $L1_2$ Ordered Alloys-II. On the Effect of Third Elements in $Ni_3Al$ Alloy," Acta Metall., Vol. 33, P. 1259, 1985.

64 T.Takasugi, N,Masahashi and O.Izumi, "Electronic and Structural Studies of Grain Boundary Strength and Fracture in $L1_2$ Ordered Alloys-III. On the Effect of Stoichiometry," Acta Metall., Vol. 35, P. 381, 1987

65 M.E.Eberhart, R.M.Latanision and K.H.Johnson, "The Chemistry of Fracture: A Basis for Analysis," Acta Metall., Vol. 33, P. 1769, 1783.

66 D.Farkas and A.Ran, "Space Group Theoretical Analysis of Grain Boundaries in Ordered Alloys," Phys. Stat. Sol. (a), Vol. 92, P. 973, 1985.

67 D.Farkas and V.Rangarajan, "Geometrical Models for Symmetrical Tilt Boundaries in $L1_2$ Ordered Compounds," Acta. Metall., Vol. 35, P. 353, 1987.

68 D.Farkas, "Structural Unit Models for High Angle Symmetrical Tilt Boundaries in Ordered Compounds with the $L1_2$ Structure," in High Temperature Ordered Intermetallic Alloys, C.C.Koch, C.T.Liu, and N.S.Stoloff, eds., Materials Reasearch Society, Pittsburgh, PA, P. 133, 1985.

69 D.Farkas, "Coincident Site Lattice Models for Grain Boundaries in Ordered Alloys," Scr. Metall., Vol. 19, P. 467, 1985.

70 H.P.Kao, C.R.Brooks and K.Vasudevan, "High Temperature Strength of Ordered and Disordered $Ni_4Mo$," in High Temperature Ordered Intermetallic Alloys, eds. N.S.Stoloff, C.C.Koch, C.T.Liu and O.Izumi, Materials Research Society, Pittsburg, PA, P. 335, 1987.

71 T.Takasugi, E.P.George, D.P.Pope and O.Izumi, "Intergranular Fracture and Grain Boundary Chemistry of $Ni_3Al$ and $Ni_3Si$," Scr. Metall., Vol. 19, P. 551, 1985.

72 T.Ogura, S.Hanada, T.Masumoto and O.Izumi, "Grain Boundary Fracture of $Cl_2$ type intermetallic Compound $Ni_3Al$," Metall. Trans. A, Vol. 16, P. 441, 1985.

73 C.J.McMohan,Jr. and V.Vitek,"The Effects of Segregated Impurities on Intergranular Fracture Energy," Acta Metall., Vol. 27, P. 507, 1979.

74 E.M.Schulson, T.P.Weihs, I.Baker, H.J.Frost and J.A.Horton, "Boron Induced Grain Boundary Accomodation of Slip in $Ni_3Al$," Scr. Metall., Vol. 19, P. 1497, 1985.

75 E.M.Schulson, T.P.Weihs, I.Baker, H.J.Frost and J.A.Horton, "Grain Boundary Accomodation of Slip in $Ni_3Al$ Containing Boron," Acta Metall., Vol. 34, P. 1395, 1986.

76 I.Baker, E.M.Schulson and J.A.Horton, "In-situ Straining of $Ni_3Al$ in Transmission Electron Microscope," Acta Metall., Vol. 35, P. 1533, 1987.

77 C.L.White, R.A.Padgett, C.T.Liu and S.M.Yalisove,"Surface and Grain Boundary Segregation in Relation to Intergranular Fracture: Boron and Sulphur in $Ni_3Al$," Scr. Metall., Vol. 18, P. 1417, 1984.

78 M.K.Miller and J.A.Horton, "Atom Probe Analysis of Grain Boundaries in Rapidly Solidified $Ni_3Al$," Acta Metall., Vol. 35, P. 133, 1987.

79 I.Baker, E.M.Schulson and J.R.Michaels, "The Effect of Boron on the Chemistry of Grain Boundaries in Stoichiometic $Ni_3Al$," Phil. Mag., in press.

80 A. Choudhury, C.L.White and C.R.Brooks, "The Role of Boron in $Ni_3Al$," in Symposium on Precious and Rare Metals, in press.

81 A.I.Taub, C.L.Briant, S.C.Huang, K.M.Huang and M.R.Jackson, "Ductility in Boron-Doped, Nickel-Based $L1_2$ Alloys Processed by Rapid Solidification," Scr. Metall., Vol. 20, P. 129, 1986.

82 A.I.Taub and C.L.Briant, "Composition Dependence of Ductility and Strength in Boron-Doped Nickel-Based $L1_2$ Alloys," Acta Metall., Vol. 35, P. 1597, 1987.

83 W.C.Oliver and C.L.White, "The Segregation of Boron and its effect on fracture of an $Ni_3Si$ Based Alloy," in High Temperature Ordered Intermetallic Alloys, eds. N.S.Stoloff, C.C.Koch, C.T.Liu and O.Izumi, Pittsburg, PA, Materials Research Society, P. 241, 1987.

84 M.A.Krimp and K.Vedula, "Effect of Boron on the Tensile Properties of B2 FeAl," Mat. Sci. Eng., Vol. 78, P. 193, 1986.

85 C.T.Liu and H.Inouye, "Control of Ordered Structure and Ductility of $(Fe,Co,Ni)_3V$ Alloys," Met. Trans., Vol. 10A, P. 1515, 1979.

86 C.T.Liu, "Physical Metallurgy and Mechanical Properties of Ductile Ordered Alloys $(Fe,Co,Ni)_3V$," Int. Met. Rev., Vol. 29, P. 168, 1984.

87 J.W.Martin and R.D.Doherty, Stability of Microstructures in Metalic Systems, Cambridge University Press, Cambridge, P. 100, 1980.

88 A.U.Seybolt, "Oxide Dispersion-Strengthened NiAl and FeAl," Trans. ASM, Vol. 59, P. 860, 1966.

89 A.G.Rozner and R.J.Wasilewski, "Tensile Properties of NiAl and NiTi," J. Inst. Met., Vol. 94, P. 169, 1966.

90 K.Aoki and O.Izumi, "On the Ductilities of Intermetallic Compound $Ni_3Al$," Trans. JIM, Vol. 19, P. 203, 1978.

91 A.A.Kuranov, I.N.Sakhanskaya and F.N.Berseneva, "Influence of Atomic Ordering on the Mechanical Properties and Character of Failure in Alloy NiPt," Phys. Met. Metall., Vol. 54(6), P. 121, 1982.

92 K.Kawahara, "Effect of Cold Rolling on the Mechanical Properties of an FeCo-2V Alloy," J. Mater. Sci., Vol. 18, P. 3437, 1983.

93 B.A.Greenberg and Yu.N.Gornostirev, "Recrystallization Features of Ordered Alloys: Part 1. Immobilization of Dislocation Structure," Scr. Metall., Vol. 19, P. 1391, 1985.

94 B.A.Greenberg and Yu.N.Gornostirev, "Recrystallization Features of Ordered Alloys: Part 2. Superstructures $L1_2$, B2 and $L1_0$," Scr. Metall., Vol. 19, P. 1397, 1985.

95 R.A.Buckley, "Microstructure and Kinetic of the Ordering Transformations in Iron-Cobalt Alloys, Fe-Co, FeCo-0.4% Cr, FeCo-2.5% V," Metal Sci., Vol. 9, P. 243, 1975.

96 R.A.Buckley, "Ordering and Recrystallizations in Fe-50Co-0.4% Cr," Metal Sci., Vol. 13, P. 67, 1979.

97 A.E.Vidoz, D.P.Lazarevic and R.W.Cahn, "Strain-Aging of Ordering Alloys, with Special Reference to the Nickel-Iron System," Acta Metall., Vol. 11, P. 17, 1963.

98 P.N.Syutkin, V.I.Syutkina, O.D.Shashkov, E.S.Yakovleva and N.N.Buynov, "Recrystallization of the Alloy CuAu on Ordering," Phys. Met. Metall., Vol. 27(6), P. 98, 1969.

99 N.D.Zemtsova and L.P.Yasyreva, "Interrelation of Ordering and Recrystallization in Alloy CuAu.," Phys. Met. Metall., Vol. 62, P. 144, 1986.

100 E.M.Schulson, "Comments on the Brittle to Ductile Transition of Long-Range Ordered Alloys," Res. Mech. Letters, Vol. 1, P. 111, 1981.

101 A.H.Cottrell, "Theory of Brittle Fracture in Steels," Trans. Metall. Soc. AIME, Vol. 212, P. 192, 1958.

102 E.M.Schulson and D.R.Baker, "A Brittle to Ductile Transition in NiAl of a Critical Grain Size," Scr. Metall., Vol. 17, P. 519, 1983.

103 I.Baker and P.R.Munroe, "Improving Intermetallic Ductility and Toughness," J. Metals, Vol. 40(2), P. 28, 1988.

104 K.Vasudevan, "The Effect of 0-4 Weight Percent Chromium on Transformations of Alpha Phase Ni-Mo-Cr Alloys with Nickel:Molybdenum Atom Ratio Equal to 4:1," MS Thesis, University of Tennessee, Knoxville, 1982.

105 H.P.Kao, "Dislocation Structure, Deformation Structure, Strengthening Mechanism and Embrittlement Causes of Ordered $Ni_4Mo$ Alloy," PhD Dissertation, University of Tennessee, Knoxville, 1986.

106 H.P.Kao, C.R.Brooks and M.Sanganeria, "Fracture and Fractography of Ordered $Ni_4Mo$," to be published in High Temperature Ordered Intermetallic Alloys, eds. N.S.Stoloff, C.C.Koch, A.I.Taub and C.T.Liu, Materials Research Society, Pittsburg, PA, 1989.

107 C.R.Brooks and M.Sanganeria, "Fracture Along Migrated Grain Boundaries in Ordered $Ni_4Mo$," Scr. Metall., Vol. 22, P. 1683, 1988.

108 F.W.Ling, R.S.Irani and R.W.Cahn, "Ordering Kinetics of Cold-worked $Ni_4Mo$," Mat. Sc. Eng., Vol. 15, P. 181, 1974.

# APPENDICES

# APPENDIX A

## Weight Percentage of Microalloying Elements

## Based on Weights Before Melting

| Sample Name | Element | Alloying element content (wt. %) |
|---|---|---|
| MC | Hf | 0.10 |
| ME | B | 0.10 |
| MG | Mn | 1.00 |
| MH | Zr | 0.10 |
| MJ | Ce | 0.12 |
| ML | Nb | 0.12 |
| MM | Mg | 0.20 |
| MN | Be | 0.12 |
| MO | La | 0.10 |

# APPENDIX B

## Chemical Compositions of Alloys

| | Alloys | | | | | | |
|---|---|---|---|---|---|---|---|
| Composition* | NMCR0 | NMCR6 | NMCR3 | NMCR1 | NMCR2 | NMCR4 | NMCR5 |
| Ni | 70.94 | 70.48 | 70.18 | 69.86 | 68.49 | 67.36 | 68.16 |
| Mo | 28.77 | 28.70 | 28.67 | 28.68 | 28.29 | 28.29 | 28.07 |
| Cr | 0.10 | 0.41 | 0.54 | 0.74 | 2.08 | 2.97 | 3.84 |
| Fe | 0.10 | 0.10 | 0.10 | 0.10 | 0.10 | 0.10 | 0.10 |
| Al | 0.05 | 0.05 | 0.05 | 0.05 | 0.05 | 0.05 | 0.02 |
| Co | 0.10 | 0.10 | 0.10 | 0.10 | 0.10 | 0.10 | 0.10 |
| Cu | 0.03 | 0.03 | 0.03 | 0.03 | 0.02 | 0.02 | 0.02 |
| Mg | 0.01 | 0.01 | 0.01 | 0.01 | 0.01 | 0.01 | 0.01 |
| Mn | 0.10 | 0.10 | 0.10 | 0.10 | 0.10 | 0.10 | 0.10 |
| Si | 0.02 | 0.02 | 0.02 | 0.02 | 0.02 | 0.02 | 0.02 |
| V | 0.01 | 0.01 | 0.01 | 0.01 | 0.01 | 0.01 | 0.01 |
| W | 0.10 | 0.10 | 0.10 | 0.10 | 0.10 | 0.10 | 0.10 |
| Zr | 0.01 | 0.01 | 0.01 | 0.01 | 0.01 | 0.01 | 0.01 |
| C | 0.005 | 0.003 | 0.006 | 0.003 | 0.006 | 0.008 | 0.005 |
| B | 0.002 | 0.005 | 0.002 | 0.002 | 0.003 | 0.003 | 0.006 |
| P | 0.006 | 0.004 | 0.004 | 0.005 | 0.004 | 0.004 | 0.004 |
| S | 0.002 | 0.002 | 0.002 | 0.002 | 0.003 | 0.002 | 0.002 |
| Ni : Mo | 4.032 | 4.015 | 4.001 | 3.981 | 3.957 | 3.892 | 3.969 |

*Composition in weight percent.

Note : Actual compositions of Fe, Al, Co, Mg, Mn, Si, V, W, B, P and S are less than the amounts indicated.

# VITA

Mahesh Sanganeria was born on December 12, 1961, in Midnapur, India. Upon completion of his secondary education, he pursued his under-graduate studies at the Indian Institute of Technology, Kharagpur, India, receiving a Bachelor of Technology degree in Metallurgical engineering in 1986. He worked for a year at TISCO, Jamshedpur, after which he joined the graduate program in metallurgical engineering at the University of Tennessee, Knoxville, Tennessee, USA. He received his MS degree from that institution in May 1989. He intends to do his Ph.D. in the area of electronics materials at N.C. State University.

He is a student member of ASM international, SAMPE and Materials Research Society.